U.PORTO

DOUTORAMENTO

BIOLOGIA BÁSICA E APLICADA

Exploring the role of pro-inflammatory signaling in myelin repair

Maria Inês Fazendeiro Cunha

D

2020

Maria Inês Fazendeiro Cunha. Exploring the role of pro-inflammatory signaling in myelin repair

Exploring the role of pro-inflammatory signaling in myelin repair

Maria Inês Fazendeiro Cunha

U.PORTO

D.ICBAS 2020

SEDE ADMINISTRATIVA

INSTITUTO DE CIÊNCIAS BIOMÉDICAS ABEL SALAZAR

FACULDADE DE CIÊNCIAS

FACULDADE DE MEDICINA

MARIA INÊS FAZENDEIRO CUNHA

Exploring the role of pro-inflammatory signaling in myelin repair

Tese de Candidatura ao grau de Doutor em Biologia Básica e Aplicada submetida ao Instituto de Ciências Biomédicas Abel Salazar da Universidade do Porto

Orientador – Prof. Dr. Med. Mikael Simons
Categoria – Professor
Afiliação – Institute of Neuronal Cell Biology (Technical University of Munich), German Center for Neurodegenerative Diseases (DZNE), Munich, Germany

Co-Orientador – Dr. João Bettencourt Relvas
Categoria – Investigador Principal
Afiliação – Instituto de Investigação e Inovação em Saúde (i3S), Universidade do Porto, Porto, Portugal

This thesis was supervised by:

Prof. Dr. Med. Mikael Simons
Professor and Head of the Group
Institute of Neuronal Cell Biology (TUM-NCB)
Technical University Munich
German Center for Neurodegenerative Diseases (DZNE)

Experimental work was conducted at:

Institute of Neuronal Cell Biology at the German Center for Neurodegenerative Diseases (DZNE), Technical University of Munich, Munich, Germany.

Financial Support:

Maria Inês Fazendeiro Cunha was supported by a fellowship (PD/BD/105749/2014) awarded by the Doctoral Program in Areas of Basic and Applied Biology (GABBA) of the University of Porto and funded by the Portuguese Foundation of Science and Technology (FCT). This work was funded by grants from the German Research foundation (SI 746/12-1, STA 1389/2-1, TRR128-2, SyNergy Excellence Cluster), ERC (Consolidator Grants to Mikael Simons) and the Dr. Miriam and Sheldon G. Adelson Medical Research Foundation.

List of Publications

Publications discussed in this thesis:

Pro-inflammatory activation following demyelination is required for myelin clearance and oligodendrogenesis

Maria Inês Cunha*, Minhui Su*, Ludovico Cantuti-Castelvetri, Stephan Mueller, Martina Schifferer, Minou Djannatian, Ioannis Alexopoulos, Franziska van der Meer, Anne Winkler, Tjakko van Ham, Bettina Schmid, Stefan Lichtenthaler, Christine Stadelmann, and Mikael Simons

J Exp Med (2020) 217 (5): e20191390.
https://doi.org/10.1084/jem.20191390

This work has been presented in poster format in the following meetings:

GABBA Annual Meeting, Porto, December 2015
Schwabing Neuroscience Summit, Munich, September 2016
DZNE PhD Retreat, Bonn, November 2016
XIV European Meeting on Glial Cells in Health and Disease, Porto, July 2019

This work has been presented in oral presentations in the following meetings:

GABBA Annual Meeting, Porto, December 2016-2019
CSD Tuesday-Noon Seminar Series, Munich, February 2017 and May 2019

À minha mãe,

Valeu a pena? Tudo vale a pena
Se a alma não é pequena.
Quem quer passar além do Bojador
Tem que passar além da dor.
Fernando Pessoa in *Mar Português*, 1934

Acknowledgements

First of all, I would like to show my gratitude to the GABBA program, which has given me this extraordinary and life-changing opportunity. To be part of GABBA is not only to be part of a PhD program. It means to be part of an academic family which helps and encourages each one of us from the moment we start this journey. It means freedom and bravery to embrace the unknown and open our minds to new ways of thinking, living and working. But it also means trust to know we have a core which supports us at any moment and decision. GABBA fosters science without borders and I am grateful to be part of it. Thank you!!

I would like to thank Mika for accepting to be my supervisor and guiding me throughout this journey. I have learnt so much being part of your lab and it definitely fostered both my personal and professional growth. Thank you for your constant availability and for your contagious enthusiasm about science. Thank you!!

I would also like to thank my co-supervisor in Porto, João Relvas, for his availability whenever necessary and for inputs given throughout these years. Thank you!!

To all members of the Simons Lab in Munich, with whom I have shared this experience, my deep, deep Thank you. Thank you for always answering my thousand million questions (per minute) with so much patience and caring. Doing a PhD is a rollercoaster of emotions and to have had the support of each one of you, believe me, made all the difference. Thank you!!

To both the animal facilities in DZNE (mouse and fish), to all the staff that makes our work possible while sharing their constant good vibes with us, Thank you!!

During this journey I was lucky to have met some wonderful people who have become part of my life and made this time really, really special, and I am very grateful for that. On the other hand, for those who already come for a long time with me, your constant support throughout these years has been crucial, Thank you!!

Finally, I would like to thank my family for being the core that provides that unlimited strength that makes us believe that anything we want is possible. And especially to the person responsible for generating that core and that keeps on making all of this possible, Obrigada Mãe!!

Table of Contents

Figure Index

1. Introduction

2. Materials and Methods

3. Research work

5. Concluding remarks and future perspectives

Table Index

Abbreviations

BBB – blood-brain-barrier

BCAS1 – breast carcinoma amplified sequence 1

Cas9 – CRISPR associated protein 9

cDNA – complementary deoxyribonucleic acid

CNPase – 2',3'-Cyclic-nucleotide 3'-phosphodiesterase

CNS – central nervous system

CNTF – ciliary neurotrophic factor

CRISPR – clustered regularly interspaced short palindromic repeats

CSF1R – colony stimulating factor 1 receptor

CXCL1 – C-X-C motif chemokine ligand 1

CXCL12 – C-X-C motif chemokine ligand 12

DAMP – damage-associated molecular patterns

DIV – days *in vitro*

dpf – days post fertilization

dpl – days post-lesion

EAE – experimental autoimmune encephalomyelitis

EDTA - ethylenediaminetetraacetic acid

eGFP – enhanced green fluorescent protein

FGF2 – fibroblast growth factor 2

GalC – galactocerebroside

GGF2 – glial growth factor 2

gRNA – guide ribonucleic acid

HGF – hepatocyte growth factor

IGF-1 – insulin-like growth factor 1

IL-10 – interleukin 10

IL-1β – interleukin 1 β

IL-6 – interleukin 6

INFγ – interferon γ

iNOS – inducible nitric oxidase synthase

IPA – ingenuity pathway analysis

IκBα – nuclear NF-κB inhibitor α

Iκκ – IκB kinase

KO – knockout

MAG – myelin-associated glycoprotein

MBP – myelin basic protein

mCSF – macrophage colony stimulating factor

MOG – myelin oligodendrocyte glycoprotein

mpeg1 – macrophage expressed gene 1

mRFP – membrane red fluorescent protein

MS – multiple sclerosis

MTZ – metronidazole

Myd88 - myeloid differentiation primary response 88

NF-κB – nuclear factor kappa B

NG2 – neuron-glial antigen 2

Nkx2.2 – NK2 homeobox 2

nls – nuclear localization signal

NSC – neural stem cells

NTR – nitroreductase

OCSC – organotypic cerebellar slice culture

Olig1 – oligodendrocyte transcription factor 1

Olig2 – oligodendrocyte transcription factor 2

OPCs – oligodendrocyte progenitor cells

OSC – organotypic slice culture

PAMP – pathogen-associated molecular patterns

PBS – Phosphate-buffered saline

PCR – polymerase chain reaction

PDGFRα – platelet-derived growth factor receptor α

PFA – paraformaldehyde

PLP – proteolipid protein

PPMS – primary progressive multiple sclerosis

PRMS – progressive relapsing multiple sclerosis

PRRs – pattern recognition receptors

PTU – 1-phenyl-2-thiourea

qPCR – quantitative polymerase chain reaction

RNA – ribonucleic acid

ROI – region of interest

RRMS – relapsing remitting multiple sclerosis

RT-PCR – reverse transcription polymerase chain reaction

SEM – standard error of the mean

Sox10 – SRY-Box transcription factor 10

SPMS – secondary progressive multiple sclerosis

Tg – transgenic

TGF-β – transforming growth factor β

TNF-α – tumor necrosis factor-α

TRIF – TIR-domain-containing adapter-inducing INF-β

WT – wild-type

Abstract

Dysregulation of immune responses in the central nervous system (CNS) is thought to underlie the development of several neurological disorders. Multiple sclerosis is the most common autoimmune disease of the CNS and it is characterized by multifocal demyelination, which is in some cases followed by spontaneous remyelination that activates myelin repair mechanisms and induces the production of new myelin. However, with the progression of the disease and the exposure to repeated demyelinating insults, remyelination efficiency decreases. The innate immune system is intimately involved in the process of remyelination. Yet, it is still unclear how microglia/macrophages activation influences the outcome of a demyelinating lesion. In this study we decided to evaluate the role of pro-inflammatory phagocyte activation in the course of a demyelinating injury. We have established a new focal demyelinating model in zebrafish larvae, through injection of lysolecithin in the spinal cord. We have monitored the degree of myelination, the kinetics of oligodendrocyte precursor cells in the lesion and their differentiation into mature oligodendrocytes, as well as the infiltration of phagocytes and their activation, throughout lesion evolution. We show that CSF1R-deficient larvae, with no microglia, have compromised remyelination, and that an initial Myd88-dependent NF-κb pro-inflammatory signaling is triggered after lysolecithin-induced demyelination. We further show that remyelination is compromised in the absence of Myd88-signaling, with impaired degradation of ingested myelin debris and phagocyte retention in lesions. Furthermore, by combining both zebrafish and mice models, we identified TNF-α as one cytokine which expression is reduced in Myd88-deficient lesions, and that its administration can foster the generation of pre-myelinating / early myelinating oligodendrocytes after lysolecithin-induced demyelination, in *ex vivo* organotypic cerebellar slice cultures. Our results support the hypothesis that an initial pro-inflammatory response is critical for myelin debris clearance and repair, as well as for inflammation resolution, and that inhibiting inflammation can compromise lesion recovery.

Keywords: Inflammation; Phagocytes; Microglia; Macrophages; Pro-inflammatory activation; Remyelination; Zebrafish; Mice

Resumo

Acredita-se que uma desregulação da resposta imunitária no sistema nervoso central (SNC) está por de trás do desenvolvimento de várias doenças neurológicas. A esclerose múltipla é a doença autoimune mais comum do SNC e caracteriza-se pela presença de lesões desmielinizantes multifocais, nas quais, em alguns casos, existe remielinização espontânea, em que se dá a ativação dos mecanismos de regeneração da mielina, induzindo assim a produção de nova mielina. No entanto, com a progressão da doença e a exposição repetida a insultos desmielinizantes, existe uma redução na eficiência da remielinização. O sistema imunitário inato está estreitamente envolvido no processo de remielinização. Contudo, ainda não é claro como é que a ativação da microglia / dos macrófagos influencia o desfecho de uma lesão desmielinizante. Neste estudo, decidimos avaliar o papel que a ativação pró-inflamatória nos fagócitos (que neste estudo se referem à microglia e aos macrófagos) tem na progressão de uma lesão desmielinizante, nomeadamente na sua entrada e retirada da lesão, na sua capacidade em eliminar os detritos de mielina (tanto em fagocitá-los como em degradá-los), assim como o seu impacto no recrutamento, sobrevivência e diferenciação das células percursoras de oligodendrócitos. Para tal, a nossa estratégia experimental consistiu em usar modelos de fagócitos subativados ou sobreativados, no contexto de uma lesão desmielinizante focal, provocada pela administração de lisolecitina.

Neste sentido, estabelecemos um novo modelo de desmielinização focal em larvas de peixe-zebra, através da injeção de lisolecitina na medula espinhal. Avaliámos o grau de mielinização, a presença das células precursoras de oligodendrócitos ao longo da evolução da lesão, assim como a sua diferenciação em oligodendrócitos maduros. Avaliámos também a infiltração e ativação dos fagócitos ao longo da evolução das lesões. Neste modelo observámos que a ausência do CSF1R nas larvas de peixe-zebra, portanto larvas sem microglia, se traduz numa redução no grau de remielinização, quando comparado com larvas selvagens. Observámos ainda que após uma lesão desmielinizante, provocada pela injeção de lisolecitina, existe uma ativação inicial pró-inflamatória, dependente da proteína adaptadora Myd88, nos fagócitos recrutados para as lesões. Mais ainda, observámos que na ausência da sinalização dependente da proteína Myd88, o processo de remielinização é comprometido, associado com uma degradação deficiente dos detritos de mielina fagocitados, assim como uma retenção dos fagócitos nas lesões.

Através da combinação do modelo de desmielinização em larva de peixe-zebra com o modelo de desmielinização em ratinho, também provocado pela injeção de lisolecitina, identificámos TNF-α como uma citocina cuja expressão se apresenta reduzida em larvas de peixe-zebra deficientes em Myd88, e que a sua administração em culturas organotípicas

de cerebelo promove a produção de novos oligodendrócitos, que expressam a proteína BCAS1.

Desta forma, os resultados obtidos neste estudo suportam a hipótese de que uma resposta inicial pró-inflamatória é necessária para a eliminação dos detritos de mielina, resultantes de um insulto desmielinizante, assim como para a resolução da resposta inflamatória e remielinização, e que a inibição da resposta inflamatória pode comprometer a recuperação de uma lesão desmielinizante.

Palavras-chave: Inflamação; Fagócitos; Microglia; Macrófagos; Ativação pro-inflamatória; Remielinização; Peixe-zebra; Ratinhos

1. Introduction

1.1. Oligodendrocyte-produced myelin and myelination in the central nervous system (CNS)

The CNS is composed by two different types of tissue, which are called gray and white matter. The gray matter is mainly composed of neuronal cell bodies, dendrites and unmyelinated axons, whereas the white matter mostly contains axons spirally wrapped in a very fatty, multilayered membrane called myelin, and the myelin-producing cells (Nave and Trapp, 2008; Snaidero et al., 2014). Myelin in the CNS is produced by a type of glial cells called oligodendrocytes, which are able to wrap several axons (generating up to 80 different myelin sheaths) (Snaidero and Simons, 2014). The major functions of myelin are to increase the speed of electrical impulse conduction, through insulation of the axon and via saltatory nerve conduction, and to provide metabolic support to axons, thereby contributing to preserve their integrity (Simons and Nave, 2015). The increase in the speed of electrical impulse propagation is achieved through the structural organization of the different domains that the myelinated axon presents. In a very simplified way, it has the internode, which corresponds to the myelinated segment, and the nodes of Ranvier, which are ~1μm non-myelinated gaps between two myelin segments, and where a high density of sodium channels cluster, allowing for saltatory conduction rather than the otherwise continuous and slow conduction along the entire length of the axon (Freeman et al., 2016). This allows for all information in the body to be transmitted rapidly, which is essential for efficient and integrated sensory, motor and cognitive functions (Fig. 1.1).

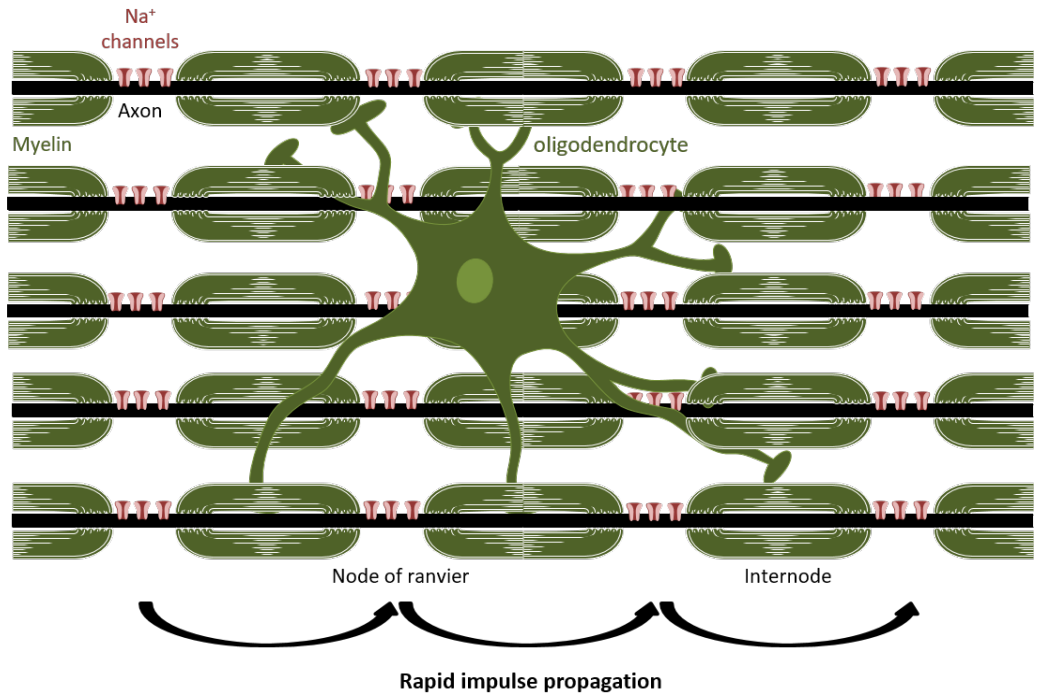

Figure 1.1 Schematic representation of myelination in the CNS. One oligodendrocyte is able to wrap multiple myelin sheaths in different axons. The myelinated axons are structured in two main different domains: the internodes, myelinated segments, and the nodes of Ranvier, non-myelinated segments. A high density of sodium channels cluster at the nodes of Ranvier and allow for saltatory conduction of the action potentials.

Myelination is an evolutionarily conserved process among vertebrates, which involves the action of different cells and their molecular signals (Ackerman and Monk, 2016). Briefly, myelination starts early in development with the migration of the oligodendrocyte precursor cells (OPCs) from the ventricular germinal zones to the entire CNS, guided by diverse chemotactic cues and promoted by receptor-ligand interactions with the extracellular matrix (Bergles and Richardson, 2015). OPCs originate from neural stem cells (NSCs) through the action of specific transcription factors like oligodendrocyte transcription factor 1 (Olig1), oligodendrocyte transcription factor 2 (Olig2), NK2 homeobox 2 (Nkx2.2) and SRY-Box transcription factor 10 (Sox10), and are also characterized by their high expression of platelet-derived growth factor receptor alpha (PDGFRα) and proteoglycan neuron-glial antigen 2 (NG2) markers (Miron et al., 2011; van Tilborg et al., 2018). These cells, initially with a bipolar morphology, proliferate and differentiate, thereby acquiring an arborized morphology driven by actin cytoskeleton dynamics, and, through extension and retraction of their multipolar filopodia-like processes, select the axons to be myelinated (Almeida, 2018; Azevedo et al., 2018; Seixas et al., 2019). Besides the increased morphological complexity, from bipolar to multipolar cells, the maturation and differentiation of oligodendrocytes is characterized by the expression of a plethora of markers depending on their developmental stage. For instance, immature, pre-myelinating / early myelinating

oligodendrocytes can be characterized by the expression of breast carcinoma amplified sequence 1 (BCAS1), the lipid antigen O4, galactocerebroside (GalC) and 2',3'-Cyclic-nucleotide 3'-phosphodiesterase (CNPase) (Fard et al., 2017; Wooliscroft et al., 2019). On the other hand, terminally differentiated, mature oligodendrocytes, ready to start the ensheathment process defined by the expansion and compaction of the myelin sheath along the axon, already express the myelin proteins myelin-associated glycoprotein (MAG), myelin oligodendrocyte glycoprotein (MOG), myelin proteolipid protein (PLP) and myelin basic protein (MBP) (Barateiro and Fernandes, 2014; Bhat et al., 1996; van Tilborg et al., 2018).

It is nowadays clear that myelin is of major importance not only for electrical insulation of the axons but also to preserve their integrity, through active metabolic dynamics between the myelin sheath and the subjacent axon. This importance is, for example, reflected through the fact that still after the peak of myelination in early development, a pool of OPCs remains in diverse areas of the CNS throughout adulthood, persisting in a quiescent state and ready to be activated whenever necessary, namely, in response to a demyelinating injury (Michalski and Kothary, 2015).

1.2. Remyelination in the CNS

Loss of myelin is accompanied by loss of metabolic support to axons and defective transmission of action potentials, both of which lead to progressive neurological impairment seen in patients (Fig. 1.2). Remyelination, or myelin repair, is the process in which after a demyelinating insult new myelin sheaths are wrapped around demyelinated axons (Franklin and Goldman, 2015). It aims at restoring the highly efficient saltatory conduction and functional defects, as well as axon survival. In the CNS, remyelination is quite a successful and efficient process, unlike axonal regeneration (McMurran et al., 2016). However, despite the restoration of saltatory conduction and regain of normal axon function, there are clear architectural differences after remyelination, in which myelin sheaths are shorter and thinner than otherwise un-lesioned myelinated axons established during development (Duncan et al., 2017). This is quite clear when large-diameter axons present with abnormally thin myelin sheaths. A possible explanation for this phenomenon is the different axonal dynamics that the myelinating oligodendrocyte encounters during the process of myelination versus remyelination. Whereas in the earlier the axon diameter is still being established, in remyelination the axon diameter has already achieved its mature size (Franklin and Ffrench-Constant, 2008). Furthermore, although considered very efficient, remyelination has been shown to be less efficient with aging, which may be of special concern when regarding demyelinating diseases that span over decades (Cantuti-Castelvetri et al., 2018; Shen et al., 2008; Sim et al., 2002).

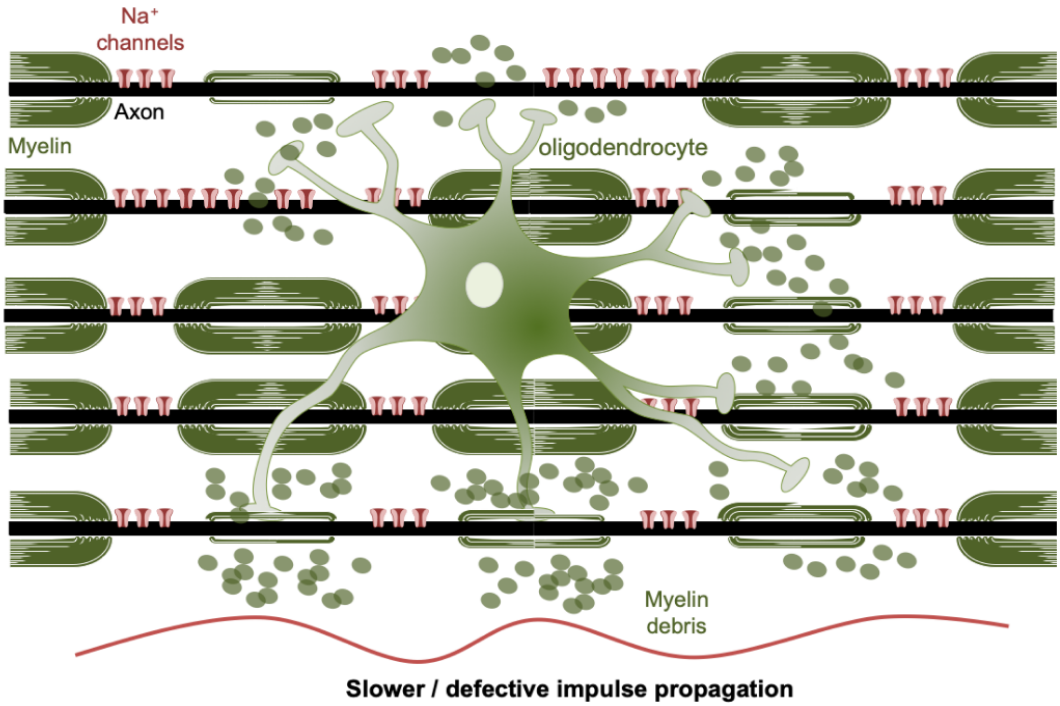

Figure 1.2 Schematic representation of demyelination in the CNS. Demyelination leads to the redistribution of sodium channels along the axon, disrupting the saltatory conduction and thereby leading to a continuous and slower impulse propagation, or, in worse cases, to a conduction block. The redistribution of sodium channels causes an increase in sodium influx and energy expenditure, which, together with the loss of metabolic support, leave the denuded axon susceptible to degeneration and subsequent neurological impairment.

The process of remyelination requires three main steps: activation of the OPCs; their proliferation and migration (recruitment) to the demyelinated site; and, their differentiation into mature oligodendrocytes, which will then remyelinate the axon (Franklin and Ffrench-Constant, 2008). OPCs are highly proliferative cells which account for around 5-8% of the CNS cell population, and can be found in both white and gray matter (Dawson et al., 2003; Kuhn et al., 2019). As mentioned before, in homeostatic conditions, these cells are characterized by the expression of specific markers, such as NG2, PDGFRα and the transcription factor Olig1 (Arnett et al., 2004; Kroehne et al., 2017; Levine et al., 1993; Redwine et al., 1997; Zhou et al., 2000). When there is a demyelinating insult, these cells shift from a quiescent to an activated state, in response to factors produced by astrocytes and microglia (Franklin and Ffrench-Constant, 2008). OPCs become then responsive to chemokines, cytokines, mitogens and growth factors. This results in morphological and gene expression changes, with increase of cell size and upregulation of the gene expression of certain transcription factors also connected with developmental myelination, such as Olig2 and Nkx2.2 (Fancy et al., 2004; Levine and Reynolds, 1999; Watanabe et al., 2004). Immediately after their activation, OPCs start to proliferate in response to the injury. This proliferation has been shown to be modulated by the cellular levels of the cell cycle

regulatory protein p27kip-1 and fostered by the growth factors PDGF, fibroblast growth factor 2 (FGF2) and glial growth factor 2 (GGF2) (Crockett et al., 2005; Li et al., 2020; Whittaker et al., 2012; Woodruff et al., 2004). Together with their proliferative response, OPCs migrate to the demyelinated area, mediated by receptor-ligand adhesions to the extracellular matrix and signaling factors. Several factors have been shown to mediate OPC migration, which include the secreted factors semaphorins, PDGF, netrin-1, C-X-C motif chemokine ligand 1 (CXCL1) and tenascin C (Boyd et al., 2013; Jarjour et al., 2003; Miron et al., 2011; Tepavcevic et al., 2014; Vora et al., 2012; Watzlawik et al., 2013). When OPCs reach the demyelinated area, they have to differentiate into mature oligodendrocytes which will then replace the damaged myelin sheath. The differentiation comprises three phases: first, the establishment of the contact with the demyelinated axon; second, the expression of myelin genes and the generation of myelin membrane; third, the wrapping and compaction of the myelin sheath (Franklin and Ffrench-Constant, 2008). The differentiation step is the one most thought to fail and consequently lead to remyelination failure in what becomes a chronic lesion (Kuhlmann et al., 2008; Skaper, 2019; Wolswijk, 1998). Various factors produced in the course of inflammation have been shown to play a role in promoting the differentiation of OPCs into post-mitotic mature oligodendrocytes following demyelination, such as thyroid hormone, ciliary neurotrophic factor (CNTF) and insulin-like growth factor 1 (IGF-1) (Franco et al., 2008; Hlavica et al., 2017; Hsieh et al., 2004; Steelman et al., 2016). Also transforming growth factor β (TGF-β) has been shown to play a major role in promoting OPC cell cycle withdrawal and subsequent oligodendrocyte differentiation, with a delay in the expression of TGF-β in old animals, following toxin-mediated demyelination, being shown to be correlated with impaired remyelination when compared to young animals (Hinks and Franklin, 2000; McKinnon et al., 1993; Palazuelos et al., 2014). In addition, microglia-derived activin-A has also been shown to promote oligodendrocyte differentiation in *in vitro* and *ex vivo* toxin-mediated demyelination models (Miron et al., 2013).

The evidence reported so far strongly suggests that the process of remyelination in the CNS is driven by a complex network of both cell-intrinsic mechanisms and environmental signals, triggered by an inflammatory response to demyelination.

1.3. CNS phagocytes and signaling pathways involved in phagocyte activation

As with any regeneration mechanism, also in remyelination the immune cells play a major role. The innate immune cells present in the CNS parenchyma are a type of tissue resident macrophages, termed microglia. These professional phagocytes account for around 10% of total glial cells, which in homeostasis perform active surveillance of the CNS parenchyma, through continuous extension and retraction of their processes (Perry, 1998; Prinz and Priller, 2014). They are involved in the regulation of several mechanisms like the migration of neural precursors, synaptic pruning, learning and social behavior, as well as myelination and OPC maintenance during adulthood (Aarum et al., 2003; Hagemeyer et al., 2017; Kierdorf and Prinz, 2017; Schafer et al., 2012; Torres et al., 2016). In response to any signs of invading pathogens or tissue damage, microglia undergo both morphological and functional changes, such as cell body hypertrophy, up-regulation of cell surface activation antigens and release of a range of cytokines and chemokines that foster an inflammatory response (Fig. 1.3) (Town et al., 2005). Often, together with CNS injury there is infiltration of peripheral monocyte-derived macrophages which are technically very challenging to distinguish from the CNS tissue resident macrophages, microglia. For this reason, and in a simplified way, in this thesis microglia/macrophages are collectively referred to as phagocytes, unless specific discrimination is made. Phagocytes have a broad spectrum of activation phenotypes, which have been related to either a more protective or more toxic action by these cells in the context of several pathologies (Kigerl et al., 2009; Mantovani et al., 2004). These cells can be activated by both pathogen-associated molecular patterns (PAMPs) and endogenous damage-associated molecular patters (DAMPs). Dependently of the stimuli by which they get activated, phagocytes present different cell-surface and intracellular markers, release different molecules and acquire different functions (Hu et al., 2015). On one extreme of the activation spectrum, these cells can present a more pro-inflammatory phenotype, with the secretion of a range of pro-inflammatory cytokines, such as IL-6, IL-1β and TNF-α, as well as the release of reactive oxygen species (ROS). On the other extreme, phagocytes are characterized by a rather anti-inflammatory phenotype, with the release of anti-inflammatory cytokines, such as IL-10, and are associated to a pro-resolving, pro-regenerative state (Akhmetzyanova et al., 2019; Lively and Schlichter, 2018).

As with any cell that is able to become activated in response to a stimulus, phagocytes must also be able to deactivate and restore their homeostatic phenotype. Otherwise, if cell deactivation is impaired, chronic activation of a cell can lead to its dystrophy, with the cell becoming senescent. In this way, the phagocyte is not able to exert its proper role in keeping tissue homeostasis anymore and it is likely to foster a chronic inflammatory process instead

(Fig. 1.3) (Caldeira et al., 2014; Koellhoffer et al., 2017; Saijo and Glass, 2011; Streit et al., 2014; van Deursen, 2014; Yu et al., 2012).

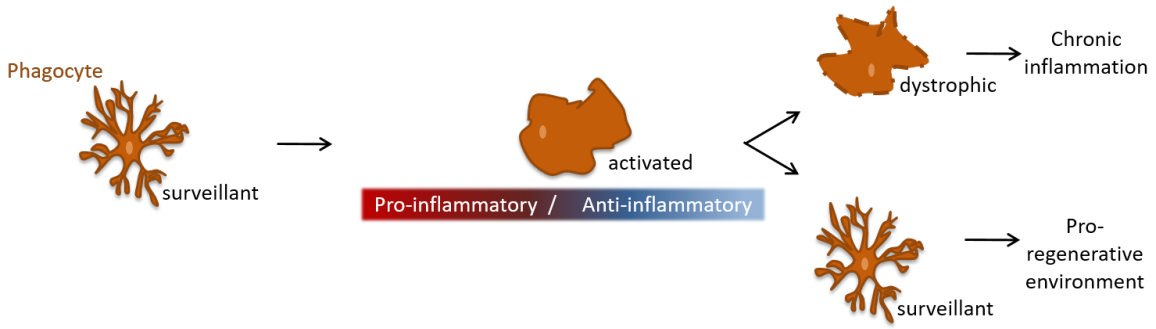

Figure 1.3 Schematic representation of the different phenotypes CNS phagocytes can acquire. In homeostasis, CNS phagocytes are very motile cells, which present a ramified morphology and are continuously surveilling the CNS parenchyma. When there is an insult, these cells become activated, thereby undergoing both functional and morphological alterations, with hypertrophy of the cell body and release of cytokines and chemokines that can range from pro- to anti-inflammatory, depending on the stimulus by which they got activated. After the insult is neutralized, the phagocytes must be able to deactivate, return to their homeostatic signature and move away from the site of injury, thereby leading to resolution of inflammation which is required for a pro-regenerative environment. If the phagocytes cannot deactivate and are in a continuous state of activation, these cells might become dystrophic and senescent, remaining in the site of injury and leading to a chronic inflammatory process.

One of the main functions of phagocytes is exactly to perform phagocytosis of either invading pathogens or damaged-derived cellular debris and dead cells. This comprises an early component of the innate immune response and it is critical to maintain tissue homeostasis. When a particle is recognized by cell surface receptors present in the membrane of a phagocyte, and is subsequentially engulfed, it undergoes a process termed phagosome maturation. Briefly, this involves the wrapping of the ingested particle in a vesicle called phagosome, through actin cytoskeleton remodeling, which goes through a series of fusions with progressively acidified endosomes containing different types of hydrolytic enzymes, that are required for the progressive degradation of the ingested particle. The last step of the phagosome maturation is the fusion of the late phagosome with the highly acidic lysosomes, which gives rise to the phagolysosome. Here, together with the hydrolytic enzymes, occurs the rapid release of ROS in a phenomenon called oxidative burst, which is of major importance for the complete degradation of the internalized particles (Fig. 1.4) (Kinchen and Ravichandran, 2008; Levin et al., 2016; Pauwels et al., 2017; Slauch, 2011).

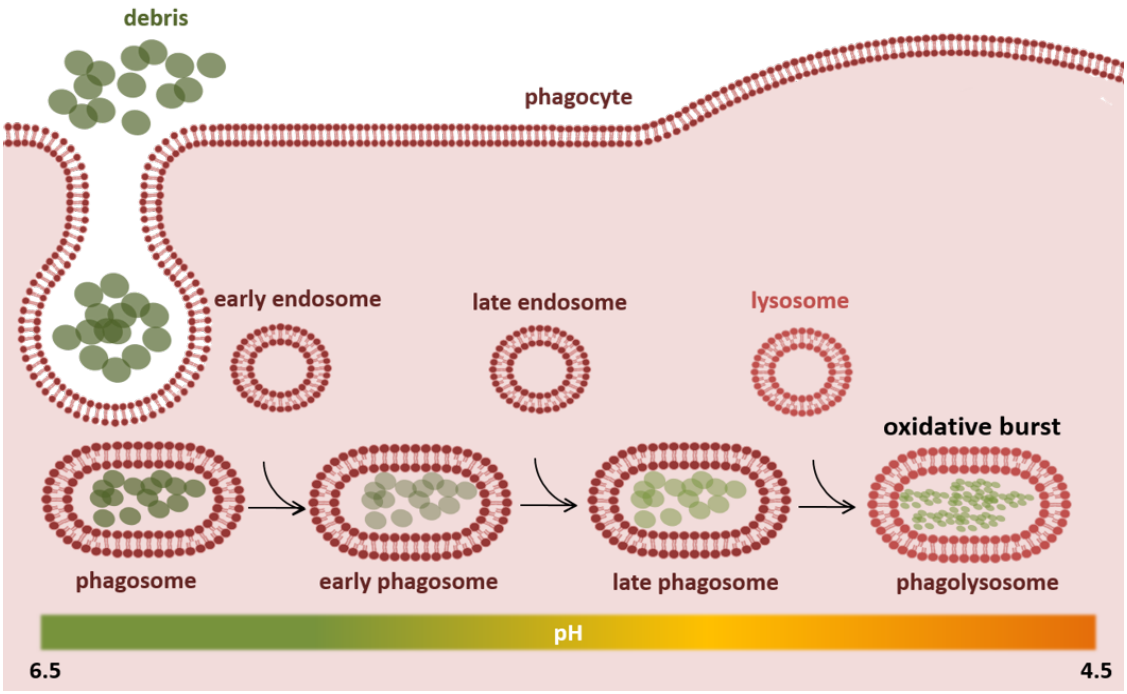

Figure 1.4 Schematic representation of the phagosome maturation process. The recognition of a particle, for instance cellular debris resultant from injury, leads to actin cytoskeleton remodeling of the phagocyte in order to internalize the particle in a structure called phagosome. The phagosome goes through a series of fusions and fissions with early and late endosomes, becoming progressively more acidic, thereby increasing its degradative capacity. Ultimately, the late phagosome fuses with lysosomes, transforming into a phagolysosome, where the oxidative burst occurs and leads to the complete degradation of the ingested particle. Adapted from (Poirier and Av-Gay, 2012).

1.3.1. Myd88-dependent pro-inflammatory signaling

The consensual model of an acute inflammation says that the initial response after an insult is pro-inflammatory and only after, once the trigger insult is neutralized, there is a shift to an anti-inflammatory, pro-resolution phenotype (Newcombe et al., 2018). Myeloid differentiation primary response 88 (Myd88) is the canonical adaptor protein critical for the activation of the pro-inflammatory signaling downstream of one of the most important pathways for innate immunity, the Toll-like receptor (TLR) pathway (Deguine and Barton, 2014). TLRs are a family of pattern recognition receptors (PRRs) and can be activated by both exogenous pathogen-derived ligands and endogenous injury-derived ligands, including glycolipids, lipoproteins and cell-secreted proteins (Erridge, 2010; Rifkin et al., 2005; Yu et al., 2010). Once engaged, TLRs (except TLR3) recruit Myd88 protein which leads to activation of the IκB kinase (Iκκ) complex. This leads to the phosphorylation of the nuclear factor kappa B (NF-κB) inhibitor α (IκBα), thereby triggering its polyubiquitination and degradation by the proteasome, leaving the transcription factor NF-κB free to translocate to the nucleus. Once in the nucleus, NF-κB activates the transcription of genes related to cell proliferation and survival, as well as pro-inflammatory chemokines and cytokines, like TNF-α, IL-1β, IL-6, among others (Liu et al., 2017; Ruland, 2011). Because if left out of control, chronic activation of an inflammatory cell might cause damage to the surrounding tissue, it should be tightly regulated (Dheen et al., 2007). Therefore, NF-κB also activates the transcription of its negative regulators, IκBα and the ubiquitin-editing enzyme A20. Following protein synthesis, IκBα binds to NF-κB in the nucleus and transports it back to the cytoplasm, inhibiting its function. Moreover, A20 deubiquitinates the Iκκ complex, leading to its disassembly and termination of the inflammatory response (Fig. 1.5) (Ruland, 2011).

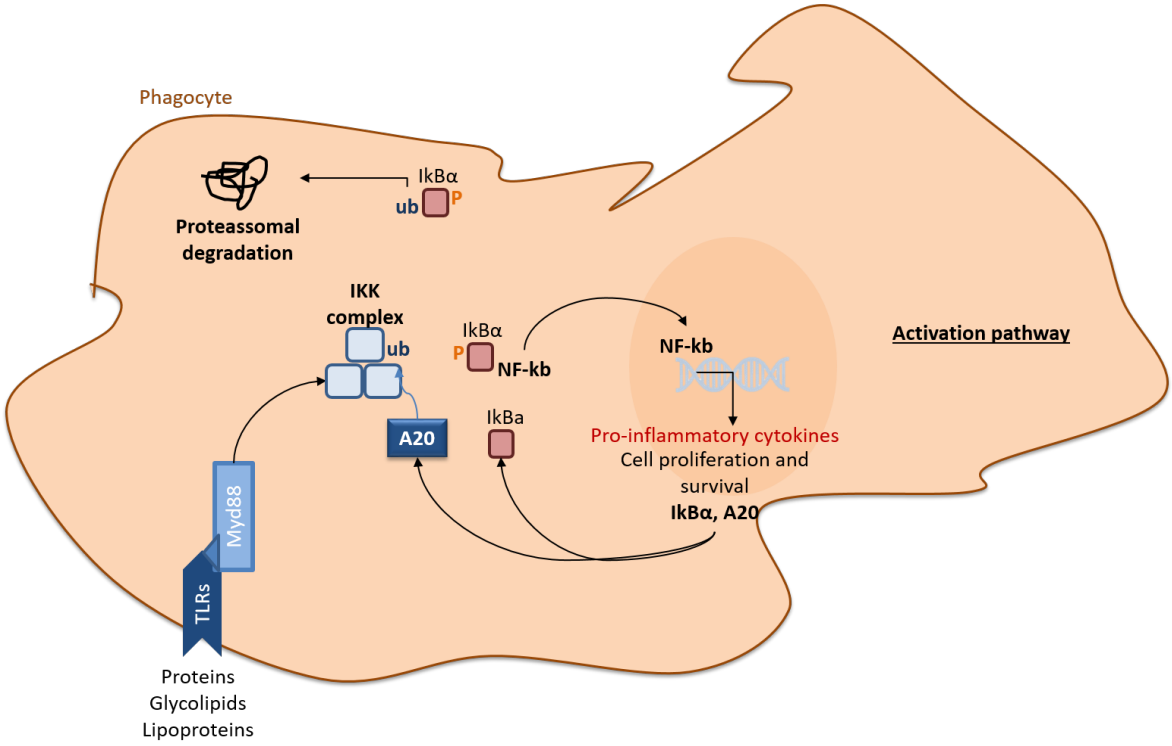

Figure 1.5 Schematic representation of Myd88-dependent TLR pro-inflammatory signaling. Proteins, glycolipids and lipoproteins are examples of ligands that can bind TLRs and activate phagocytes. This binding leads to the recruitment of Myd88 adaptor protein which is critical for the signaling of the rest of the activation pathway that culminates with the translocation of NF- κB into the nucleus thereby activating the transcription of genes related with pro-inflammatory cytokines, as well as cell proliferation and survival. NF- κB also activates the transcription of its negative regulators, IκBα and A20, which will in turn shutdown the activation pathway.

1.4. CNS phagocytes and their role in remyelination

The role of inflammation is to prepare injured tissue for regenerative processes, and there is now several evidence that the innate immune response to a demyelinating injury is critical to remyelination. For instance, in toxin-induced demyelination models, both ablation of macrophages, with systemic treatment of clodronate liposomes, as well as their pharmacological inhibition with corticosteroids, have been shown to lead to decreased inflammation and impaired remyelination (Chari et al., 2006; Kotter et al., 2001; Kotter et al., 2005; Li et al., 2005). Conversely, promotion of inflammation, by stimulation of TLR2, was shown to foster myelination by transplanted OPCs (Setzu et al., 2006). In addition, being a type of phagocytic cell, CNS phagocytes play a major role in the clearance of myelin debris from the demyelinated area (Hadas et al., 2012; Lampron et al., 2015; Natrajan et al., 2015; Neumann et al., 2009). This is of major importance since myelin debris have been shown to contain inhibitors of oligodendrocyte differentiation, which is suggested to function as a way of keeping the pool of progenitor cells from differentiating in the absence of a demyelinating injury, which could likely cause their apoptosis (Kotter et al., 2006; Natrajan et al., 2015; Plemel et al., 2013; Robinson and Miller, 1999; Syed et al., 2008). The clearance of myelin debris involves both their uptake and digestion and when phagocytes are not able to clear the ingested myelin debris, due for instance to aging senescence, this results in impaired resolution of inflammation which has been correlated with impaired remyelination (Cantuti-Castelvetri et al., 2018; Safaiyan et al., 2016).

Microglia, together with astrocytes, are thought to be the major source of factors promoting the proliferation and differentiation of OPCs in response to a demyelinating insult (Franklin and Ffrench-Constant, 2008). Indeed, in MS patients, active demyelinating lesions with ongoing inflammation, were shown to have the highest numbers of OPCs and better remyelination (Franklin and Ffrench-Constant, 2008; Kuhlmann et al., 2008; Miron, 2017). The released factors include galectin 3, TGF-β, TNF-α, IL-1β, IGF-1, activin A, hepatocyte growth factor (HGF), PDGF-AA and C-X-C motif chemokine ligand 12 (CXCL12) (Arnett et al., 2001; Dillenburg et al., 2018; Hinks and Franklin, 2000; Lloyd and Miron, 2019; Mason et al., 2001; Pasquini et al., 2011). Furthermore, phagocytes might facilitate OPC recruitment by the expression of matrix metalloproteinases, which degrade the extracellular matrix components and chondroitin sulfate proteoglycans, that were reported to be inhibitors of OPC migration and differentiation (Lloyd and Miron, 2019; Pu et al., 2018).

It has been shown, both in toxin-mediated and immune-mediated demyelination models, that phagocytes which are present in the early stages of lesion formation are characterized by a pro-inflammatory phenotype, with predominance of inducible nitric oxidase synthase (iNOS) positive cells, and that this phenotype is shifted to a more anti-

inflammatory one at later stages of lesion progression, at the start of remyelination / lesion resolution, with the predominance of arginase-1 (Arg-1) marker (Locatelli et al., 2018; Miron et al., 2013). The presence of these different phenotypes throughout the course of demyelinating lesions has been further reported both in animal models, as well as in human MS lesions (Hammond et al., 2019; Voss et al., 2012). Furthermore, this shift in phagocyte phenotypes has been shown to play a major role in promoting oligodendrocyte differentiation, without which remyelination was impaired (Miron et al., 2013; Sun et al., 2017). In this way, the evidence reported so far suggests that phagocytes secrete factors essential for the different phases of remyelination, which correlate with the phenotype acquired during each phase. This together with their major role in the phagocytosis of myelin debris seem to comprise the main functions of the innate immune cells during remyelination (Fig. 1.6).

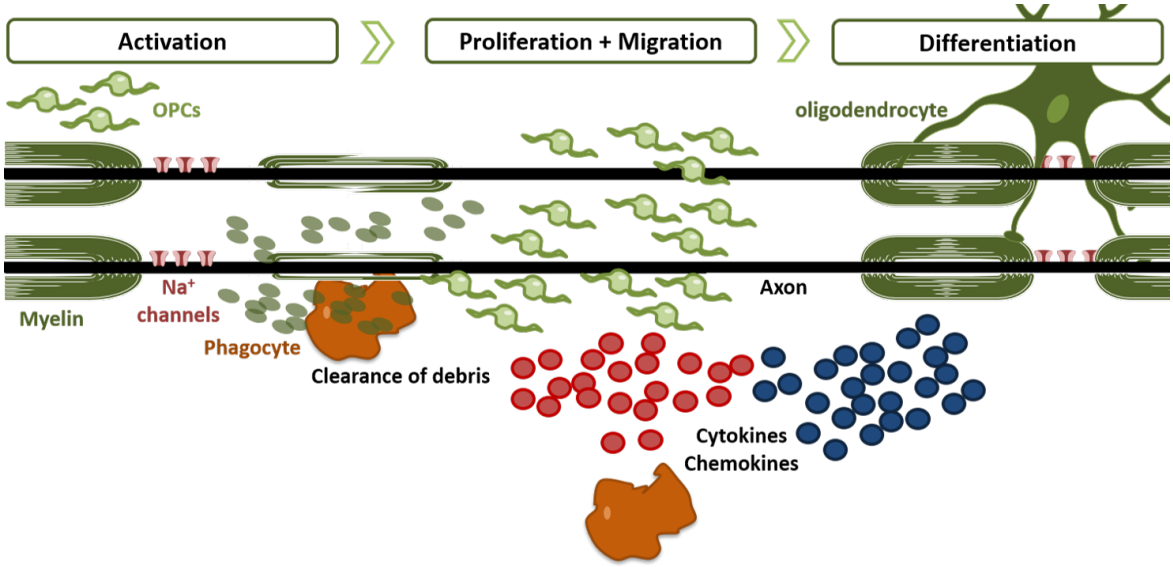

Figure 1.6 Schematic representation of the role of CNS phagocytes in remyelination. Following a demyelinating insult, OPCs shift from a quiescent state to an activated state, in which they start to proliferate and migrate to the site of injury, where they differentiate into mature myelinating oligodendrocytes that remyelinate the axon. This process is mediated by phagocytes that become activated and clear the myelin debris from the injury site, which are inhibitory for the differentiation of mature oligodendrocytes and subsequent remyelination, and also release a range of cytokines and chemokines important for the different steps of the remyelination process.

This favorable and critical role of the innate immune-mediated inflammation in remyelination is also seen in other different regeneration processes, where depletion of macrophages in different models has led to impaired tissue regeneration (Godwin et al., 2013; Mirza et al., 2009).

1.5. Autoimmune / inflammatory demyelinating disorders of the CNS

Demyelinating disorders of the CNS can have causes intrinsic to the oligodendrocytes, such as inherited white matter leukodystrophies, or extrinsic to oligodendrocytes, namely in their inflammatory environment. Here we focus on the latter, of which the inflammatory demyelinating diseases of the CNS include acute disseminated encephalomyelitis, neuromyelitis optica disorders (NMOSD) and multiple sclerosis (MS), the latter being the most common inflammatory demyelinating disease of the CNS.

1.5.1. Multiple Sclerosis

MS affects approximately 2.5 million people worldwide. It is the leading cause of non-traumatic neurological disability in young adults with age between 20-40 years old, affecting around 2.3 to 3.5 times more women than men (Harbo et al., 2013; Simone et al., 2000). For an unknown reason, it seems to be most prevalent in Nordic countries and in more temperate climates (Wade, 2014). Usually the disease starts with a pattern of relapsing and remitting episodes (relapsing remitting MS - RRMS) and in about 10-20 years, it develops to a progressive course (secondary progressive MS - SPMS). However, it can also develop as a continuum of worsening disability from the onset of symptoms, without previous relapses or remissions (primary progressive MS - PPMS) (Dobson and Giovannoni, 2019). MS has a broad spectrum of symptoms, common to a myriad of other diseases, therefore the diagnosis is usually not straightforward from the beginning. Symptoms usually include monocular visual loss, ataxia, limb weakness, sensory loss, fatigue, pain and spasms, among others (Filippi et al., 2018). The genetic component of MS can only explain very little of its cause. In fact, monozygotic twins have only around 30% concordance in disease development, implying a significant role for environmental risk factors in disease susceptibility (Willer et al., 2003). Nonetheless, a recent large-scale meta-analysis of MS genetic data has identified more than 200 variants which are associated significantly with MS susceptibility. They report an enrichment of MS related genes in the peripheral innate and adaptive immune system, as well as in the CNS resident innate immune cells, microglia (Gao, 2019).

The characteristic pathology of MS is the presence of multifocal lesions which can be spread both in space, throughout the CNS (in the white and gray matter of the brain and spinal cord), and in time (Reich et al., 2018). The main pathological hallmark of MS is demyelination, with lesions being characterized by loss of myelin and oligodendrocytes. Neuroaxonal loss, as well as brain atrophy, seems to be secondary, occurring gradually

with disease progression (Dendrou et al., 2015). In MS both demyelination and remyelination processes are concurrent. Complete remyelination is reported to occur in lesions of MS patients (termed shadow plaques); however its efficiency decreases with the progression of the disease (Bruck et al., 2003; Lassmann et al., 1997). Another hallmark of MS, besides demyelination, is the infiltration of peripheral innate and adaptive immune cells into the CNS, as monocyte-derived macrophages, autoreactive T cells and B cells (Filippi et al., 2018). However, it seems that peripheral infiltration fades away at later stages of the disease independently of therapy, while a CNS-intrinsic chronic inflammatory process is driven by cells that have become or are CNS resident, by producing neurotoxic inflammatory mediators (cytokines, chemokines and ROS), which can sustain and fuel neuroaxonal damage (Fig. 1.7) (Dendrou et al., 2015; Friese and Fugger, 2007; Kutzelnigg et al., 2005; Rasmussen et al., 2007).

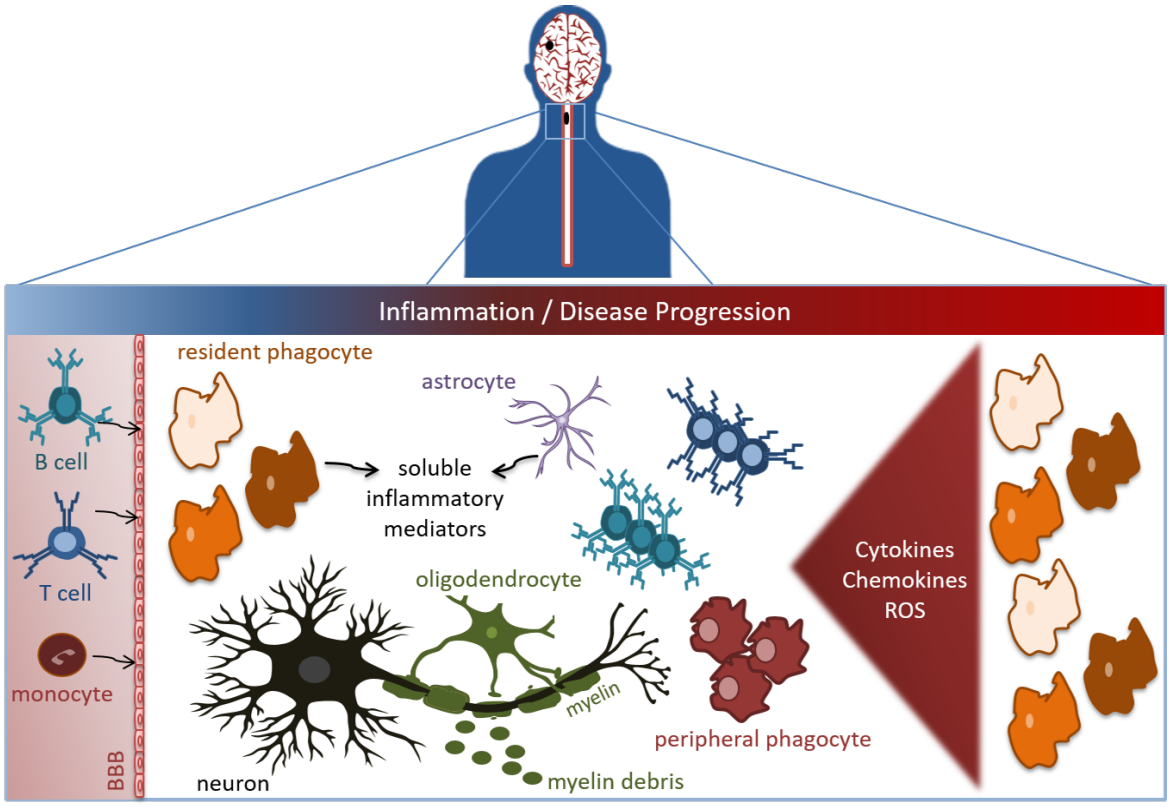

Figure 1.7 Schematic representation of an inflammatory-mediated demyelinating lesion, with main focus on the role of phagocytes. Clusters of activated CNS phagocytes can be found in normal appearing white matter, in early stages of disease. Peripheral immune cell infiltration is present in active lesions, characterized by the extravasation of autoreactive T and B cells and monocytes through the blood-brain barrier (BBB), and seems to dissipate at later stages of the demyelinating lesion. Astrocytes, together with activated phagocytes, can fuel the inflammatory process with the release of soluble inflammatory mediators. In later stages of disease progression, chronic active lesions seem to be sustained by persistent activation of CNS resident immune cells. Adapted from (Dendrou et al., 2015).

Even in what appears to be normal-appearing white matter (NAWM), in early stages of the disease, phagocyte numbers and activation are increased, together with reduction of myelin and axonal pathology (Beer et al., 2016; Friese and Fugger, 2007; van Horssen et al., 2012). Lesion evolution in MS is characterized by a series of phagocyte activation and demyelination events which can extend over months to years, and range from pre-phagocytic to inactive lesions (Stadelmann et al., 2019). Briefly, lesions are reported to evolve from a pre-phagocytic stage, where pathology of oligodendrocytes (presenting condensed nuclei) and myelin loss starts, and there is the presence of activated phagocytes. It then proceeds to an active demyelinating lesion, where there is massive infiltration of foamy phagocytes together with active phagocytosis of myelin, infiltration of peripheral lymphocytes, as well as a slight reduction on OPCs density, whereas the density of oligodendrocytes seems to be close to normal (Bruck et al., 1994; Cui et al., 2013; Grajchen et al., 2018). After, lesions may become chronic active or smoldering. These lesions are characterized by slow expansion, a rim of activated and foamy phagocytes with ingested myelin products, axonal pathology, as well as active demyelination in the peripheral rim, opposite to a cellular inactive center (Filippi et al., 2018). Smoldering lesions have been found more often in patients with progressive disease, rather than in patients with acute or relapsing-remitting disease, and correlate with incomplete remyelination (Bramow et al., 2010). The final stage of lesion evolution is called inactive lesion. Here, the lesions are characterized by a lack of cellularity (mature oligodendrocytes, phagocytes and OPCs), few myelin sheaths and no signs of myelin phagocytosis, as well as variable severity of axonal reduction, with the remaining ones being surrounded by astrocyte processes which form a glial scar (Stadelmann et al., 2019).

Despite the hundreds of years of research, there is still no cure, or even highly efficient treatment, for inflammatory demyelinating diseases. In order to preserve axonal integrity and avoid neurodegeneration, which ultimately lead to the irreversible neurological disability seen in patients, strategies to promote remyelination seem to comprise the ultimate therapeutic goal.

1.6. Current therapies for enhanced remyelination

Even though remyelination occurs in patients with demyelinating diseases, such MS, it is often incomplete and eventually fails with disease progression. This failure is thought to be mostly due to impairment of oligodendrocyte differentiation, mainly because around 70% of demyelinated MS lesions have been found in pathological studies to have rather immature oligodendrocytes over terminally differentiated mature cells (Kuhlmann et al., 2008; Lucchinetti et al., 1999). Based on the knowledge gathered from the research in demyelinating injuries so far, strategies to promote remyelination consist mainly of fostering myelin debris clearance, increasing the number of OPCs, as well as promoting their differentiation (Wooliscroft et al., 2019). For instance, oligodendrocyte differentiation has been shown to be negatively regulated by LINGO-1, one component of the Nogo receptor, of which mice treated with antibody against LINGO-1 or completely LINGO-1 deficient mice, have been reported to have increased remyelination in animal models of demyelination (Mi et al., 2007; Zhang et al., 2015). Following these discoveries, an antibody targeting LINGO-1, opicinumab, has been the first therapy targeting directly remyelination, to reach phase I of clinical trials and is being currently evaluated (Kremer et al., 2019; Ruggieri et al., 2017).

On the other hand, some of the immunomodulatory therapies currently available include the first main drugs in the treatment for MS, the interferon-β therapies, which dampen inflammation through suppression of T cell activation and a shift to anti-inflammatory cytokine production; fingolimod, which keeps lymphocytes in the lymph nodes, thereby preventing the infiltration of autoreactive lymphocytes into the CNS; as well as the monoclonal antibodies rituximab and ocrelizumab, which lead to depletion of circulating B cells by targeting the surface-expressed CD20 molecule, and natalizumab, which prevents leukocyte trafficking inside the CNS, by acting as an antagonist of the α4 integrin present in the surface of lymphocytes, monocytes and eosinophils (Brandstadter and Katz Sand, 2017; Jakimovski et al., 2018; Scott, 2011; Yamout et al., 2018).

However, both the currently in use, or under development, remyelination-directed therapy and the immunomodulatory therapies, the latter focusing mainly on inhibiting the adaptive immune response and impairing leukocyte trafficking through the brain-blood barrier (BBB), seem to only be successful in reducing relapse rates in MS, however fall short of halting long-term disease progression. This implies that we might have to re-evaluate our therapeutic targets and further understand the molecular mechanisms driving remyelination failure.

1.7. Models of de- and remyelination

Although still no model fully recapitulates a chronic inflammatory demyelinating disease, like MS, there are several models that together have shed light onto the mechanisms of de- and remyelination and from which currently therapies have emerged.

1.7.1. Autoimmune / inflammatory models

1.7.1.1. Experimental autoimmune encephalomyelitis (EAE)

EAE mimics some of the pathological events occurring in MS, as infiltration of peripheral immune cells into the CNS, demyelination, gliosis and axonal loss. It is induced by an active immunization with myelin antigens (MBP - myelin basic protein, PLP - proteolipid protein, MOG - myelin oligodendrocyte glycoprotein) given together with a bacterial adjuvant (complete Freund's adjuvant) in order to boost the activation of the peripheral immune system, by priming of myelin-specific autoreactive T cells (Glatigny and Bettelli, 2018). It generally follows a predictable relapsing-remitting course, leading to an ascending paralysis from hind to fore-limbs (Robinson et al., 2014). However, depending on the animal strain and antigen used, the animals might develop different disease processes. Major drawbacks of this model are the concurrent demyelination and remyelination processes, the complex ongoing inflammatory pathogenesis and the fact that the localization of the lesions is not possible to be predicted, which make it difficult to study independently the mechanisms of remyelination.

1.7.2. Chemical lesion models

The toxin-induced models of demyelination represent a good alternative for studying discrete demyelination and remyelination processes in the absence of a primary adaptive immune response. These can be administered systemically, as the cuprizone model, or focally, as the ethidium bromide and lysolecithin models.

1.7.2.1. Cuprizone

In the cuprizone model, young mice (8-10 weeks age) are fed for up to 6 weeks with a diet containing 0.2-0.3% of the copper chelator cuprizone. This results in progressive

demyelination through specific death of oligodendrocytes, possibly as a result of mitochondrial dysfunction (Faizi et al., 2016). Mice fed with cuprizone present patterns of demyelination in the corpus callosum, superior cerebellar peduncles and in the cortex, as well as axonal loss and activation of both astrocytes and phagocytes (Gudi et al., 2014; Torkildsen et al., 2008). In this model, the BBB remains intact and T-cell activation is mostly absent, opposite of what happens in MS and in the EAE model. The course of demyelination is complete around 5 weeks after the start of cuprizone diet and remyelination can be observed as early as 4 days after cuprizone withdrawal. However, a caveat of this model is, for instance, that the toxicity of cuprizone is dependent on the amount of food intake, which can vary per mice thereby leading to very high variability in the results obtained.

1.7.2.2. Ethidium bromide

Together with the lysolecithin model, the injection of ethidium bromide into the CNS white-matter corresponds to a model of focal demyelinating lesion, representing good models for the study of isolated processes of remyelination, where the localization and timing of the lesion are well known. This model has been widely used in the rat spinal cord as model of demyelination and is mainly characterized by loss of both oligodendrocytes and astrocytes, while axons seem to remain mainly intact (Bammens et al., 2014). Here, inflammation is resolved by 3-4 weeks. However, the mode of action of the ethidium bromide is thought to be through its DNA intercalating properties, making it non-specific to myelinating cells but rather to all nucleated cell types located in the site of injection (Bjelobaba et al., 2018; Blakemore and Franklin, 2008).

1.7.2.3. Lysolecithin

Lysolecithin promotes especially damage to myelinating cells. In comparison, it mostly spares the other cell types, and lesions remyelinate faster, when compared to the ethidium bromide model (Woodruff and Franklin, 1999). Lysolecithin (L-α-Lysophosphatidylcholine) is a membrane-dissolving toxin. Usually, it is focally injected as a 1% solution in the white matter of rodents, most frequently in the spinal cord and the corpus callosum, but also in other areas, as the optic nerve or the caudal cerebellar peduncle (Blakemore and Franklin, 2008; Hall, 1972). The injection of lysolecithin in the white matter tracts, leads to a rapid loss of myelin and great part of the mature oligodendrocytes, together with massive influx of phagocytes, leading to a demyelination process which extends through the first 4 days

after injection (Cantuti-Castelvetri et al., 2018). In lysolecithin-induced demyelinating lesions there is also some degree of axonal loss (Woodruff and Franklin, 1999). Typically, remyelination occurs spontaneously between 7 and 21 days after injection; between 3 and 7 days there is OPC recruitment; and from 7 to 10 days there is oligodendrocyte differentiation, with remyelination being maximal between 14 to 21 days after injection (Keough et al., 2015; Miron et al., 2013).

Besides its *in vivo* application, lysolecithin-mediated demyelination has also been adapted to *ex vivo* organotypic slice cultures (OSC). OSC represent a rather simple model to study CNS biological mechanisms, where the 3D cytoarchitecture of the tissue is kept, together with intercellular connectivity. Cerebellar slices have been used for investigating mechanisms of myelination, demyelination and remyelination, with the advantages of keeping all the different stages of both oligodendrocyte maturation and axon myelination, since cerebellar slice cultures are prepared when the majority of axons are still not myelinated, while preserving an active neuronal network, resembling the *in vivo* conditions (Doussau et al., 2017). Organotypic cerebellar slice cultures (OCSC) are prepared from mouse pups, postnatal day 8-12. When the slices are put in culture, myelination occurs in the first 7 days *in vitro* (DIV) (Birgbauer et al., 2004; Thetiot et al., 2019). After myelination is complete, lysolecithin was shown to be able to induce reproducible demyelination when added to OCSC for a period of 15-16h, with damage of the myelin structure, observed by a punctate immunostaining for myelin components, as MBP, MOG and PLP, instead of a rather even staining occurring in the absence of the toxin, and eventually an almost complete loss of myelin proteins immunostaining, albeit with preserved axonal integrity (Birgbauer et al., 2004; Thetiot et al., 2019). Spontaneous remyelination was shown to occur, with recovery of MBP, MOG and PLP markers immunostaining, starting as soon as 2 days after lysolecithin treatment and with detection of fully remyelinated slices 6 days after treatment (Birgbauer et al., 2004; Thetiot et al., 2019).

1.7.3. Zebrafish transgenic models

Zebrafish (*Danio rerio*) myelination mechanisms are considered representative of vertebrate myelination, with myelin structure and myelin-related gene expression being very much conserved between zebrafish and mammals (Czopka, 2016; Fang et al., 2014). This animal model brings a lot of advantages in comparison to rodents. For instance, they are of easy maintenance, produce in very short time at least hundreds of progeny in a single mating per week, allowing for large-scale rapid genetic and chemical screens (Vacaru et al., 2014). These organisms undergo external fertilization and the transparent embryos are

of fast development. In addition, the optically transparent larvae allow for high-resolution live imaging experiments in a quite straightforward way. Furthermore, they represent a quite useful, fast and not so challenging models for genetic engineering (Preston and Macklin, 2015). To date, there are numerous reporter lines available to study the most diverse biological mechanisms, including myelination and innate immune responses (Auer et al., 2018; Czopka and Lyons, 2011; Djannatian et al., 2019; Early et al., 2018; Mazzolini et al., 2020; Novoa and Figueras, 2012; Oosterhof et al., 2018; Tsarouchas et al., 2018). Up to two-weeks post fertilization, the zebrafish larvae exhibit almost no markers of adaptive immunity, being also a very good model to study specifically innate immune mechanisms (Lam et al., 2004). In fact, a lot of insight into the mechanisms of the CNS immune cells, microglia, has been gained from studies in zebrafish larvae (Mazaheri et al., 2014; Peri and Nusslein-Volhard, 2008; Villani et al., 2019).

However, there are not many zebrafish models of de- and remyelination available to study remyelination mechanisms *in vivo*. In 2013, the first transgenic model of remyelination in zebrafish was generated. In this model, the bacterial nitroreductase enzyme (NTR) was expressed specifically in the oligodendrocytes, under the control of the *mbp* or *sox10* promoter. When the drug metronidazole (MTZ) was added to the medium containing the transgenic larvae, NTR converted it into a cytotoxic DNA-cross linking agent leading to rapid ablation of around 2/3 of oligodendrocytes and consequent demyelination, within 48h of treatment. Remyelination with recovery of myelination and oligodendrocytes is said to occur 7 - 16 days after withdrawn of the drug (Chung et al., 2013; Karttunen et al., 2017). In this model, the innate immune response, orchestrated by macrophages labeled by the reporter line Tg(mpeg1:eGFP), was observed to peak at 4 days after MTZ treatment, with macrophages observed to contain myelin debris inside, and to progressively fade away in the consecutive days (Karttunen et al., 2017). However, a not so appealing feature of this model for the study of the role of inflammatory cells in remyelination, is the very modest inflammatory response that is instigated and also the fact that complete depletion of the oligodendrocyte population is not a characteristic of demyelinating diseases.

1.8. Significance of the study and global aims

A better understanding of the molecular mechanisms determining remyelination success or failure is required, in order to enable the design of efficient therapeutic strategies aiming at promoting long-term regeneration and stop relentless demyelinating disease progression. For this and taking into account the already reported evidence of the major role that phagocytes play in remyelination, further unravelling of the role of the innate immune system in myelin damage and repair is needed.

In this study, the major aim was to understand how pro-inflammatory phagocyte activation influences the course of a demyelinating lesion, namely:

- In phagocyte influx to and efflux from the lesion site
- In phagocyte clearance ability of myelin debris (both uptake and digestion)
- The direct impact in OPCs recruitment, survival and differentiation

To address these questions, our experimental strategy was to generate both under-activated and overactivated phagocytes, in the context of a lysolecithin-induced focal demyelinating lesion.

The under-activated model consisted in a global Myd88 KO of both zebrafish larvae and mice, in which we have performed lysolecithin injections in the spinal cord. Here we have also used mice organotypic cerebellar slice cultures, upon treatment with lysolecithin.

The over-activated model consisted in phagocyte-specific Myd88-constitutively active transgenic zebrafish (Tg(mpeg1:myd88-L265P)^{fh507}), in which we have injected lysolecithin in the spinal cord, and a phagocyte-specific A20-depleted mice (A20$^{flox/flox}$CX3CR1$^{CreERT2/wt}$), in which we have injected lysolecithin in the corpus callosum.

2. Materials and Methods

Part of the materials and methods section here described was published in the manuscript Cunha et al., *J Exp Med* (2020) 217 (5): e20191390.

2.1. Zebrafish husbandry

Zebrafish were kept under standard conditions at the DZNE fish facility, in Munich, and handled according to local animal welfare regulations. Zebrafish to be raised were kept in 3.5L tanks with constant water flow and water temperature of ~28°C, pH ~7.6 and conductivity ~300µS. The light cycle was 12h light/ 12 h dark (with half-hour of light deeming in the morning and in the evening). Adult zebrafish were transferred to individual breeding boxes overnight for mating until next day, when the eggs were collected and transferred to petri dishes. Fertilized eggs were raised at 28.5°C in E3 medium. When the fish were to be raised to adults, 1dpf embryos were sorted by viability and bleached in clutches of 30. After bleaching, pronase was added to the fresh E3 medium in order to facilitate the hatching. At 5dpf, larvae were transferred to 3.5 l tanks and started to be fed, with both powder food and artemia. 1-Phenyl-2-thiourea (PTU, Sigma) was added to the petri dish at 1 dpf when the larvae were to be used in experiments, in order to prevent pigmentation. At 5dpf, larvae were kept in 300ml E3 medium, at 28.5°C, and started to be given powder food, everyday once until the experiment was finished. Fish lines used in this work are indicated in Table 2.1.

2.2. Mouse husbandry

Mice were handled according to local animal welfare regulations and kept under standard conditions at the DZNE mouse facility, in Munich. Mice were housed in GreenLine IVC GM500 cages enriched with woodchips and a red house. The cages were kept in a ventilated rack system, inside rooms with temperature at 20°C-22°C, 45% to 65% relative humidity and a light cycle of 12h light/ 12h dark (with half-hour of light deeming in the morning and in the evening).

2.3. Zebrafish genotyping

Whole larvae and fin clips from adult zebrafish were lysed at 55°C with Proteinase K (17mg/ml) and Tris-EDTA buffer, for 4hrs. Inactivation of Proteinase K was done at 65°C for 5min. Next, amplification of the genomic DNA was performed using the primers specified in Table 2.2 and the product digested with the appropriate restriction enzymes for 2hrs (see Table 2.3). PCR products, both undigested and digested, were loaded in a 2% agarose gel, and electrophoresis was performed for 50min at 180 V. Gel scanning was performed in a BioRad Gel Doc XR+ system.

2.4. Lysolecithin injection in the spinal cord of zebrafish larvae

Larvae at 6dpf were anesthetized in E3 medium by adding tricaine (MS-222, Pharmaq Limited) and placed one by one in an agarose mold. After, the majority of the medium was removed, and larvae were placed laterally to the injection setup. Using a microscope and a Nanoliter 2010 + Micro4 Controller injection setup, larvae were injected in the anterior part of the spinal cord, with a glass needle (World Precision Instruments, 504949) previously pulled by a DMZ-Universal puller. Needle preparation was as follows: the glass needle was completely filled with mineral oil; after, 2000nl of the oil were discarded and 500nl of air were pulled inside the needle; next, 900nl of lysolecithin (L-alfa-Lysophosphatidylcholine from egg yolk, Sigma) in PBS were withdrawn. The injections were performed at a rate of 23nl/sec. After injection, larvae were put in 300ml of fresh E3 medium, fed with powder food and left at 28.5°C for the remaining time of the experiment (Fig 2.1).

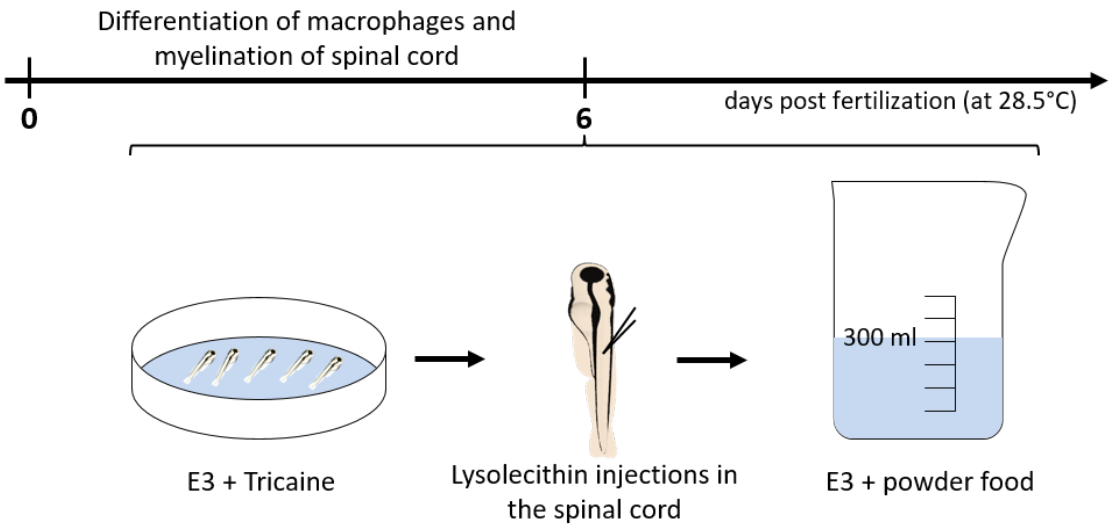

Figure 2.1 Schematic representation of the injection protocol for zebrafish larvae.

2.5. *In vivo* confocal imaging of zebrafish larvae

For *in* vivo confocal live imaging, larvae were immersed in E3 medium with tricaine in order to become anesthetized. After, larvae were positioned laterally in 0.8% low melting agarose, placed in a glass bottom dish filled with the anesthetic solution (tricaine in E3 medium). Mounted larvae were imaged using a Leica TCS SP8 confocal laser scanning microscope coupled with a climate chamber (set to 28.5°C), with a 20× air or 40× water immersion objectives and 488 nm and 552 nm lasers. For lysosomal quantification, 10 μM LysoTracker® Red DND-99 dye was added to E3 medium containing the larvae, in a 24-well plate. The plates were incubated at 28.5°C, for 1 h 30 in the dark. After, the larvae were washed with fresh E3 medium 4 times. After imaging, larvae were taken out of the mounting agarose and sacrificed. In case imaged larvae resulted from heterozygous in crosses, they were at this point lysed and genotyped.

2.6. Image analysis of live imaging experiments in zebrafish

Quantification of myelination, phagocyte infiltration and axons, was determined using Fiji software by measuring the total amount of mbp:mCherry-CAAX, mpeg1:eGFP or cnt1b:mCherry positive pixels, respectively, using maximum intensity projections and assessing in a predefined region of interest (ROI). Huang method was the threshold used for these quantifications and the final result corresponds to the percentage of the signal by the total ROI measured. NF-κB activation in phagocytes was quantified using the 3D surpass view of the software Imaris, through manually thresholding the NF-κB and phagocyte channel in every image and generating surfaces of both NF-κB signal and phagocytes. The determination of the percentage of co-localized NF-κB surface per total amount of phagocytes was performed using the plugin Surface-Surface Coloc of Imaris. This method was also used for the quantification of myelin and lysosomes in the phagocytes. The number of mature oligodendrocytes was quantified by counting manually in the dorsal spinal cord, the amount of mbp:nls-eGFP positive objects in maximum intensity projections. The number of OPCs was determined by counting manually in the dorsal spinal cord, the number of olig1:nls-mApple positive objects, in maximum intensity projections. The threshold method used was IJ-IsoData method.

2.7. Quantitative RT-PCR of zebrafish larvae lesions

One hundred lesions were collected per genotype and immediately snap-frozen in dry ice, for determination of gene expression. RNeasy Mini Kit (Quiagen) was used to extract and isolate RNA, according to the QIAshredder dissociation protocol available. SuperScript III First-Strand Synthesis system (Thermofisher) was used to obtain cDNA. Roche LightCycler®480 Instrument II Real Time PCR system was used to perform qPCR, using PowerUP SYBR Green Master Mix (Thermofisher). Normalization of gene expression was performed using the housekeeping gene *elf1a* and determination of relative fold gene expression was done using the $\Delta\Delta$Ct method. Each sample was run in triplicate and the experiment performed three times. Primers used are indicated in Table 2.2.

2.8. Microinjection of zebrafish eggs

Site-directed zebrafish transgenesis using phiC31 integrase system was performed as previously described (Mosimann et al., 2013). Embryos from an in-cross of Tg(phiC31.attP.2B, -0.8cmlc2:eGFP) and TLF were injected with 1nl injection mix of plasmid DNA (mpeg1:cas9/CY) and phiC31 integrase mRNA, at one-cell stage. The injection mix was prepared right before injection and contained: 1.5µl of mpeg1:cas9/CY DNA plasmid (449.4 ng/µl), 1.5µl of phiC31 integrase mRNA (888.75 ng/µl) and 23µl of nuclease-free water. The F0 generation was then outcrossed to wild-type fish and the progeny was assessed for stable integration and germline transmission of the mpeg1:cas/CY plasmid.

2.9. Intraperitoneal injection of tamoxifen for inducible, conditional KO mice

8 weeks old mice were injected intraperitoneally with 100µl of 10 mg/ml tamoxifen once every 24h for 5 consecutive days. Tamoxifen was prepared accordingly to The Jackson Laboratory recommendations. Briefly, tamoxifen was dissolved in corn oil to 10mg/ml in a tube wrapped in aluminium foil, at 37°C shaking overnight. The day after and until further use, tamoxifen was kept in the dark at 4°C. Mice were monitored and weighted every day, during the injections period. For assessment of successful Cre/loxP recombination and gene knockout, microglia were isolated 5 weeks after tamoxifen injection (time point when lesions were analyzed).

2.10. Stereotactic injection of lysolecithin in the corpus callosum of mice

10 weeks old mice were anesthetized intraperitoneally with a mixture of Medetomidin 0.5mg/kg, Midazolam 5.0mg/kg, Fentanyl 0.05mg/kg (MMF), accordingly to the weight of the mice. After exposing the skull, the coordinates were defined relative to bregma: ± 1mm (X), - 0.1mm (Y), - 1.38mm (Z). A hole was drilled in those coordinates until reaching the brain, without damaging it. 1% Lysolecithin (L-alfa-Lysophosphatidylcholine from egg yolk, Sigma) in PBS was warmed to 37°C and briefly sonicated. 1% Monastral Blue 3% solution filtered and autoclaved was added to the lysolecithin solution in order to track the lesion site. The injections were performed using a Nanoliter 2010 + Micro4 Controller injection setup, set to inject 1µl of Lysolecithin at a rate of 100 nl/min. The needle was only withdrawn 2min after the injection finished, to avoid reflux. 0.05 -0.1mg/kg of the analgesic Buprenorphine was injected subcutaneously right after surgery. The skin was sutured and a mixture of Atipamezole 2.5mg/kg, Flumazenil 0.5mg/kg, Naloxone 1.2mg/kg (AFN) was injected subcutaneously as an antagonist of the anesthesia, for the mice to wake up. Mice were placed in a 37°C chamber for initial recovery until they wake up.

2.11. Mice tissue preparation for histology

Mice at the appropriate stage of the experiment were anesthetized intraperitoneally with MMF and tissues were fixed by transcardial perfusion with 4% PFA in PBS, after washing out the blood with ice cold PBS. The brain was isolated and placed immediately in 4% PFA at 4°C overnight. The day after, the brain was rinsed twice with PBS and placed on a 30% sucrose solution in PBS, for two overnights at 4°C. When the brain was completely sunk in the sucrose solution, it was transferred to a plastic cube filled with Optimal Cutting Temperature compound (OCT). The cube was then transferred to a metal bucket filled with isopentane, placed in dry ice, until the OCT froze completely. After, the cube was wrapped in aluminium foil and parafilm and stored at -80°C until further processing. Prior to sectioning, the brains embedded in OCT were transferred to -20°C for 1h. Then, frozen sections of 20µm thickness were coronally cut in a cryostat and mounted on SuperFrost™ Plus Microscope Slides (Thermo Scientific). The slides were stored at -20°C until further processing.

2.12. Immunohistochemistry (IHC)

For IHC, slides were first incubated at 37°C to dry, followed by 3x 10min wash with PBS, at room temperature. After, sections were permeabilized with 0.3% Triton 100X in PBS, for 10min, followed by 3x 5min wash with PBS, Then, sections were circled with an hydrophobic marker and incubated with 1X blocking solution (4X: 2.5% fetal calf serum, 2.5% bovine serum albumin, 2.5% fish gelatin, PBS), for 1h at room temperature. The sections were washed 3x 10min in PBS for 10min and incubated with primary antibody (Iba1 rabbit, Wako 019-19741 – 1:1000), diluted in staining solution (1:4 of 1X blocking solution, in PBS) overnight, at 4°C. the day after, the slides were placed at room temperature for 1h, followed by 3x 10min wash with PBS. The sections were then incubated with secondary antibody (Alexa 555 goat anti-rabbit, Thermofisher Scientific A-21428, 1:500), diluted in staining solution, for 2h, at room temperature. The sections were washed 3x 10min with PBS, for 10min and incubated with FluoroMyelin™ Green Fluorescent Myelin Stain (Thermofisher Scientific F34651, 1:350 in PBS) for 20min, at room temperature. The sections were washed again 3x 10min with PBS, mounted with mowiol mounting medium and left to dry before imaging overnight, at room temperature.

2.13. Fluorescent *in situ* hybridization

Fluorescent *in situ* hybridization for detection of TNF-α mRNA was performed with the commercially available RNAscope® Multiplex Fluorescent Reagent Kit (v2) (Advanced Cell Diagnostics, Inc.), accordingly to instructions of the manufacturer. Coronal tissue sections of 12μM, containing the lesions, were mounted in SuperFrost Plus slides (Thermo Scientific) followed by treatment with hydrogen peroxide and target retrieval. The sections were then treated with Protease III at 40°C, for 30min. Next, probe hybridization (TNF-α probe 1:50) was achieved at 40°C, for 2h, followed by signal amplification and washing steps. Development of fluorescent in situ hybridization signals was performed using the Opal 570 fluorophore (1:2000), followed by counterstaining with DAPI for 30sec at room temperature. The slides were then mounted with ProLong Gold Antifade Mountant. Assay success and RNA integrity were checked with a specific probe targeting the housekeeping gene cyclophilin B (PPIB). Assessment of the background staining (negative control) was performed with a probe specific to the bacterial gene dapB. Imaging was done with a Leica TCS SP8 confocal laser scanning microscope, with 40× water immersion objective and 405nm and 552nm lasers.

2.14. Organotypic cerebellar slice culture and demyelination

All steps were performed under sterile conditions, with tools being sterilized by UV irradiation prior to use. Postnatal day (P) 8-9 mouse pups *Myd88* $^{-/-}$ or C57BL/6J (WT) were decapitated using scissors, with one clean cut. Followed brain dissection, the cerebellum was placed in ice-cold HBSS (with calcium and magnesium). The cerebella were cut into 300µm sagittal slices with the McIlwain Tissue Chopper and rapidly placed in ice-cold dissection media (15mM HEPES (Gibco), 1× HBSS with calcium and magnesium (Gibco), 0.57% Glucose 45% (Sigma)). The slices were separated and placed, up to 3, in one insert. Previously prepared 6-well plates containing 0.4µM, 30mm diameter cell culture inserts and 1 ml slice culture media (5% BME with Earle's salts, 1× GlutaMAX™ 100× (Gibco), 50% MEM 10× no glutamine and with Earle's salts, 0.5% Penicillin/Streptomycin, 0.648% Glucose 45%, 25% Horse serum, 7.5% $NaHCO_3$ for pH adjust to ~7.2 and autoclaved deionized water), were placed for at least 2h in the incubator (37°C, 5% CO_2), before placing the slices, in order to oxygenate the media and for acclimatization of the insert membranes. Slice culture media was changed right the day after the culture was done and, after that, every 3 days. Slice culture demyelination using lysolecithin, was performed as previously published (Thetiot et al., 2019). After 7DIV, the cerebellar slices were transferred to fresh media containing 0.5mg/ml lysolecithin (L-alfa-Lysophosphatidylcholine from egg yolk, Sigma) in PBS, and placed in the incubator for 16h. Fixation of the slices was performed with 4% paraformaldehyde (PFA), after being washed with PBS.

2.15. Image analysis of mouse lesions and slice culture experiments

ImageJ/Fiji software was used for automated TNF-α mRNA quantification in mice lesions, by using manually thresholded maximum intensity projections and quantifying the total area occupied by positive pixels, in the whole field of view. The same method was applied for the quantification of $BCAS1^+$ cells in the slice culture experiments, but the quantification here was restricted to and normalized to the total area of the cerebellar slice. Quantification of the lesion volume and phagocyte infiltration volume, in mice corpus callosum lesions, was done by calculating the volume of negative FluoroMyelin and positive IBA1 staining, respectively, throughout the lesion, as published previously by the lab (Cantuti-Castelvetri et al., 2018). Briefly, areas of the respective lesion staining were measured using Fiji software and volume was calculated using the truncated cone formula:

$$V = \sum_{i=1}^{n-1} \frac{1}{3}\pi(r_i^2 + r_{i+1}^2 + r_i r_{i+1})d$$

, where *n* equals to the number of sections, *r* corresponds to the radius of the lesion area and *d* equals the distance of consecutive sections.

2.16. Scanning Electron Microscopy

Zebrafish larvae were fixed in a solution of 2.5% glutaraldehyde (EM grade, Science Services), 2 mM calcium chloride in 0.05M sodium cacodylate buffer (pH 7.4) placed in a microwave (BioWave, Pelco 100W, 450W, 5 cycles). After, they were incubated at 4°C for 24-48h (Czopka and Lyons, 2011). The spinal cord of 7-8 weeks old mice was dissected and fixed by brief immersion in 2% PFA (EM grade, Science Services), 2.5% glutaraldehyde, 2mM calcium chloride in 0.1M sodium cacodylate buffer (pH 7.4). After, the samples were mounted in 20% gelatin for vibratome sectioning in 0.1M PBS and further fixed for 24-48h at 4°C. Both fish and mouse tissue were post fixed in a solution of 2 % osmium tetroxide (Science Services), 2mM calcium chloride in 0.1M (mouse) and 0.05M (fish) sodium cacodylate and after placed in 2.5% potassium hexacyanoferrate (Sigma) as a reducing step. After thiocarbohydrazide (1% in water, Sigma) incubation, the tissue samples were contrasted by a solution of 2% aqueous osmium and incubation in uranylacetate (1%, EMS), overnight, dehydrated at increasing concentrations of ethanol and finally embedded in LX112. For imaging, tissue was sectioned in 100 nm thin sections (Leica UC7 ultramicrotome) which were adsorbed onto carbon nanotube tape strips (Science Services) (Kubota et al., 2018). The relocation of zebrafish larvae spinal cord lesions was done according to anatomical landmarks. The embedded tissue was trimmed in 50µm sections and the screening of the lesion site was done in ultrathin sections. Imaging of the spinal cord samples was done on a Crossbeam 340 (Zeiss), with images taken at 10 ×10 ×100nm. Image analysis was performed using ImageJ/TrackEM2 software (Cardona et al., 2012).

2.17. Statistics

Statistics are specified in each figure legend, according to experiments and were performed using GraphPad Prism7. Two-way ANOVA with Tukey's or Sidak's multiple comparisons test, one-way ANOVA with Tukey's multiple comparisons test, Kruskal-Wallis test with Dunn's multiple comparisons test or unpaired *t* test with Welch's correction were used, depending on each experiment. All data was tested for normality. *$p < 0.05$, **$p < 0.01$, ***$p < 0.001$, ****$p < 0.0001$, n.s. indicates no significance. *n* = number of animals and data are presented as mean ± SEM (standard error of the mean), unless stated differently in the respective figure legends.

Table 2.1 – List of zebrafish lines used in this study

Lines	Source
Tg(mpeg1:eGFP)	Francesca Peri lab
Tg(mbp:eGFP-CAAX)	Tim Czopka lab
Tg(mbp:mcherry-CAAX)	Tim Czopka lab
Tg(olig1:nls-mApple)	Tim Czopka lab
Tg(sox10:mRFP)	Tim Czopka lab
Tg(mpeg1:mCherry-F)	Georges Lutfalla lab
Tg(pNF-KB:egfp)	Yi Feng lab
myd88^{hu3568}	Annemarie Meijer lab
cfs1ra/b DKO	T.J. van Ham lab
Tg(mpeg1:myd88-L265P)^{fh507}	Minna Roh-Johnson lab

Table 2.2 – List of zebrafish primers used in this study

Target gene	5´ - 3’
myd88 fwd	GAGGCGATTCCAGTAACAGC
myd88 rev	GAAGCGAACAAAGAAAAGCAA
tnf-α fwd qPCR	CTCCATAAGACCCAGGGCAAT
tnf-α rev qPCR	ATGGCAGCCTTGGAAGTGAA
ef1a fwd qPCR	AGCAGCAGCTGAGGAGTGAT
ef1a rev qPCR	GTGGTGGACTTTCCGGAGT
csf1rb fwd	CTTGCTGACAAATCCAGCAG
csf1rb rev	GAGCTAACCGGACAAACTGG

Table 2.3 – List of enzymes used for zebrafish genotyping

Restriction enzyme	Target gene	Temperature of activity (°C)	Expected bands (bp)
MseI	*myd88*	37	Wt - 300 Het - 300, 200, 100 Hom – 200, 100
MspI	*csf1rb*	37	Wt – 203, 132 Het – 331, 203, 132 Hom - 331

Table 2.4 – List of mouse lines used in this study

Lines	Source
Myd88	Arthur Liesz lab
$A20^{Fl}$	Hiroaki Honda, Research Institute for Radiation Biology and Medicine
$CX3CR1^{CreERT2}$	Steffen Jung lab

Table 2.5 – List of mouse primers used in this study

Target gene	5´ - 3’
myd88 fwd	GTTGTGTGTGTCCGACCGT
myd88 rev	GTCAGAAACAACCACCACCATGC
$A20^{Fl}$ fwd	CTATCTGTGGTGGACAAAGGCTACTCTCGG
$A20^{Fl}$ rev	GAATCGCCTACCTAGGAATCAGCTGTCCAG
CreERT2 fwd	TATCTTCTATATCTTCAGGCGC
CreERT2 rev	GTGAACGAACCTGGTCGAAATCAG

3. Research work

Part of the research work here presented was published as a manuscript in Cunha et al., *J Exp Med* (2020) 217 (5): e20191390.

3.1. Establishment of a lysolecithin-induced demyelination model in the spinal cord of zebrafish larvae

Lysolecithin-induced focal demyelinating lesions have been widely used in rodents. However, these models are not yet the most suitable for high-resolution live imaging experiments. The optically transparent zebrafish larvae have been extensively used for the study of myelin biology and innate immune responses, which are conserved between zebrafish and mammals (Almeida et al., 2011; Auer et al., 2018; Czopka and Lyons, 2011; Forn-Cuni et al., 2017; Mitchell et al., 2018; Peri and Nusslein-Volhard, 2008; Villani et al., 2019). We wondered if we could combine the strengths of the lysolecithin model with the advantages of zebrafish larvae. For that we have first established the optimal concentration of lysolecithin to be injected. We prepared 1%, 10% and 40% solutions of lysolecithin dissolved in PBS and injected each in 4, 10 and 100nl volumes in the spinal cord of 6 days post fertilization (dpf) larvae, age where spinal cord myelination is reported to be mostly completed, and stable, and the differentiation and migration of resident CNS phagocytes already took place (Buckley et al., 2010; Herbomel et al., 2001; Rossi et al., 2015). We assessed larvae survival, as well as myelination and phagocyte infiltration at 2 days post injection (dpi), by using pre-existing reporter lines for visualizing myelin and phagocytes (Tg(mbp:mCherry-CAAX) and Tg(mpeg1:eGFP), respectively). We have observed that 4nl of 40% lysolecithin in PBS, is the best concentration for inducing a noteworthy focal demyelinating lesion with substantial inflammatory response (Fig. 3.1 A – D).

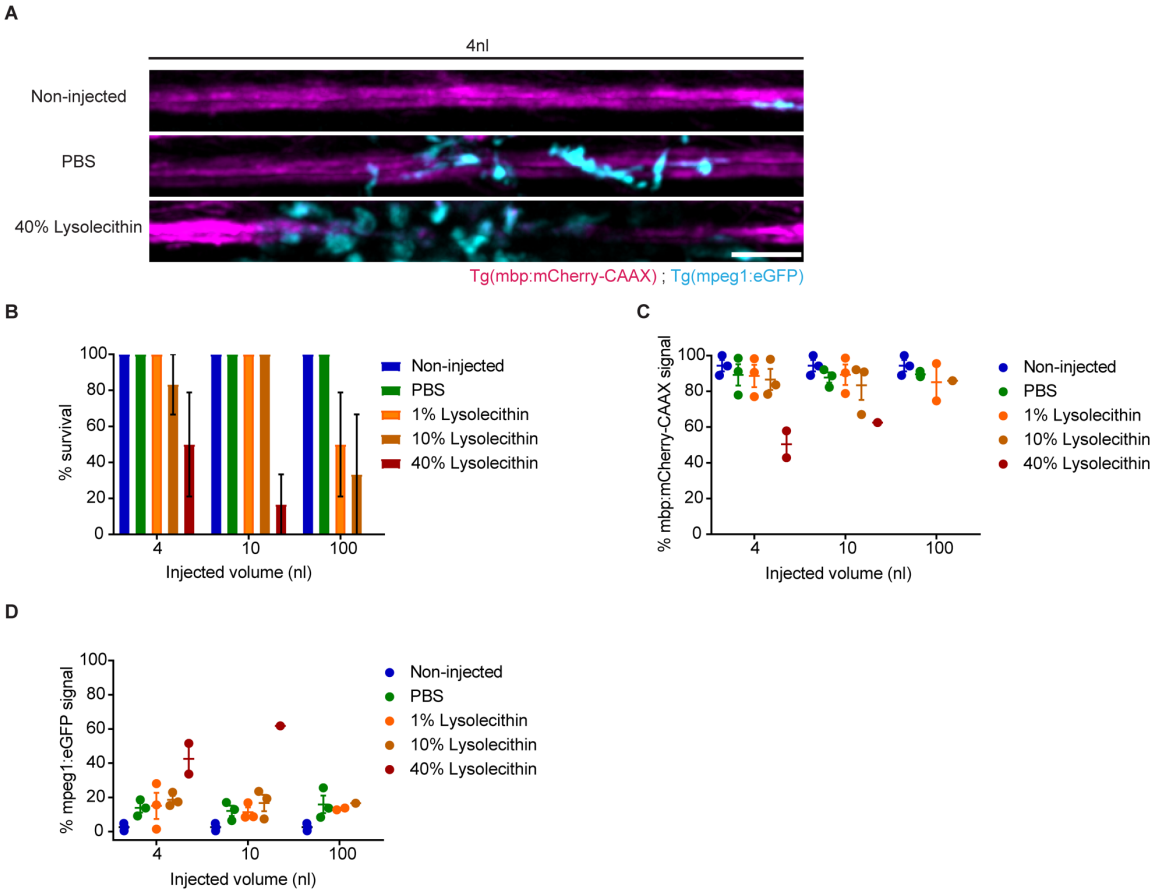

Figure 3.1 Establishment of the lysolecithin concentration to be injected in the spinal cord of zebrafish larvae. (A) Maximum intensity projections showing myelin in the spinal cord (magenta) and phagocytes (cyan), in non-injected and larvae injected with 4nl of PBS or 40% lysolecithin, at 2dpi. *n* = 3 larvae. (B) Assessment of larvae survival was performed at 2dpi, in non-injected and larvae injected with PBS or lysolecithin in the spinal cord. (C) Myelination was quantified by the total amount of mbp:mCherry-CAAX signal in the dorsal spinal cord. (D) The infiltration of phagocytes was quantified by the total amount of mpeg1:eGFP signal in the dorsal spinal cord. *n* = 1-3 larvae. Images show lateral views of the lesion site, dorsal is down and anterior is left. Data are mean ± SEM (error bars). Scale bar is 50µm (A).

After establishing the right concentration and volume of lysolecithin to be injected, we assessed the kinetics of the lesion by looking at myelination and phagocyte infiltration at 6 hours post injection (hpi), 2, 4 and 7dpi. We observed that the lysolecithin injection leads to a reduction of the mbp:mCherry-CAAX signal until 2dpi which is increased from 4dpi. The fact that PBS values remain comparable to non-injected larvae shows that this drop in the signal was not a consequence of an injury caused by the needle. We further observed that there is a rapid recruitment of mpeg1:eGFP phagocytes, with the peak of infiltration at 2dpi which is then decreased at 4dpi, contrary to PBS injection in which phagocyte numbers return to baseline immediately at 2dpi (Fig. 3.2 A-C). In order to know if remyelination, and the subsequent increase in MBP signal, was a result of the generation of new oligodendrocytes or if it was performed by the ones that remained in the spinal cord after the injection of lysolecithin, we injected larvae that have labeled the nucleus of mature oligodendrocytes (Tg(mbp-nls:eGFP-CAAX)), and observed that the injection of lysolecithin leads to a reduction in mature oligodendrocyte numbers until 2dpi and that these numbers are increased at 4dpi (Fig. 3.2 D and E). To completely characterize the demyelination / remyelination kinetics, we also assessed the recruitment of OPCs to the lesion, by looking at Tg(olig1-nls:mApple) larvae. We observed that OPCs, normally present in the spinal cord of the larvae, are mostly lost immediately after lysolecithin injection, at 6hpi and 1dpi, and that new cells are present in the lesion site from 2dpi, with values comparable to non-injected larvae (Fig. 3.2 F and G).

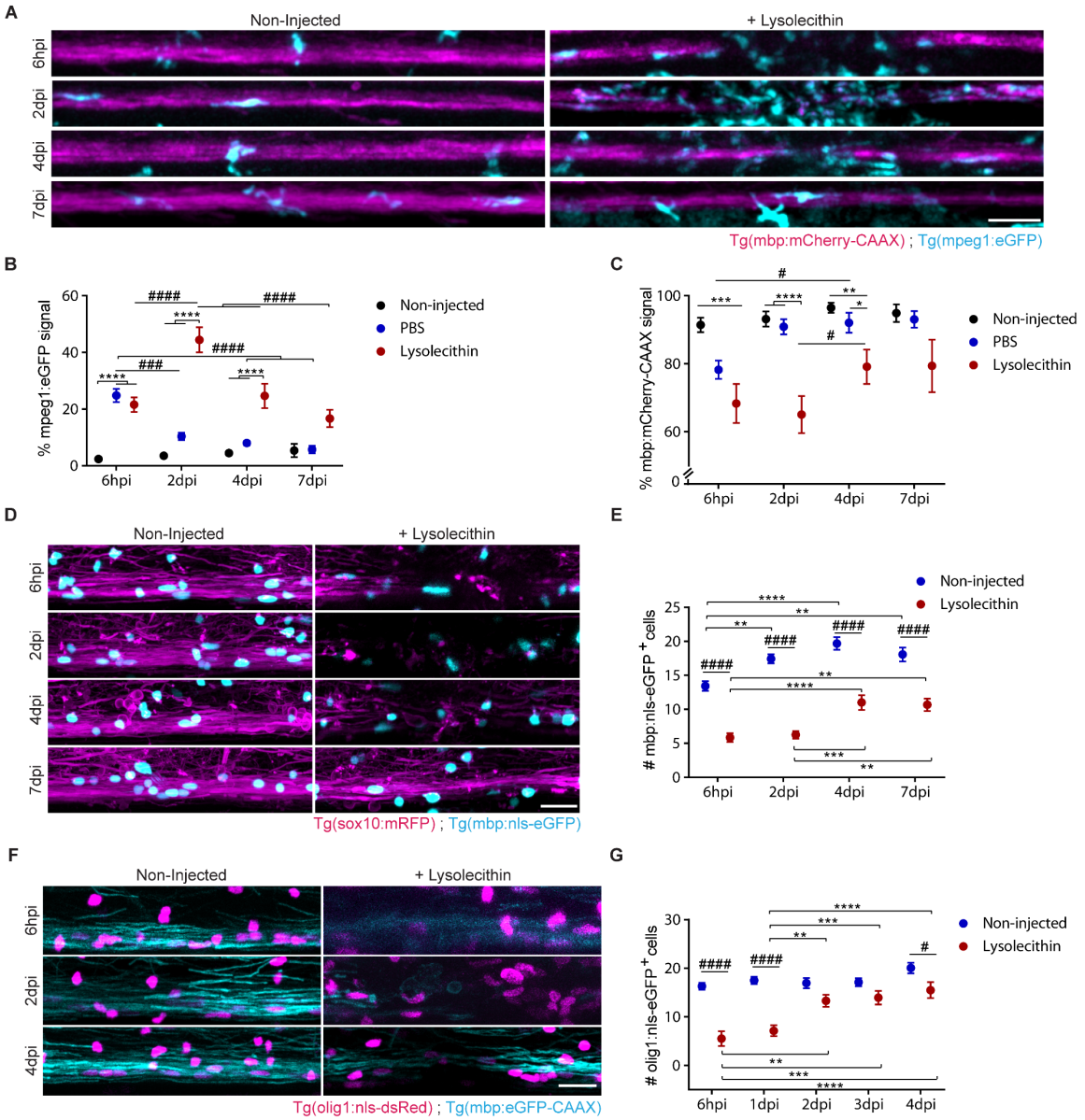

Figure 3.2 Lysolecithin-induced model of spinal cord demyelination in zebrafish larvae. (A) Maximum intensity projections showing myelin in the spinal cord (magenta) and phagocytes (cyan), in non-injected and lysolecithin-injected larvae, over time. (B) The infiltration of phagocytes was quantified by the total amount of mpeg1:eGFP signal in the dorsal spinal cord. (C) Myelination was quantified by the total amount of mbp:mCherry-CAAX signal in the dorsal spinal cord. *n* = 9-12 (6hpi), 15-16 (2dpi), 13-20 (4dpi), 4-8 (7dpi) larvae. (D) Maximum intensity projections showing the nucleus of mature oligodendrocytes (cyan) and the myelinated spinal cord (magenta), in non-injected and lysolecithin-injected larvae, over time. (E) Quantification of the mature oligodendrocytes number was performed by counting the mbp:nls-eGFP nuclei in the dorsal spinal cord, over time. *n* = 20-21 (6hpi), 16-21 (2dpi), 20-22 (4dpi), 12-15 (7dpi) larvae. (F) Maximum intensity projections showing the nucleus of OPCs (magenta) and the myelinated spinal cord (cyan), in non-injected and lysolecithin-injected larvae, over time. (G) Quantification of the number of OPCs number was performed by counting the olig1:nls-mApple nuclei in the dorsal spinal cord, over time. *n* = 8-10 (6 hpi), 12-16 (1dpi), 16 (2dpi), 17 (3dpi), 16-17 (4dpi) animals. Images show lateral views of the lesion site, dorsal is down and anterior is left. Data are mean ± SEM (error bars); *p < 0.05, **p < 0.01, *** p < 0.001 and **** p < 0.0001, by 2-way ANOVA, with Tukey's multiple comparisons test (B, C, E, G). # indicates statistical significance when compared to WT (B and C). Scale bars are 50µm (A) and 20µm (D and F).

Next, we wanted to know whether our model was exclusively targeting myelin and the myelinating cells or if it was inducing off-target injury to neurons and the wider tissue. For that we have performed lysolecithin injections into double transgenic Tg(mbp:eGFP-CAAX) / Tg(cntn1b:mCherry) to visualize both myelin and axons, respectively. While we have observed a ~25% reduction in mbp:eGFP-CAAX signal at 2dpi, the lysolecithin injection only led to a ~3% reduction in cntn1b:mCherry signal (Fig. 3.3 A-C). Furthermore, we have performed scanning electron microscopy in larvae at 2dpi and 4dpi to further characterize the extent of demyelination and remyelination, respectively. At 2dpi, we observe the presence of demyelinated axons and myelin fragments, as well as phagocytes engulfing myelinated axons, all of which are features of demyelinating lesions. At 4dpi, there are still demyelinated axons present, but we could already observe at this time-point axons with loose myelin wraps (partially myelinated axons), which are likely to represent remyelinated axons (Fig. 3.3 D). In order to further assess the integrity of the neurons in the lesion site, we have looked at the axonal morphology in depth and could observe that throughout the different lesion stages and independent of the myelin phenotypes, the axons, as well as classical features of the nervous system, as synapses, remained morphological intact (Fig. 3.3 E).

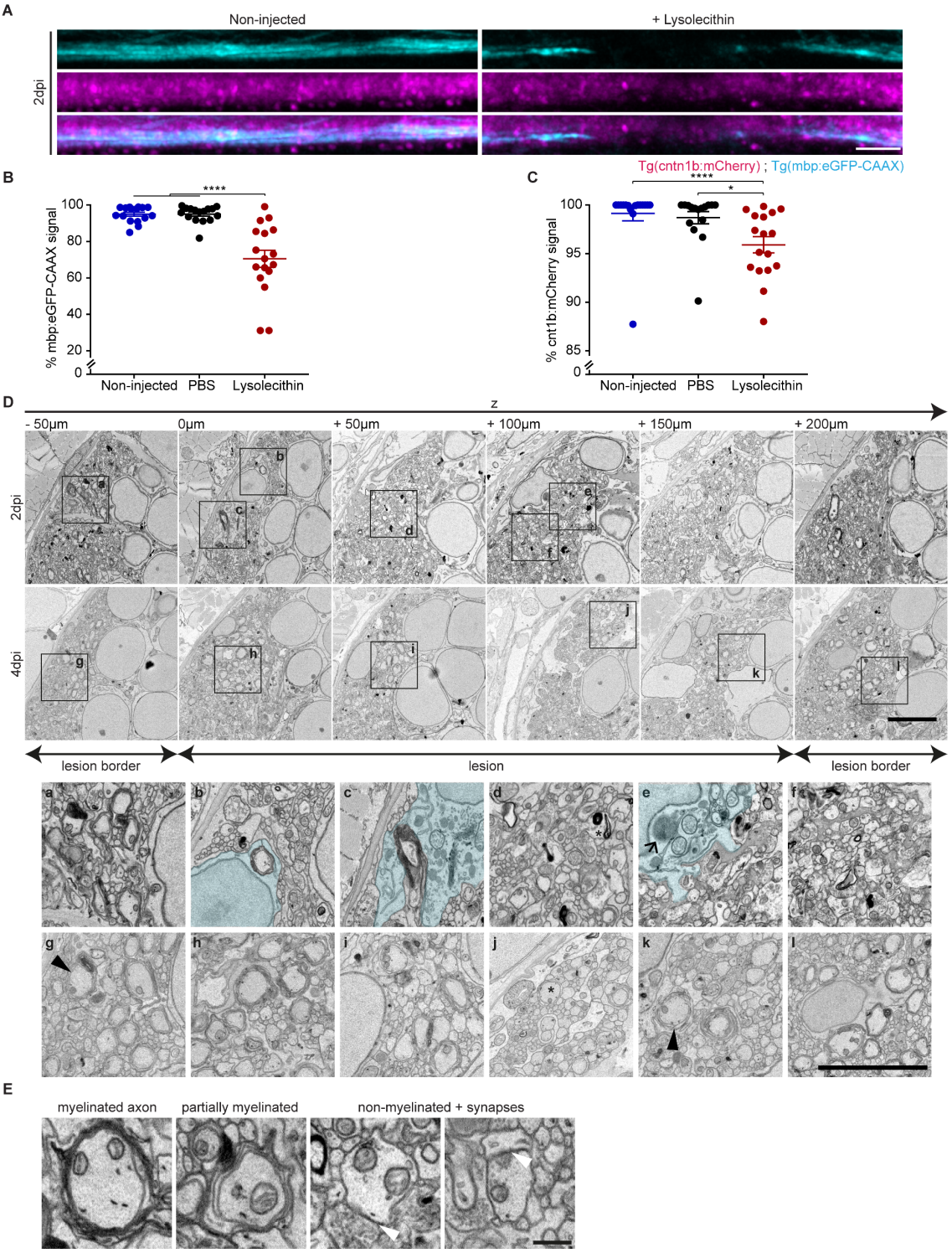

Figure 3.3 Axonal integrity is mainly preserved after lysolecithin-induced demyelination. (A) Maximum intensity projections showing myelin in the spinal cord (cyan) and axons (magenta), in non-injected and lysolecithin-injected larvae, at 2dpi. (B) Myelination was quantified by the total amount of mbp:eGFP-CAAX signal in the dorsal spinal cord. (C) Axonal density was quantified by the total amount of cntn1b:mCherry signal in the dorsal spinal cord. *n* = 16-17 larvae. (D) Electron microscopy images of serial cross sections of the spinal cord of lysolecithin-injected WT larvae, at 2 and 4 dpi. (D-a, b, d, e and f) Close-up images of the demyelinating lesion showing myelin debris, at 2dpi. (D-b, c) Close-up images of the demyelinating lesion showing a phagocyte (cyan) taking up a myelinated axon, at 2dpi. (D-c, e) Close-up images of the demyelinating lesion showing phagocytes with lysosomes (arrow), at 2dpi. (D-b, d, f, j) Close-up images of the demyelinating lesion showing demyelinated axons (star). (continues on the bottom of the next page)

It is well known that in a demyelination / remyelination context in rodents, phagocytes play an important role in myelin debris phagocytosis and clearance, as well as in the secretion of factors said to be necessary for the repair process to initiate (Kotter et al., 2001; Kotter et al., 2005; Lampron et al., 2015; Miron et al., 2013). In order to validate our zebrafish larvae lysolecithin-induced demyelination model, we have performed injections in larvae lacking the colony-stimulating factor 1 receptor a and b (*csf1r*$^{-/-}$), in which the CNS resident phagocytes (microglia) were previously shown to be almost completely absent (Oosterhof et al., 2018). We observed that *csf1r* mutant larvae show reduced mbp:eGFP-CAAX signal at 4dpi, when compared to wild-type controls, implying impaired remyelination in the absence of CNS phagocytes (Fig. 3.4 A and B).

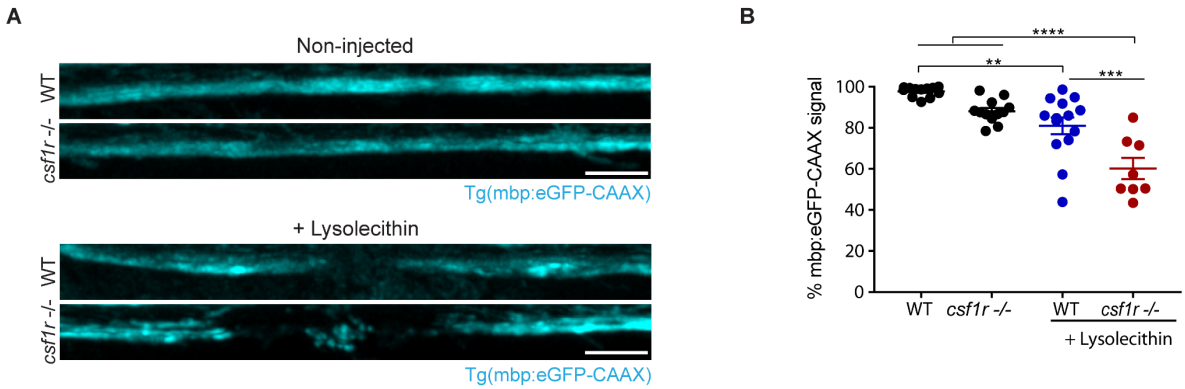

Figure 3.4 CNS phagocytes are important for remyelination after lysolecithin-induced demyelination in the spinal cord of zebrafish larvae. (A) Maximum intensity projections showing myelin in the spinal cord (cyan), in non-injected and lysolecithin-injected larvae, at 4dpi. (B) Myelination was quantified by the total amount of mbp:eGFP-CAAX signal in the dorsal spinal cord. *n* = 8-14 larvae. Images show lateral views of the lesion site, dorsal is down and anterior is left. Data are mean ± SEM (error bars); **p < 0.01, *** p < 0.001 and **** p < 0.0001, by 1-way ANOVA, with Tukey's multiple comparisons test (B). Scale bars are 50µm (A).

Taken all together, we have established a lysolecithin-induced model of spinal cord demyelination in zebrafish larvae, in which there is rapid demyelination, with loss of mature oligodendrocytes, together with a required influx of phagocytes, followed by recruitment of OPCs, generation of new oligodendrocytes, phagocyte efflux and subsequent remyelination.

Figure 3.3 (continuation) (D-g, h, j, k) Close-up images of the demyelinating lesion showing partially myelinated axons (arrow), at 4dpi. (E) Close-up electron microscopy images showing the integrity of axons in the different myelinating phenotypes across lesion stages (arrows show synapses). Data are mean ± SEM (error bars); p < 0.05, **** p < 0.0001 by 1-way ANOVA, with Tukey's multiple comparisons test (B) or Kruskal-Wallis test, with Dunn's multiple comparisons test (C). Scale bars are 50µm (A), 5µm (D) and 0.5µm (E).

3.2. Impaired myelin clearance in *myd88* mutant zebrafish larvae

In this study we intended to explore how phagocyte pro-inflammatory activation influences the course of a demyelinating lesion. For that, we first started by determining if the demyelinating injury induced a pro-inflammatory activation of the recruited phagocytes. We have used a previously published reporter line for NF-κB activation, Tg(NF-κb:eGFP), and observed that immediately at 6hpi there was a strong induction of NF-κb:eGFP signal in the phagocytes recruited to the lesion, which was decreased in the subsequent days, meaning that pro-inflammatory NF-κB activation occurred in the early stages of the demyelinating injury (Fig. 3.5 A and B) (Kanther et al., 2011). In order to determine the impact of phagocyte under-activation in a demyelinating lesion, we have targeted one of the major activation pathways essential to innate immunity response: the TLR pathway. As seen in the previous sections, most TLRs (with exception of TLR3), when signaled by either exogenous PAMPs or endogenous DAMPs, require the recruitment of an adaptor protein called Myd88, which is essential to then trigger the rest of the activation pathway which culminates with the translocation of NF-κB to the nucleus and the transcription of pro-inflammatory cytokines. Thus, in order to test if phagocyte under-activation had an impact in the regenerative response after demyelination, we have used *myd88* mutant larvae. We started by validating our model with the previously used NF-κb activation reporter line and have observed that although there is an initial activation at 6hpi, this is reduced in comparison with wild-type control phagocytes and completely gone by 2dpi, which allowed us to use this line as a phagocyte under-activated model (Fig. 3.5 A and B).

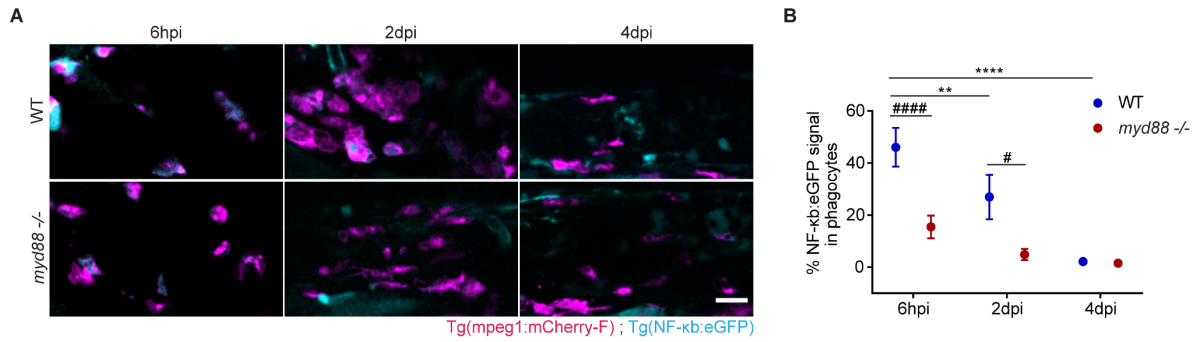

Figure 3.5 Myd88-dependent pro-inflammatory signaling is triggered early after lysolecithin-induced demyelination. (A) Maximum intensity projections of the spinal cord lesion showing phagocytes (magenta) and NF-κB activation, in lysolecithin-injected larvae, over time. (B) Quantification of NF-κB activation in phagocytes was performed by determining the colocalized signal of mpeg1:mCherry with NF-κB:eGFP relative to total mpeg1:mCherry signal. *n* = 9-10 (6hpi), 7 (2dpi), 10-11 (4dpi) larvae. Images show lateral views of the lesion site, dorsal is down and anterior is left. Data are mean ± SEM (error bars); * $p < 0.05$, **$p < 0.01$, and **** $p < 0.0001$, by 2-way ANOVA, with Tukey's multiple comparisons test (B). # indicates statistical significance when compared to WT (B). Scale bars are 50μm (A).

Next, we wondered if phagocytic ability was impaired in *myd88* mutants. When we looked at wild-type lesions, we observed that at the peak of demyelination, at 2dpi, the phagocytes were loaded with intracellular myelin debris and were actively stripping it off from axonal tracts (Fig. 3.6 A and supplementary video 1). Phagocytosis of myelin debris was not affected in *myd88* mutants, since a comparable amount of mpeg1:eGFP phagocytes with internalized mbp:mCherry-CAAX, was found at 2dpi, between *myd88* $^{-/-}$ and wild-type larvae. However, when we looked at later stages of the lesion, while wild-type phagocytes had largely reduced the amount of phagocytes with internalized myelin debris at 4dpi, *myd88* mutants revealed similar values between 2 and 4dpi (Fig. 3.6 B and C). Since lysosomes are the cell organelles in charge of intracellular degradation, we wondered if *myd88* mutant phagocytes had impaired lysosomal biogenesis. To label lysosomes we have used the extensively used dye LysoTracker, for its high selectivity for acidic organelles (Sasaki et al., 2017). We found that lysosomal biogenesis is largely induced in phagocytes at 2dpi, in both wild-type and *myd88* mutants, consistent with their role in the phagocytosis of myelin debris (Fig. 3.6 D-G). However, when we looked at 4dpi, we observed that the amount of Lysotracker signal remained high in *myd88*$^{-/-}$ phagocytes, while wild-type controls had reduced the amount of signal inside phagocytes from 2 to 4dpi, implying an accumulation of lysosomes in the absence of Myd88 signaling (Fig. 3.6 F and G).

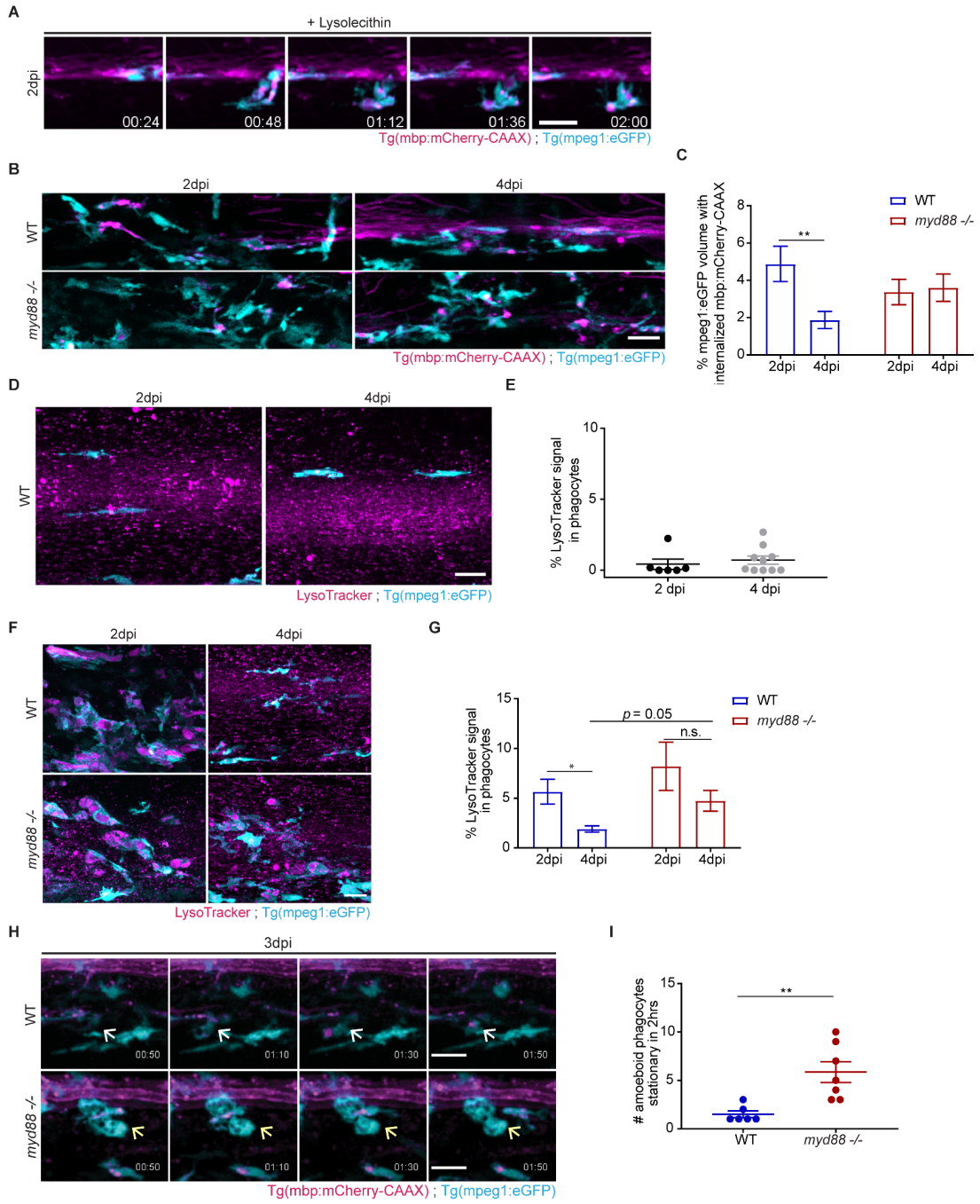

Figure 3.6 Myelin degradation is impaired in Myd88 deficient animals. (A) Maximum intensity projections of a 2h time-lapse of a lesion showing phagocytes (cyan) and the myelinated spinal cord and myelin debris (magenta), in WT larvae, at 2dpi. (B) Maximum intensity projections of spinal cord lesions showing phagocytes (cyan) and the myelinated spinal cord and myelin debris (magenta), at 2 and 4 dpi. (C) Quantification of the ingested myelin debris was performed by determining the colocalized signal of mpeg1:eGFP with mbp:mCherry-CAAX relative to total mpeg1:eGFP signal. n = 11-15 (2dpi), 15-17 (4dpi) larvae. (D) Maximum intensity projections of spinal cord showing phagocytes (cyan) and lysosomes (magenta), in non-injected WT larvae, at 2 and 4dpi. (E) Quantification of lysosomes was performed by determining the colocalized signal of mpeg1:eGFP with Lysotracker relative to total mpeg1:eGFP signal. n = 6 (2dpi), 10 (4dpi) larvae. (F) Maximum intensity projections of spinal cord lesions showing phagocytes (cyan) and lysosomes (magenta), at 2 and 4 dpi. (G) Quantification of lysosomes was performed by determining the colocalized signal of mpeg1:eGFP with Lysotracker relative to total mpeg1:eGFP signal. n = 8-10 (2dpi), 14-25 (4dpi) larvae. (continues on the bottom of the next page)

Since there seemed to be an impairment in the degradation of myelin debris with accumulation of lysosomes inside *myd88* $^{-/-}$ phagocytes, we sought to visualize how phagocytes were handling internalized myelin during the degradation process. Because we observed that myelin digestion should be taking place from 2 to 4dpi, we have performed time-lapse imaging of lesions at 3dpi. We found that the majority of phagocytes present in the lesions were highly motile but there were an increased number of amoeboid stationary phagocytes in *myd88* $^{-/-}$ lesions compared to controls (Fig. 3.6 H and I and supplementary videos 2 and 3).

In order to further understand the mechanisms leading to impaired myelin clearance by the phagocytes, we have performed cell culture experiments with wild-type and Myd88-deficient microglia isolated from mice pups. By assessing the fusion rate of myelin vacuoles with either lysosomes or reactive oxygen species (ROS) compartments, both of which we observed to be decreased in *Myd88* mutants, we have found that phagosome maturation was impaired in Myd88-deficient microglia when treated with myelin debris (Cunha et al., 2020).

Figure 3.6 (continuation) (H) Maximum intensity projections of a 2h time-lapse of lesions showing phagocytes (cyan) and the myelinated spinal cord and myelin debris (magenta), at 3dpi. White arrows show phagocytes actively moving; yellow arrows show amoeboid phagocytes stationary. (I) Quantification of the number of amoeboid stationary phagocytes was determined by counting phagocytes that did not move in all frames of the 2h time-lapse. *n* = 6-7 larvae. Images show lateral views of the lesion site, dorsal is down and anterior is left. Data are mean ± SEM (error bars); * $p < 0.05$, ** $p < 0.01$ and n.s corresponds to no significance, by 2-way ANOVA, with Tukey's multiple comparisons test (C) or Sidak's multiple comparisons test (G), and unpaired t-test with Welch's correction (I). Scale bars are 20µm.

3.3. Oligodendrocyte generation and remyelination are impaired after lysolecithin-induced demyelination in *myd88* mutant animals

Having found that the lack of phagocyte pro-inflammatory activation led to consequent impairment in myelin debris degradation, we sought to determine the impact it had in remyelination. We have first observed that *myd88* mutant zebrafish larvae did not show any abnormalities in developmental myelination, by looking at the amount of mbp:mCherry-CAAX signal, the number of mature oligodendrocytes (mbp:nls-EGFP) and OPCs (olig1:nls-mApple), in the spinal cord, from 6 to 10dpf (Fig. 3.7 A-G). Also, the number of myelinated axons at 6dpf in the dorsal spinal cord was the same between *myd88* mutant larvae and control larvae, as assessed by scanning electron microscopy (Fig. 3.7 H-I). This was in accordance to what happened in mice, since *Myd88* $^{-/-}$ mice also did not show any differences between the number of myelinated axons in the spinal cord at 7-8 weeks old, nor in myelin thickness, as assessed by g-ratio measurements (Fig. 3.7 J-L).

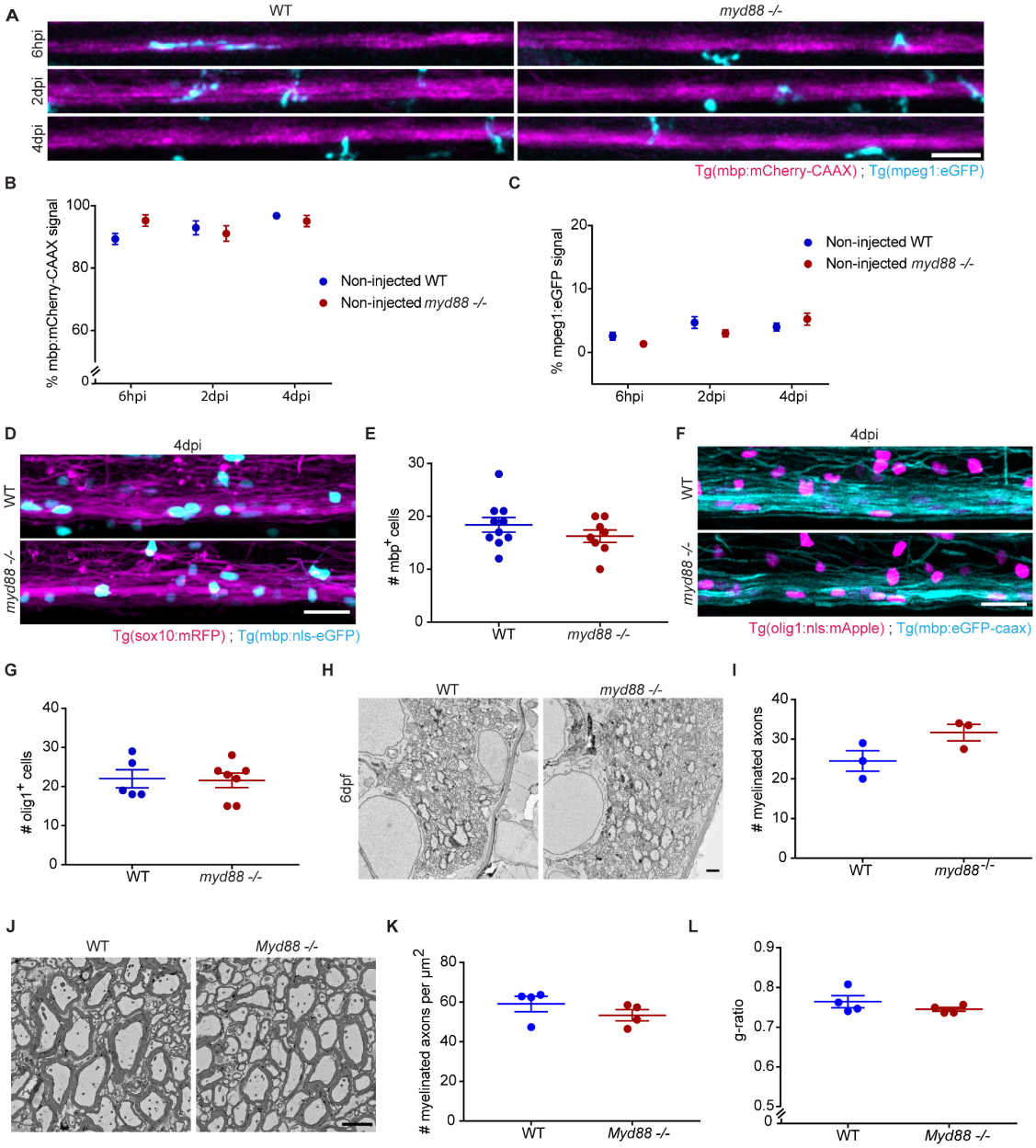

Figure 3.7 Myelination is not impaired in the absence of Myd88 signaling. (A) Maximum intensity projections showing myelin in the spinal cord (magenta) and phagocytes (cyan), in non-injected larvae, over time. (B) Myelination was quantified by the total amount of mbp:mCherry-CAAX signal in the dorsal spinal cord. (C) The infiltration of phagocytes was quantified by the total amount of mpeg1:eGFP signal in the dorsal spinal cord. *n* = 15-19 (6hpi), 11-17 (2dpi), 13-17 (4dpi) larvae. (D) Maximum intensity projections showing the nucleus of mature oligodendrocytes (cyan) and the myelinated spinal cord (magenta), in non-injected larvae, at 4dpi. (E) Quantification of the mature oligodendrocytes number was performed by counting the mbp:nls-eGFP nuclei in the dorsal spinal cord, in non-injected larvae, at 4dpi. *n* = 8-10 larvae. (F) Maximum intensity projections showing the nucleus of OPCs (magenta) and the myelinated spinal cord (cyan), in non-injected larvae, at 4dpi. (G) Quantification of the number of OPCs number was performed by counting the olig1:nls-mApple nuclei in the dorsal spinal cord, in non-injected larvae, at 4dpi. *n* = 5-7 larvae. (H) Electron microscopy images of spinal cord cross sections, of non-injected larvae, at 6dpf. (I) Quantification of the number of myelinated axons was performed in a representative cross section per larvae. *n* = 3 larvae. (J) Electron microscopy images of spinal cord cross sections, of 2months old non-lesioned mice. (K) Quantification of the number of myelinated axons was performed in 2-3 1600µm^2 per mice. *n* = 4 mice. (L) G-ratios to assess myelin thickness were calculated in 225µm^2 per mice. *n* = 4 mice. (continues on the bottom of the next page)

Then, we have performed injections in double transgenic Tg(mpeg1:eGFP) / Tg(mbp:mCherry-CAAX), in both *myd88* mutant and control larvae. We found that while the extent of demyelination was the same in Myd88-deficient larvae compared to wild-type, the recovery of mbp:mCherry-CAAX signal seen in control larvae at 4dpi, did not occur in *myd88* $^{-/-}$ lesions (Fig. 3.8 A and B). We have also found that the amount of mpeg1:eGFP signal in 4dpi lesions, was higher in *myd88* mutant compared to control animals, implying a delayed resolution of inflammation (Fig. 3.8 A and C). In order to further explore the lack of mbp:mCherry-CAAX signal recovery in *myd88*$^{-/-}$ lesions, we have performed injections in Tg(mbp:nls-eGFP) and found that there were also less mature oligodendrocytes present in the lesions at 4dpi, consistent with impaired remyelination in Myd88-deficient animals (Fig. 3.8 D and E). We then wondered if this was a consequence of shortage of OPCs in the site of injury. By using Tg(olig1:nls-mApple) larvae, we have found that there were also less progenitor cells present in the lesions of *myd88*$^{-/-}$ larvae, at 4dpi (Fig. 3.8 F and G).

In addition, we have performed lysolecithin injections in the spinal cord of *Myd88* $^{-/-}$ mice and have observed that also in the mammalian model, the absence of Myd88 signaling results in impaired remyelination, with reduced OPCs and pre-myelinating / early myelinating oligodendrocytes at the start of remyelination, as well as reduced mature oligodendrocyte numbers and remyelinated axons, compared to wild-type controls (Cunha et al., 2020).

Figure 3.8 (continuation) Images show lateral views of the spinal cord, dorsal is down and anterior is left (A, D and F). Data are mean ± SEM (error bars). Scale bars are 50μm (A), 20μm (D and F), 1μm (H) and 100μm (J).

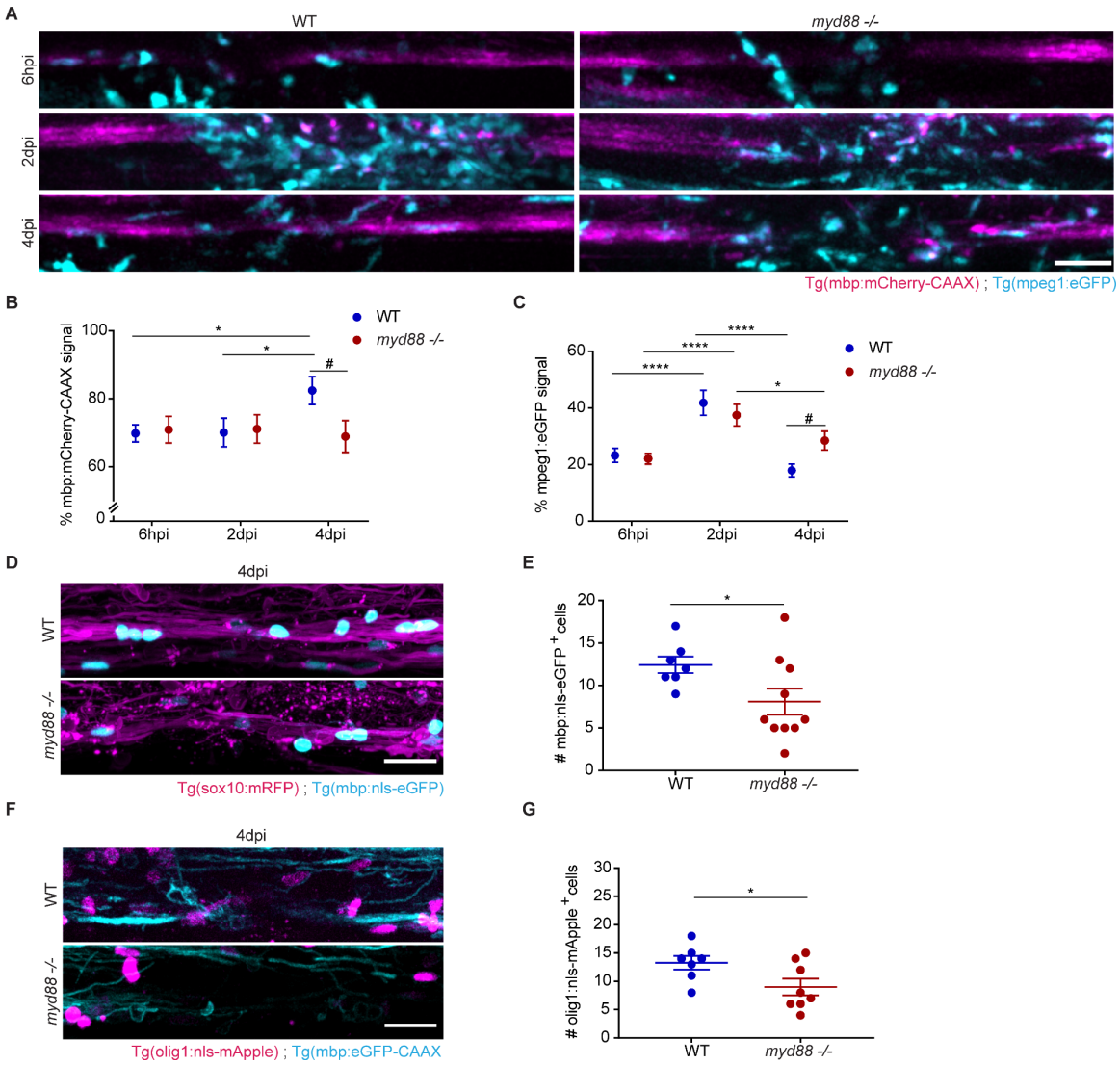

Figure 3.8 Inflammation resolution and remyelination are impaired in Myd88-deficient larvae. (A) Maximum intensity projections showing myelin in the spinal cord (magenta) and phagocytes (cyan), in lysolecithin-injected larvae, over time. (B) Myelination was quantified by the total amount of mbp:mCherry-CAAX signal in the dorsal spinal cord. (C) The infiltration of phagocytes was quantified by the total amount of mpeg1:eGFP signal in the dorsal spinal cord. *n* = 15-19 (6dpi), 11-17 (2dpi), 13-17 (4dpi) larvae. (D) Maximum intensity projections showing the nucleus of mature oligodendrocytes (cyan) and the myelinated spinal cord (magenta), in lysolecithin-injected larvae, at 4dpi. (E) Quantification of the mature oligodendrocytes number was performed by counting the mbp:nls-eGFP nuclei in the dorsal spinal cord, at 4dpi. *n* = 7-10 larvae. (F) Maximum intensity projections showing the nucleus of OPCs (magenta) and the myelinated spinal cord (cyan), in lysolecithin-injected larvae, at 4dpi. (G) Quantification of the number of OPCs number was performed by counting the olig1:nls-mApple nuclei in the dorsal spinal cord, at 4dpi. *n* = 7-8 larvae. Data are mean ± SEM (error bars); *p < 0.05 and **** p < 0.0001, by 2-way ANOVA, with Tukey's multiple comparisons test (B, C) and unpaired t-test with Welch's correction (E and G). Controls WT and *myd88*$^{-/-}$ non-injected larvae represented in Figure 3.7 A-C are included in the statistical analysis of B and C. # indicates statistical significance when compared to WT (B and C). Scale bars are 50µm (A) and 20µm (D and F).

3.4. TNF-α promotes oligodendrocyte generation in the absence of Myd88

Taken together, the lack of Myd88 signaling in a context of focal demyelination seems to lead to under-activation of phagocytes, resulting in impaired myelin debris clearance, impaired phagocyte efflux from lesions, together with impaired remyelination. These results led us to further question which pathways are activated in phagocytes in the presence of myelin debris. For this, we have performed proteomic analysis of cultured microglia treated with myelin debris, and the differentially expressed proteins between *Myd88* $^{-/-}$ and wild-type microglia were subsequently taken for pathway analysis. Interestingly, myelin debris seemed to trigger the activation of pro-inflammatory pathways in cultured wild-type microglia, with TNF-α being one common predicted upstream regulator, identified by Ingenuity Pathway Analysis (IPA). Conversely, TNF-α pathway was inhibited in *Myd88* $^{-/-}$ microglia treated with myelin debris, identifying TNF-α as a candidate cytokine regulator of the response to myelin debris (Cunha et al., 2020). In order to validate these results in lysolecithin-induced demyelinating lesions, we have performed *in situ* hybridization targeting TNF-α in mice spinal cord lesions, and found that TNF-α transcription was induced to a lesser extent in *Myd88*$^{-/-}$ lesions, compared to wild-type controls (Fig. 3.9 A and B). Additionally, by real-time PCR we observed that TNF-α mRNA expression was induced to a much higher extent in spinal cord lesions of wild-type larvae compared to *myd88* $^{-/-}$ mutants (Fig. 3.9 C).

To determine the source of damage-induced TNF-α expression, we combined the *in situ* hybridization against TNF-α with immunohistochemistry targeting IBA1, in mice spinal cord lesions at 4dpi, and observed that ~80% of TNF-α positive cells showed colocalization with IBA1 signal (Fig. 3.9 D and E). These results imply a role for phagocyte-induced TNF-α after a demyelinating injury. These observations raised two questions, on one hand does TNF-α have any effect in the degradation of myelin debris by the phagocytes? On the other hand, does TNF-α have any effect in the generation of new oligodendrocytes after demyelination? To answer the first question, we have again treated cultured microglia with myelin debris for 2h, washed myelin away from the cultures, and after, added TNF-α to the media, in order to specifically assess its role in the degradation of intracellular myelin debris, rather than in its phagocytosis. We found that after 6h of incubation with recombinant TNF-α, microglia cells had less amount of myelin debris inside compared to controls non-treated cells, meaning it enhanced phagocyte degradation of myelin debris (Cunha et al., 2020). Next, to answer the second question, we have used organotypic cerebellar slice cultures of wild-type and Myd88-deficient mice pups P8-9, and induced demyelination by 16h incubation with 0.5mg/ml lysolecithin, a model of demyelination / remyelination previously established (Birgbauer et al., 2004; Thetiot et al., 2019). After, we have let the slices recover

for 48h with or without the addition of recombinant TNF-α to the slice culture medium, and performed immunohistochemistry against BCAS1, in order to determine the amount of pre-myelinating and early myelinating oligodendrocytes. We have found that wild-type slices recovered BCAS1 signal 48h after lysolecithin incubation, but not *Myd88* $^{-/-}$ slices. However, in the presence of TNF-α in the slice culture medium, we could observe an increase in BCAS1 signal in *Myd88* $^{-/-}$ slices. The increase of BCAS1 immunoreactivity in wild-type slices was independent of, and not further increased by, the addition of TNF-α (Fig. 3.9 F and G). These results suggest that in the absence of Myd88, TNF-α administration after a demyelinating insult is able to enhance lesion recovery.

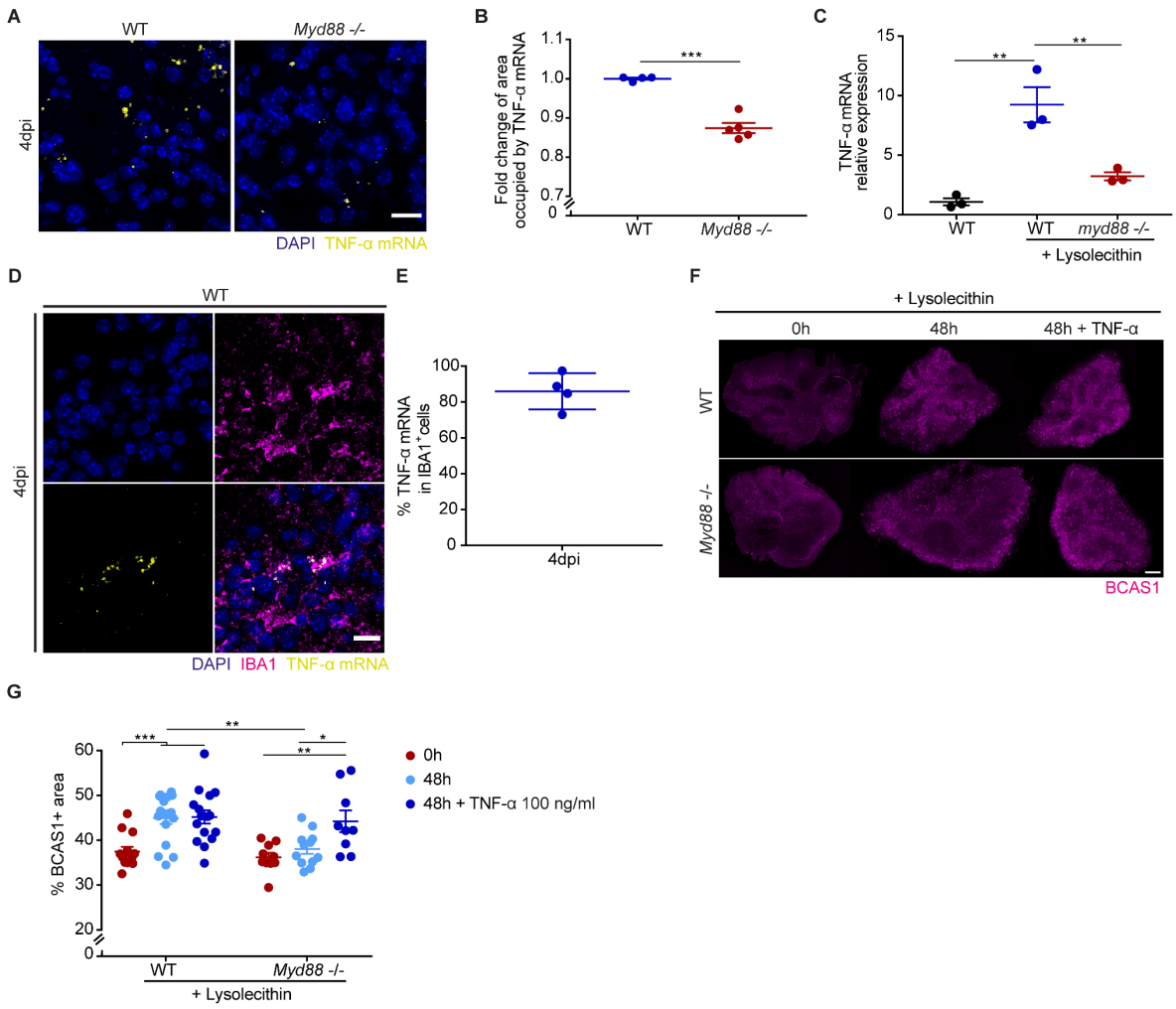

Figure 3.9 Recombinant TNF-α was able to rescue the generation of BCAS1⁺ oligodendrocytes in the absence of Myd88. (A) Maximum intensity projections of *in* situ hybridization performed with RNAscope® targeting TNF-α mRNA (yellow) in mice spinal cord lesions, at 4dpi. (B) Quantification of TNF-α mRNA in mice spinal cord lesions was performed by determining the total amount of signal in the lesions, at 4dpi. *n* = 4-5 lesions. (C) Quantification of TNF-α mRNA in zebrafish larvae spinal cord lesions was performed by quantitative RT-PCR of non-injected and lysolecithin-injected spinal cord tissue, at 6hpi. *n* = 3 independent experiments. (D) Maximum intensity projections of combined immunohistochemistry and *in* situ hybridization targeting Iba1 phagocytes (magenta) and TNF-α mRNA (yellow) in WT mice spinal cord lesions, at 4dpi. (E) Quantification of TNF-α mRNA in phagocytes was performed by determining the colocalized signal of Iba1 with TNF-α mRNA relative to the total amount of TNF-α mRNA signal, in WT mice spinal cord lesions, at 4dpi. *n* = 4 lesions. (F) Images of OCSCs showing pre-myelinating / early myelinating BCAS1⁺ oligodendrocytes (magenta), 0h and 48h after treatment with lysolecithin, with or without TNF-α (100ng/ml) for 48h. (G) Quantification of pre-myelinating / early myelinating oligodendrocytes was performed by determining the total amount of BCAS1 signal in the slices. *n* = 9-17 slices. Data are mean ± SEM (error bars); * p < 0.05, **p < 0.01 and *** p < 0.001, by unpaired t-test with Welch's correction (B), 1-way ANOVA with Tukey's multiple comparisons test (C) and 2-way ANOVA with Tukey's and Sidak's multiple comparisons test (G). Scale bars are 20µm (A and D) and 500µm (F).

Taken together, these data point towards a Myd88-dependent induction of TNF-α after lysolecithin-induced demyelination, which is able to enhance the phagocytic degradation of myelin debris and the generation of pre-myelinating / early myelinating oligodendrocytes. To further elucidate the impact of phagocyte-induced TNF-α in remyelination, we sought to generate a phagocyte-conditional knockout of TNF-α in zebrafish larvae. For that we have generated a mpeg1:Cas9 zebrafish line, by microinjection of a mpeg1:cas9/CY plasmid (harboring an α-crystallin:Venus (CY) as a transgenesis lens marker) into one-cell stage embryos (Fig. 3.10 A). Site-directed transgenesis into specific pre-determined genomic landing sites, has been established as an optimal alternative to random, multicopy Tol2-mediated transgene integration in various genomic loci. Briefly, the integrase phiC31 specifically recognizes the sequence of heterotypic binding sites called *attB* and *attP*. Therefore, the injection of a plasmid containing the *attB* site together with the mRNA of the integrase phiC31, into an organism containing the *attP* site in a known genomic location, results in the recombination of the binding sites and the generation of new *attL* and *attR* sites which are not recognized by the integrase, thus making the integration of the site-directed vector irreversible (Mosimann et al., 2013). Hence, we have confirmed successful integration of the plasmid through the green fluorescence expression under the control of the α-crystalin lens promoter present in the plasmid, and by the presence of the recombination sites *attL* and *attR* in the injected larvae (Fig. 3.10 B and C). After having confirmed the stable integration and germline transmission of the mpeg1:cas9/CY vector, we have further crossed this line with the reporter lines Tg(mpeg1:eGFP) and Tg(mbp-CAAX:mCherry). Therefore, we have now available zebrafish reporter lines that not only allow the visualization of phagocytes and myelin, but also, simultaneously, allow us to perform phagocyte-specific gene targeting. This, together with our newly established model of lysolecithin-induced demyelination in the spinal cord of the zebrafish larvae, represents a powerful tool for rapid assessment of phagocyte-specific functions in remyelination.

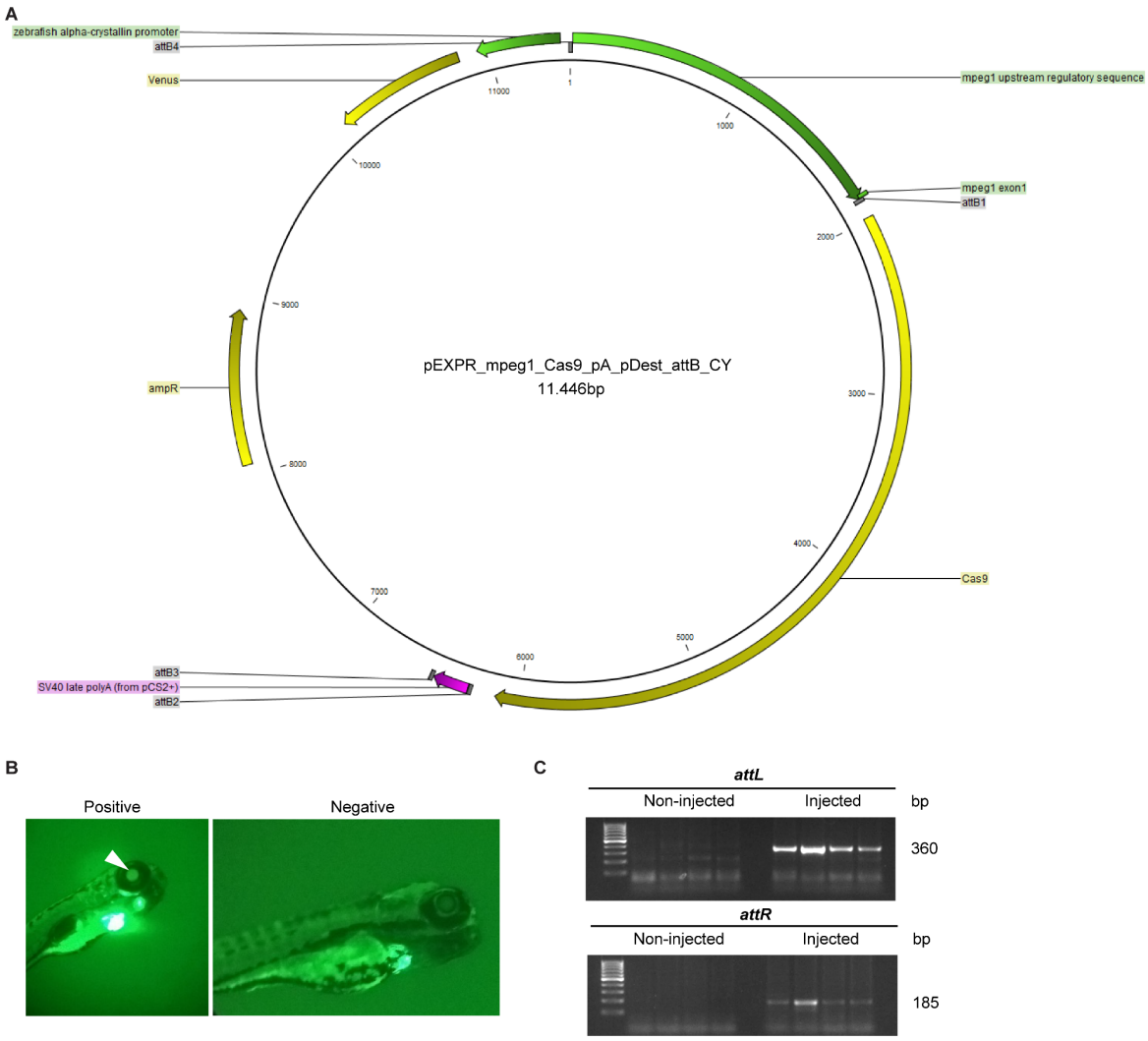

Figure 3.10 Generation of mpeg1:Cas9 transgenic zebrafish line. (A) Representation of the mpeg1:Cas9/CY plasmid vector injected in the *attP*-carrier zebrafish embryos at one cell stage. (B) Representative fluorescent images of injected larvae showing the positive α-crystallin:Venus (CY) lens marker vs. the negative non-injected larvae, at 5dpf. (C) Image of an agarose gel electrophoresis showing the presence of recombinant *attL* and *attR* sites in the injected vs. the non-injected larvae DNA, at 5dpf.

3.5. Early boost of phagocyte pro-inflammatory signaling seems to improve remyelination

Collectively, our results suggest that after a lysolecithin-induced demyelinating lesion, under-activation of phagocytes, by absence of pro-inflammatory Myd88 signaling, compromises remyelination and inflammation resolution, through impaired myelin debris degradation and oligodendrogenesis. We then wondered if, conversely, the overactivation of phagocytes through over-expression of pro-inflammatory Myd88 signaling, would lead to an overall improved lesion recovery, by means of faster inflammation resolution and remyelination. For that, we have used double transgenic Tg(mpeg1:eGFP) / Tg(mbp:mCherry-CAAX) zebrafish larvae, in which macrophages harbor a mutated version of the Myd88 protein (the substitution of a conserved amino acid, L265P), which increases Myd88 downstream signal (hereafter called constitutively active Myd88) (Roh-Johnson et al., 2017). We found that Myd88 constitutively active phagocytes did not seem to differ in their recruitment and infiltration into the site of injury, at 2 days post injection of lysolecithin in the spinal cord (Fig. 3.11 A and B). However, when we looked at the amount of mbp:mCherry-CAAX signal in the dorsal spinal cord, this seemed to be increased already at this time point, in the presence of phagocytes with constitutively active Myd88, compared to wild-type controls (Fig. 3.11 A and C).

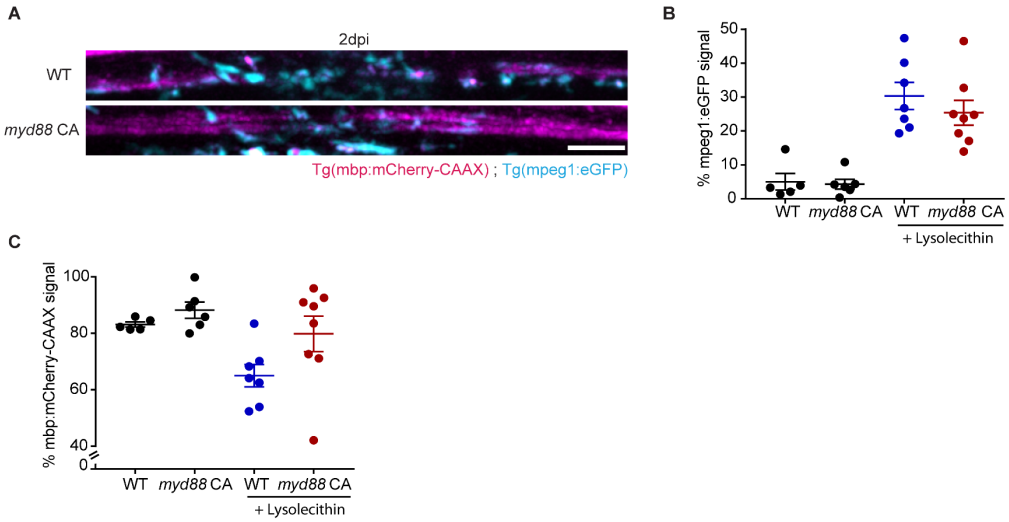

Figure 3.11 Larvae with Myd88-constitutively active phagocytes seem to have smaller lesions compared to controls. (A) Maximum intensity projections showing myelin in the spinal cord (magenta) and phagocytes (cyan), in lysolecithin-injected larvae, at 2dpi. (B) The infiltration of phagocytes was quantified by the total amount of mpeg1:eGFP signal in the dorsal spinal cord. (C) Myelination was quantified by the total amount of mbp:mCherry-CAAX signal in the dorsal spinal cord. *n* = 5-8 larvae. Images show lateral views of the lesion site, dorsal is down and anterior is left. Data are mean ± SEM (error bars). Scale bar is 50µm (A).

We then asked if the same was true in a mammalian model. As mentioned in previous sections, the ubiquitin-editing enzyme A20 plays a major role in shutting down the NF-κB pro-inflammatory pathway, by deubiquitination of the Ικκ complex. Therefore, we have induced lysolecithin-mediated demyelination in the corpus callosum of 2 months old $A20^{flox/flox}CX3CR1^{CreERT2/wt}$ ($A20^{CX3CR1\text{-}KO}$) mice, in which phagocytes are depleted of the A20 enzyme after tamoxifen injection, as previously reported (Voet et al., 2018). There was no difference in the weight of $A20^{CX3CR1\text{-}KO}$ mice, either after tamoxifen injections or in the first 3 days after lysolecithin injections in the corpus callosum, compared to $A20^{flox/flox}CX3CR1^{wt/wt}$ controls ($A20^{FL}$), implying that phagocyte-specific depletion of A20 did not compromise mice health *a priori* (Fig. 3.12 A and B). Next, we assessed the extent of demyelination at 21 days post lesion (dpl), time point where lysolecithin-induced demyelinating lesions in the corpus callosum of 2 months old wild-type mice are reported to already present robust remyelination (Crawford et al., 2016; Gregg et al., 2007; Jeffery and Blakemore, 1995). Notably, we found that $A20^{CX3CR1\text{-}KO}$ mice seemed to have smaller lesion volumes compared to their littermates, $A20^{FL}$ controls, by analyzing the volume of FluoroMyelin-depleted signal in the corpus callosum of lysolecithin-injected animals (Fig. 3.12 C and D). Furthermore, through analysis of the volume occupied by IBA1 signal, there also seemed to be less phagocyte infiltration in $A20^{CX3CR1\text{-}KO}$ lesions compared to $A20^{FL}$ controls, at 21dpl (Fig. 3.12 C and E).

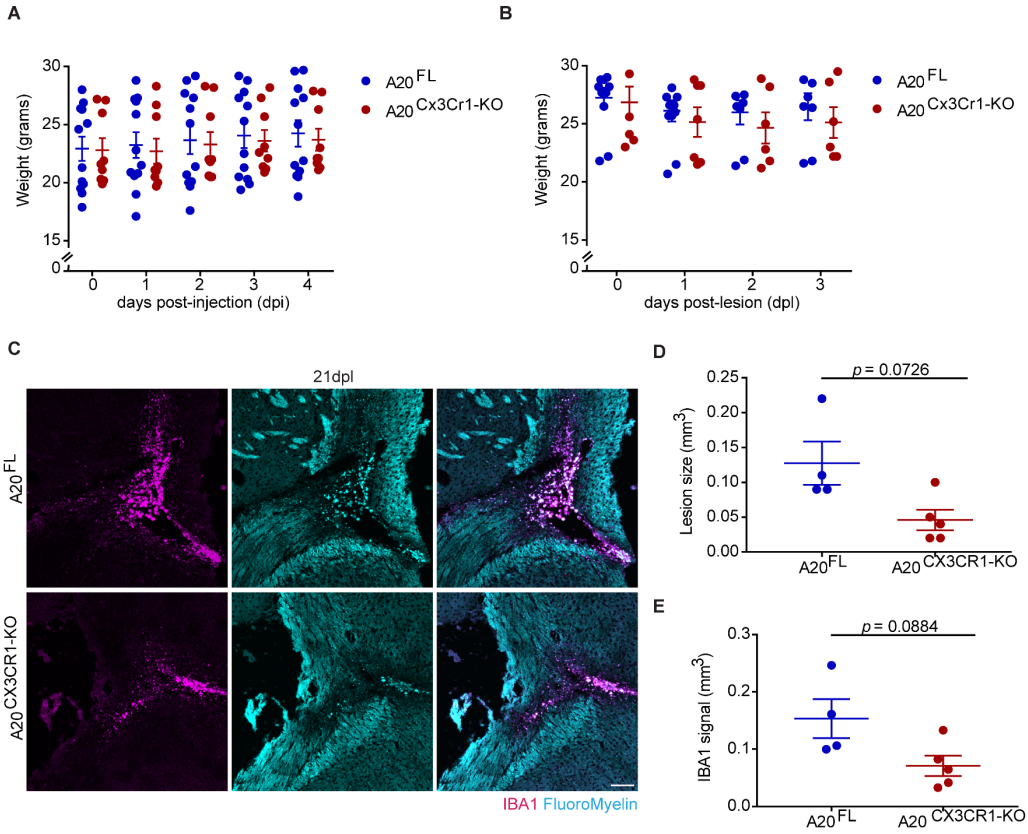

Figure 3.12 Phagocyte-specific A20 depletion in mice seems to result in better remyelination and faster inflammation resolution compared to controls. (A) Mice at 2 months were injected intraperitoneally with tamoxifen, once per day, for 5 days and weighed. (B) Two weeks after tamoxifen injection, mice were injected with lysolecithin in the corpus callosum and weighed before the surgery and 3 days after. (C) Images of the corpus callosum lesions showing phagocytes (magenta) and myelin (cyan), at 21dpl. (D) Lesion volumes were quantified by the lack of FluoroMyelin staining in the corpus callosum. (E) Phagocyte infiltration volume was quantified by determining the area occupied by the Iba1 signal throughout the entire lesion. *n* = 4-5 mice. Data are mean ± SEM (error bars). p values were calculated by unpaired t-test with Welch's correction (D and E). Scale bar is 100µm (C).

Altogether, these preliminary results suggest that an early boost of phagocyte-specific pro-inflammatory signaling after a lysolecithin-induced focal demyelinating lesion, might lead to improved remyelination.

4. Discussion

MS is the most common inflammation-mediated demyelinating disease of the CNS. Regardless of the years of research and the advances made in the development of new therapeutics, which significantly improve the exacerbation of symptoms in the acute stages of disease, we are still not able to stop its progression and chronicity. This results from the fact that we are still unclear about its etiology and we do not fully understand the molecular pathology, as well as the complex cellular interactions driving its progression. Phagocytes, here referred to microglia and macrophages, have been implicated in the different stages of the disease, due to their activation both in the early stages, before peripheral immune cell infiltration, as well as in later stages, after peripheral infiltration is no longer observed. In this study, we intended to understand the impact of phagocyte pro-inflammatory activation in the progression of a focal demyelinating lesion. We have established a new toxin-induced focal demyelination model in the spinal cord of zebrafish larvae and, in combination with the widely used mice lysolecithin model, found that Myd88-dependent pro-inflammatory signaling, following a demyelinating insult, is necessary for myelin debris clearance, and subsequent inflammation resolution, as well as for oligodendrocyte generation and remyelination. We further identified reduced expression of TNF-α in lesions of Myd88-deficient animals, and that addition of TNF-α after lysolecithin-induced demyelination was able to promote the generation of pre-myelinating / early myelinating oligodendrocytes.

Zebrafish represents an excellent model for dissecting the role of innate immune system in myelin repair. In addition to its advantages as a model organism, including the optically transparent larvae, which provide a strong tool for high-resolution *in vivo* live imaging, both myelination and inflammation basic mechanisms are conserved between zebrafish and mammals (Buckley et al., 2008; Forn-Cuni et al., 2017). We were interested in visualizing the *in vivo* cellular dynamics occurring after a focal demyelinating insult is induced. For that we have combined the strengths of the lysolecithin-induced demyelination model in mice with the advantages of the zebrafish larvae as a model organism. The kinetics of demyelination and remyelination in zebrafish spinal cord, as well as the recruitment of phagocytes into the lesion, occurred comparable with what we know from the mammalian system, although much faster. After a demyelinating insult, there is an influx of phagocytes which peak during demyelination, followed by their efflux correlated with the process of remyelination (Jeffery and Blakemore, 1995). Lysolecithin has been used as a focal demyelination model in the zebrafish before. In this case, it was used to induce demyelination in the optic nerve of adult zebrafish (Munzel et al., 2014). Here, the lesions, induced by a lysolecithin-soaked absorbable gelatin foam applied in the optic nerve, were characterized by phagocyte infiltration at day 4, demyelination at day 8, phagocyte efflux at day 14, an increase in oligodendrocytes at day 21 and full remyelination at day 28. However,

this model doesn't seem to bring any advantages over the mammalian model, since the time course seems to be very similar and, since it is performed in an adult zebrafish, it also does not take advantage of the optical transparency of the zebrafish larvae, therefore meaning that laborious IHC methods also have to be applied.

Phagocytes get in contact with and start clearing myelin debris the moment they arrive at the lesion site. This clearance has been reported to be critical for remyelination, since myelin debris were reported to inhibit oligodendrocyte differentiation and subsequent remyelination (Kotter et al., 2006; Lampron et al., 2015). CSF1R has been reported to play an important role in the development of most tissue-resident phagocytes, namely in their viability, proliferation and differentiation, and the lack of it in zebrafish and mice has been shown to lead to an absence of microglia (Ginhoux et al., 2010; Oosterhof et al., 2018; Stanley and Chitu, 2014). In our newly-established demyelination model, lysolecithin-induced demyelination in the spinal cord of zebrafish larvae lacking CNS resident phagocytes, through the depletion of CSF1R, results in compromised remyelination. This is in agreement with previous studies in which depletion of phagocytes has led to impaired remyelination, likely due to impaired myelin debris clearance and lack of secretion of pro-remyelination factors (Kondo et al., 2011; Kotter et al., 2001). Consistently with what we know from the mammalian model, concurrent with the peak of phagocyte infiltration following demyelination in zebrafish larvae, there was recruitment of OPCs to the site of injury, and together with phagocyte efflux there was an increase in MBP signal and in the number of mature oligodendrocytes (Jeffery and Blakemore, 1995; Keough et al., 2015; Miron et al., 2013; Ousman and David, 2000). Through both confocal and electron microscopy, we have observed that axonal damage occurs, although to a minimum extent. Nonetheless, essential features of the nervous system, as synapses, are preserved after lysolecithin injection in the spinal cord of zebrafish larvae. Also in the mammalian model of lysolecithin-induced demyelination, it has been shown that some axons are lost following the injection of lysolecithin (Woodruff and Franklin, 1999). Furthermore, in human MS lesions, axonal pathology and neuronal loss are also present as a secondary event following demyelination (Bitsch et al., 2001; De Stefano et al., 1998; Trapp et al., 1998). In this way, our study provides a new model of toxin-mediated demyelination in the spinal cord of zebrafish larvae, in which there is a conserved role of phagocytes, together with conserved kinetics of cellular dynamics in de- and remyelination, and minimal disruption of axonal integrity, comparable to the mammalian system, and from which we were able to acquire further insights on phagocyte function in remyelination.

In our zebrafish larvae model of demyelination, there is an early NF-κB pro-inflammatory activation in phagocytes after the demyelinating insult, which is Myd88-dependent. This is in agreement with previous studies using the immune-mediated EAE and the lysolecithin-

mediated models of demyelination in mice, in which phagocytes present in early stages of lesion formation are characterized by high expression of iNOS, and at later stages, concomitant with the start of remyelination, there is a shift in phagocyte activation characterized by high expression of Arg-1 (Locatelli et al., 2018; Miron et al., 2013). One of the studies further reports that iNOS$^+$ phagocytes are required for OPC proliferation, and that the shift to the latter anti-inflammatory phenotype is necessary for oligodendrocyte differentiation and remyelination (Miron et al., 2013). These results suggest that an early pro-inflammatory signaling in phagocytes after a demyelinating insult is necessary for recruiting the progenitor cells, which will drive remyelination through their differentiation into mature oligodendrocytes, if signaled by the late anti-inflammatory phagocytes (Lloyd et al., 2019; Lloyd and Miron, 2019; Miron and Franklin, 2014).

Notably, we found that in the absence of Myd88-dependent pro-inflammatory signaling, remyelination is impaired, with decreased OPC numbers, as well as mature oligodendrocytes and MBP signal, in the lesion site. This could be due to the lack of pro-remyelination signals, like secreted cytokines and growth factors. In fact, the absence of the pro-inflammatory cytokine TNF-α has been shown to lead to impaired remyelination in a cuprizone model of demyelination, through reduced OPC proliferation and subsequent reduced number of mature oligodendrocytes (Arnett et al., 2001). Accordingly, we have found that lesions of Myd88-deficient animals had decreased expression of TNF-α, and that the addition of TNF-α into lysolecithin-induced demyelinated *ex vivo* OCSCs, was able to promote the generation of new pre-myelinating / early myelinating oligodendrocytes, in the absence of Myd88. This is in contrast with previous reports where inhibition of soluble TNF-α in a cuprizone model of demyelination in mice is said to improve remyelination, but it is rather in line with clinical evidence in which treatment of MS patients with anti-TNF antibody has worsened disease progression, by an increase in the gadolinium-enhancing lesions, as well as leukocyte numbers and immunoglobulins in their cerebrospinal fluid (Karamita et al., 2017; van Oosten et al., 1996). Furthermore, treatment of MS patients, mainly relapsing-remitting MS, with a TNF-receptor fusion protein, lenercept, have shown increased and earlier exacerbations, characterized by the occurrence of a new symptom or the aggravating of a previous existent one, for at least 24h with no fever, and followed by a period of stability lasting 28 days (1999). Additionally, also the lack of the pro-inflammatory cytokine IL-1β has been found to lead to a reduced number of mature oligodendrocytes, and subsequent compromised remyelination, which was correlated with the lack of IGF-1 expression and not due to reduced phagocyte infiltration (Mason et al., 2001). Not long after, IL-1β was shown to promote the differentiation and maturation of oligodendrocytes, as well as their survival, possible through a p38 mitogen-activated protein kinase (MAPK) pathway, an important signal transduction pathway for the production of pro-inflammatory

cytokines (Vela et al., 2002). Together, these results further support the idea that the initial pro-inflammatory signal triggered after a demyelinating insult is critical for the release of pro-remyelinating factors, essential for driving a successful remyelination process.

Our results further show that in the absence of Myd88-dependent pro-inflammatory signaling, phagocytes are not able to fully degrade myelin debris, following phagocytosis, and that this is parallel with accumulation of lysosomes in Myd88-deficient phagocytes. Previous reports, using *in vitro* cultures of macrophages, have shown that the process of phagosome maturation, after phagocytosis of bacteria, is mediated and induced by Myd88 signaling, with increased fusion rates of bacteria-containing phagosome and lysosomes, in WT rather than Myd88-deficient macrophages, while the kinetics of phagosome maturation after internalization of apoptotic cells was the same (Blander and Medzhitov, 2004). This raises an interesting hypothesis in which myelin internalization seems to follow the same pattern as the defense against an invading pathogen. This could be related to the increased complexity of the multilayered, highly lipidic myelin membrane, which might require a strong antimicrobial defense in order to fully degrade it. Notably, our proteome analyses of *in vitro* primary microglia cultures, showed that the addition of myelin debris to microglia induces a pro-inflammatory response, characterized by upregulation of pathways classically involved in pathogen defense, like the INF-γ and TNF-α pathways, which are oppositely regulated in the absence of Myd88 signaling. This is in agreement with previous studies, where the addition of myelin to phagocytes *in vitro*, triggers a pro-inflammatory response, characterized by secretion of pro-inflammatory cytokines, like TNF-α, as well as nitric oxide and increased oxidative burst / ROS production (Liu et al., 2006; van der Laan et al., 1996; Wang et al., 2015; Williams et al., 1994).

It is interesting to think that while phagosome maturation may vary accordingly to different stimuli, such as cytokines, being stimulated in order to prevent presentation of self-peptides and autoimmunity, or delayed for the opposite, an under-activation by the lack of pro-inflammatory cytokines within an antigen-presenting cell, as the CNS resident phagocytes, might have direct implications in CNS autoimmunity (Pauwels et al., 2017). Interestingly, the blockage of TNF-α has been correlated with the onset of MS in more than one clinical case, treated with either a TNF-receptor soluble fusion protein, etanercept, or with TNF-α monoclonal antibodies, adalimumab and infliximab (Hare et al., 2014; Mohan et al., 2001; Sicotte and Voskuhl, 2001; Titelbaum et al., 2005). Notably, our results show that treatment of *in vitro* microglia cultures with TNF-α enhances the degradation of internalized myelin. This is in agreement with a previous study, showing that the same TNF-α blockers correlated above with the onset of MS, impaired phagosome maturation in macrophages and, conversely, the addition of TNF-α increased the phagosome maturation process of internalized *mycobacterium tuberculosis* (Harris et al., 2008).

The enhancement of myelin debris degradation through pro-inflammatory signaling, might explain why we observe impaired phagocyte efflux from the lesion site, and consequent defective remyelination, in Myd88-deficient animals. In fact, previous results from our lab have shown that defective clearance of myelin-derived cholesterol by phagocytes, after a demyelinating insult, leads to impaired inflammation resolution and compromised remyelination, together with stimulation of the inflammasomes (Cantuti-Castelvetri et al., 2018). In addition, it has been reported that continuous activation of phagocytes leads to their senescence, thereby making them functionally impaired, and our lab has also previously shown that increased myelin fragmentation, normally occurring with aging, contributes to microglia senescence (Safaiyan et al., 2016; Yu et al., 2012). Therefore, it is reasonable that the retention of non-responsive, myelin-loaded phagocytes in the site of injury, can prevent the generation of a pro-regenerative environment where recruited progenitor cells would be able to differentiate.

Previous reports have shown that TLR2 is present in oligodendrocytes and that inhibiting TLR2 activation increased oligodendrocyte maturation and remyelination, in a Myd88-dependent mechanism (Sloane et al., 2010; Wasko et al., 2019). Our results reveal that the overall inhibition of pro-inflammatory signaling, through a central inflammatory mediator as Myd88, overcomes the effects of TLR2-specific signaling in oligodendrocyte maturation, likely due to the lack of signals for OPC recruitment to the lesions, as well as their survival during differentiation into mature oligodendrocytes. Consistently with this is a previous report, showing that the administration of a TLR2 ligand into the retina of adult rats, causing inflammation seen through an increase in macrophages, astrocytes, and secreted cytokines, considerably enhances myelination by transplanted OPCs, characterized by an increase in MBP^{+} myelin sheaths (Setzu et al., 2006). Moreover, TLR2/4 stimulation, through LPS intraperitoneally injections in mice, was found to increase OPC recruitment to ethidium bromide-induced demyelinating lesions, improve myelin debris clearance, and enhance the expression of transcripts for myelin-related proteins, PLP and MOG (Glezer et al., 2006).

In line with a key role of innate immune pro-inflammatory activation in remyelination, early treatment of mice with mCSF together with an FDA-approved drug, amphotericin B, which stimulates phagocyte activation through a TIR-domain-containing adapter-inducing INF-β (TRIF) / Myd88-dependent manner, thereby causing an increased production of TNF-α, resulted in higher number of OPCs in lysolecithin-induced lesions, and a significant improvement in remyelination (Doring et al., 2015).

Remyelination can be observed in many active lesions, mainly in early or acute stages of disease progression, and recently it was reported that MS patients with more aggressive disease present a substantial increase in oligodendrocyte generation rate (Lassmann et al.,

1997; Yeung et al., 2019). Although evidently still in need of further experiments, our preliminary results with overactivation of pro-inflammatory signaling, through phagocyte-specific depletion of a critical negative regulator of the NF-κb-mediated activation, the deubiquitinase A20, or the constitutively active form of Myd88 in zebrafish larvae, suggest a consequent improvement in remyelination. Overactivation of phagocytes is usually related to detrimental and damage-inducing effects in several neuropathologies (Block et al., 2007; Prinz and Priller, 2014). Accordingly, previous results on the phagocyte-specific depletion of A20 in mice have reported to worsen EAE-induced demyelination (Voet et al., 2018). However, this contrasting results with our preliminary results might be due to the fact that in the EAE model, both demyelination and remyelination processes are concurrent, thus making it technically challenging to establish a specific correlation with either of the processes. On the other hand, our results are well in line with a previous report on the early induction of TLR4 / NF-κB signaling, through the administration of a synthetic TLR4 agonist (E6020) at the same time of lysolecithin-induced spinal cord demyelination in mice, which was shown to promote early phagocyte activation (based on CD11b immunoreactivity), improve myelin debris clearance, increase OPC proliferation and augment the number of remyelinated axons (Church et al., 2017). Our model of overactivation in mice consists of tamoxifen-inducible Cre-lox recombination, in which it is possible that, with the induction of an acute injury and the consequent turnover of myeloid cells, this phenotype is vanished in peripheral phagocytes at later stages of lesion evolution (Yona et al., 2013). It has been shown that in the absence of any injury, inducible Cre-lox recombination in microglia is achieved in ~80% of the cells and it is stable for at least 1 month after tamoxifen injection. On the other hand, peripheral phagocytes only show ~40% recombination 1 week after tamoxifen injection, which is progressively vanished, with recombination efficacy after 1 month dropping to ~10% (Zoller et al., 2018). However, it has been reported that peripheral phagocytes are mostly present only in the acute early stages of lysolecithin-induced demyelinating lesions and that microglia are the dominant phagocytic cell in these lesions, meaning that most of the phagocytes present throughout the course of the demyelinating lesion are likely depleted of the A20 enzyme, and thus, prompted to an exacerbated pro-inflammatory activation (Plemel et al., 2020). Nevertheless, it is conceivable that our model might represent only an early boost of pro-inflammatory signaling in phagocytes, rather than a persistent pro-inflammatory activation. It is possible that the cellular response to the process of myelin degradation, for instance through peroxisome proliferator-activated receptor (PPAR) pathway, is enough to counterbalance the increased pro-inflammatory signaling caused by A20-depletion, thus preventing a persistent overactivation of the cells (Bogie et al., 2013; Boven et al., 2006). Additionally, it is also reasonable that once the demyelinating-induced damage signals are neutralized by the phagocytes, the lack of TLR

stimuli in these cells also dampens the exacerbated pro-inflammatory signaling, triggered either by the A20-depletion in mice or the Myd88 constitutively active form in zebrafish.

In any case, that immune cell exhaustion, rather than its hyperactivation, may contribute to decreased remyelination efficiency, is strongly supported by studies in which old mice paired with young mice through parabiosis show enhanced remyelination with increased recruitment of phagocytes (Miron et al., 2013; Ruckh et al., 2012). This, together with our results, suggests that specific early pro-inflammatory activation in innate immune cells after a demyelinating insult in the CNS, is likely necessary to boost a regenerative response, and potentially enhance immune cell function in an overwhelmed system.

5. Concluding remarks and future perspectives

A large body of literature suggests that innate immune system hyperactivation in the CNS is guilty and causative of the development and fostering of several neurological disorders. But is this true or is it, in contrast, that the lack of activation, making the innate immune system functionally impaired, drives disease progression? Our study argues that lack of phagocyte activation in the CNS may be in the core of white matter pathology. This raises awareness and caution to the idea that shutting down all, and in a non-specific way, immune cell activation, holds the key to stop inflammatory-mediated disease progression, and is very much in line with the fact that current therapies aiming to stop inflammatory-mediated demyelinating diseases, which dampen peripheral inflammation, are factually not successful in ceasing disease progression.

Inflammation has the purpose of clearing the injured tissue of its harmful insult and prepare it for healing and regeneration, being responsible for returning it to a state of equilibrium. It is characterized by different phases which, given their existence in a temporally coordinated pattern, have different roles and purposes, important for the success of the regenerative process.

Our study underscores the importance of stimulating phagocyte activation in order to promote remyelination, following a demyelinating injury. We show that early pro-inflammatory activation of phagocytes is required to trigger the mechanisms of clearance of the ingested myelin debris, and that this is necessary for inflammation resolution, characterized by the efflux of phagocytes from the lesion, important to create a pro-regenerative environment, with the necessary signals for oligodendrocyte survival and subsequent remyelination (Fig. 5.1).

Nevertheless, this study still warrants further investigation in the effect of an early boost of pro-inflammatory signaling in myelin clearance and repair. For instance, the activation of the A20-depleted / Myd88-constitutively active phagocytes throughout the lesion evolution must be assessed, as well as the kinetics of myelin debris clearance and the kinetics of OPC recruitment and their differentiation. Additionally, a critical question regarding which specific signal(s) trigger phagocyte recruitment to the site of a demyelinating insult in the first place, is still to be answered. Therefore, we anticipate our newly established model of focal demyelination in the spinal cord of zebrafish larvae, to be a useful tool to, in combination with the mammalian model, further unravel the role of the innate immune system in myelin damage and repair. This will hopefully contribute to a better understanding of the etiology of autoimmune demyelination processes, and so, shed light on to novel potential targets for long-term regenerative therapeutics.

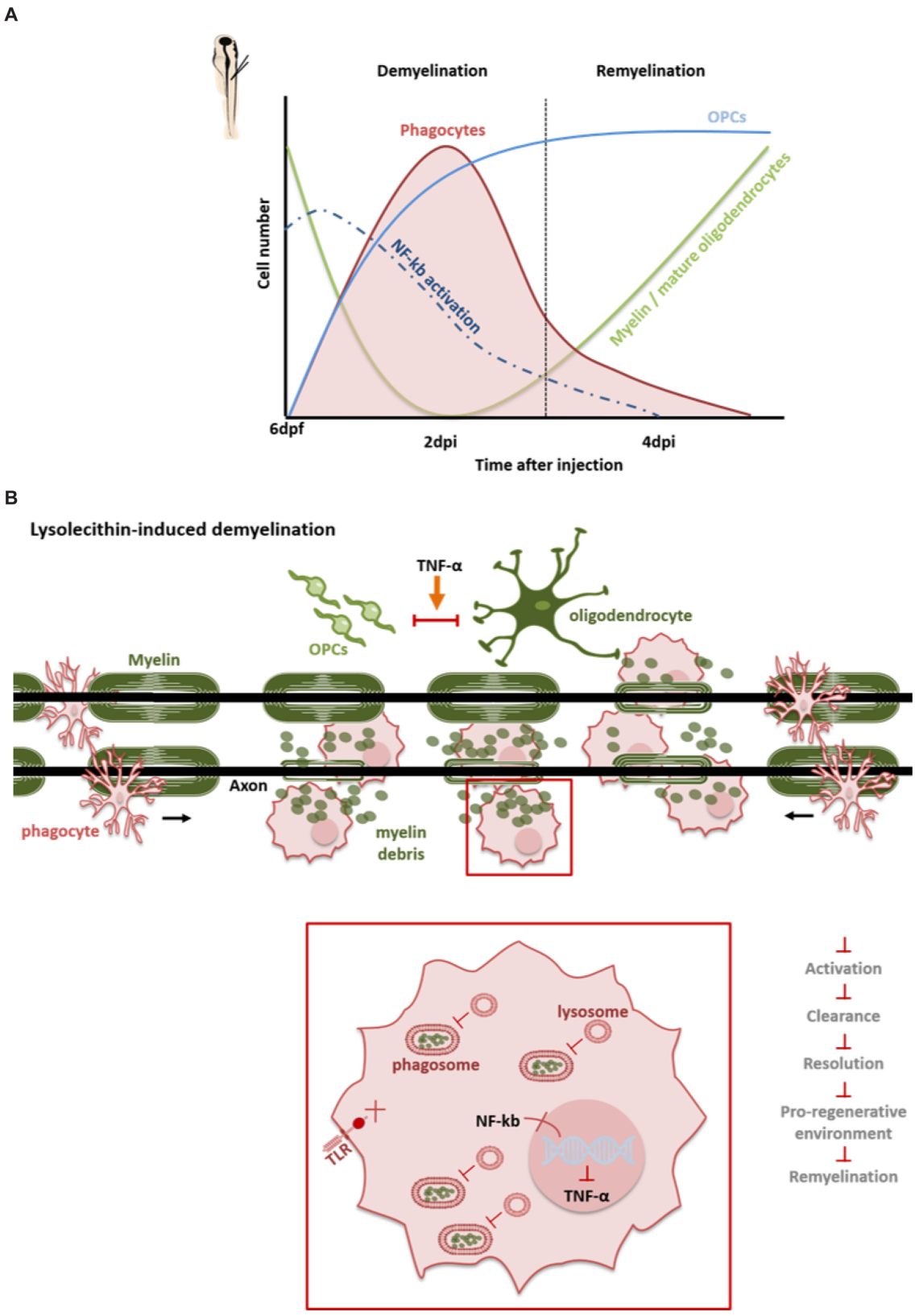

Figure 5.1 Schematic representation of the main findings of this study. (A) Focal injection of lysolecithin in the spinal cord of 6dpf zebrafish larvae, leads to a demyelination process, characterized by loss of myelin and mature oligodendrocytes, which extends up to 2dpi; this phase is also characterized by a fast infiltration of phagocytes into the lesion site, which peaks at 2dpi, together with the recruitment of OPCs; additionally, lysolecithin-induced demyelination triggers an early Myd88-dependent NF-κb activation in the recruited phagocytes, which progressively declines with lesion evolution. (continues on the bottom of the next page)

Figure 5.1 (continuation) This is followed by a phase of spontaneous remyelination observed at 4dpi, characterized by generation of new mature oligodendrocytes and recovery of myelin, as well as phagocyte efflux from the lesion. (B) After a lysolecithin-induced demyelinating insult, in zebrafish larvae and mice, phagocytes lacking Myd88-signaling are normally recruited to the lesion site and perform phagocytosis of myelin debris; however, in the absence of Myd88-signaling, the fusion rate of lysosome to myelin-containing phagosomes is reduced, compared to wild-type conditions, thereby leading to an accumulation of myelin debris and lysosomes inside the phagocytes; the impairment in internalized-myelin debris degradation leads to phagocyte retention in the lesions, which in turn is associated with reduced number of OPCs, a consequent reduced number of mature oligodendrocytes and impaired remyelination. Lack of Myd88-signaling leads to a reduced production of TNF-α in the lesions, and treatment of OCSC with TNF-α, after lysolecithin-induced demyelination, rescues the generation of pre-myelinating / early myelinating oligodendrocytes. In sum, the results obtained in this study imply that lack of phagocyte pro-inflammatory activation, after lysolecithin-induced demyelination, leads to impaired myelin debris clearance, which in turn leads to impaired inflammation resolution; consequently, under-activated phagocytes fail to provide a pro-regenerative environment, promoting OPC survival and differentiation, thereby compromising the remyelination process.

6. Supplementary information

The following supplementary videos can be found online in the original publication:

Pro-inflammatory activation following demyelination is required for myelin clearance and oligodendrogenesis

Maria Inês Cunha*, Minhui Su*, Ludovico Cantuti-Castelvetri, Stephan Mueller, Martina Schifferer, Minou Djannatian, Ioannis Alexopoulos, Franziska van der Meer, Anne Winkler, Tjakko van Ham, Bettina Schmid, Stefan Lichtenthaler, Christine Stadelmann, and Mikael Simons

J Exp Med (2020) 217 (5): e20191390.
https://doi.org/10.1084/jem.20191390

Video 1 – 2h time-lapse imaging of a spinal cord lesion showing phagocytes (cyan) actively stripping-off myelin (magenta) from the axons, at 2dpi. Time interval between frames was 12min. Scale bar is 20μm.

Video 2 – 2h time-lapse imaging of a spinal cord lesion showing phagocytes (cyan) actively moving with ingested myelin debris (magenta), in WT larvae, at 3dpi. Time interval between frames was 10min. Scale bar is 20μm.

Video 3 – 2h time-lapse imaging of a spinal cord lesion showing phagocytes (cyan) amoeboid and immobile and myelin (magenta), in *myd88* $^{-/-}$ larvae, at 3dpi. Time interval between frames was 10min. Scale bar is 20μm.

7. References

1999. TNF neutralization in MS: results of a randomized, placebo-controlled multicenter study. The Lenercept Multiple Sclerosis Study Group and The University of British Columbia MS/MRI Analysis Group. *Neurology* 53:457-465.

Aarum, J., K. Sandberg, S.L. Haeberlein, and M.A. Persson. 2003. Migration and differentiation of neural precursor cells can be directed by microglia. *Proc Natl Acad Sci U S A* 100:15983-15988.

Ackerman, S.D., and K.R. Monk. 2016. The scales and tales of myelination: using zebrafish and mouse to study myelinating glia. *Brain Res* 1641:79-91.

Akhmetzyanova, E., K. Kletenkov, Y. Mukhamedshina, and A. Rizvanov. 2019. Different Approaches to Modulation of Microglia Phenotypes After Spinal Cord Injury. *Front Syst Neurosci* 13:37.

Almeida, R.G. 2018. The Rules of Attraction in Central Nervous System Myelination. *Front Cell Neurosci* 12:367.

Almeida, R.G., T. Czopka, C. Ffrench-Constant, and D.A. Lyons. 2011. Individual axons regulate the myelinating potential of single oligodendrocytes in vivo. *Development* 138:4443-4450.

Arnett, H.A., S.P. Fancy, J.A. Alberta, C. Zhao, S.R. Plant, S. Kaing, C.S. Raine, D.H. Rowitch, R.J. Franklin, and C.D. Stiles. 2004. bHLH transcription factor Olig1 is required to repair demyelinated lesions in the CNS. *Science* 306:2111-2115.

Arnett, H.A., J. Mason, M. Marino, K. Suzuki, G.K. Matsushima, and J.P. Ting. 2001. TNF alpha promotes proliferation of oligodendrocyte progenitors and remyelination. *Nat Neurosci* 4:1116-1122.

Auer, F., S. Vagionitis, and T. Czopka. 2018. Evidence for Myelin Sheath Remodeling in the CNS Revealed by In Vivo Imaging. *Curr Biol* 28:549-559 e543.

Azevedo, M.M., H.S. Domingues, F.P. Cordelieres, P. Sampaio, A.I. Seixas, and J.B. Relvas. 2018. Jmy regulates oligodendrocyte differentiation via modulation of actin cytoskeleton dynamics. *Glia* 66:1826-1844.

Bammens, B., D. Peeters, J. Jaekers, K.J. Claes, P. Evenepoel, D. Kuypers, B. Meijers, M. Naesens, Y. Vanrenterghem, and D. Monbaliu. 2014. Postimplantation X-ray parameters predict functional catheter problems in peritoneal dialysis. *Kidney Int* 86:1001-1006.

Barateiro, A., and A. Fernandes. 2014. Temporal oligodendrocyte lineage progression: in vitro models of proliferation, differentiation and myelination. *Biochim Biophys Acta* 1843:1917-1929.

Beer, A., V. Biberacher, P. Schmidt, R. Righart, D. Buck, A. Berthele, J. Kirschke, C. Zimmer, B. Hemmer, and M. Muhlau. 2016. Tissue damage within normal appearing white matter in early multiple sclerosis: assessment by the ratio of T1- and T2-weighted MR image intensity. *J Neurol* 263:1495-1502.

Bergles, D.E., and W.D. Richardson. 2015. Oligodendrocyte Development and Plasticity. *Cold Spring Harb Perspect Biol* 8:a020453.

Bhat, R.V., K.J. Axt, J.S. Fosnaugh, K.J. Smith, K.A. Johnson, D.E. Hill, K.W. Kinzler, and J.M. Baraban. 1996. Expression of the APC tumor suppressor protein in oligodendroglia. *Glia* 17:169-174.

Birgbauer, E., T.S. Rao, and M. Webb. 2004. Lysolecithin induces demyelination in vitro in a cerebellar slice culture system. *J Neurosci Res* 78:157-166.

Bitsch, A., T. Kuhlmann, C. Stadelmann, H. Lassmann, C. Lucchinetti, and W. Bruck. 2001. A longitudinal MRI study of histopathologically defined hypointense multiple sclerosis lesions. *Ann Neurol* 49:793-796.

Bjelobaba, I., V. Begovic-Kupresanin, S. Pekovic, and I. Lavrnja. 2018. Animal models of multiple sclerosis: Focus on experimental autoimmune encephalomyelitis. *J Neurosci Res* 96:1021-1042.

Blakemore, W.F., and R.J. Franklin. 2008. Remyelination in experimental models of toxin-induced demyelination. *Curr Top Microbiol Immunol* 318:193-212.

Blander, J.M., and R. Medzhitov. 2004. Regulation of phagosome maturation by signals from toll-like receptors. *Science* 304:1014-1018.
Block, M.L., L. Zecca, and J.S. Hong. 2007. Microglia-mediated neurotoxicity: uncovering the molecular mechanisms. *Nat Rev Neurosci* 8:57-69.
Bogie, J.F., W. Jorissen, J. Mailleux, P.G. Nijland, N. Zelcer, T. Vanmierlo, J. Van Horssen, P. Stinissen, N. Hellings, and J.J. Hendriks. 2013. Myelin alters the inflammatory phenotype of macrophages by activating PPARs. *Acta Neuropathol Commun* 1:43.
Boven, L.A., M. Van Meurs, M. Van Zwam, A. Wierenga-Wolf, R.Q. Hintzen, R.G. Boot, J.M. Aerts, S. Amor, E.E. Nieuwenhuis, and J.D. Laman. 2006. Myelin-laden macrophages are anti-inflammatory, consistent with foam cells in multiple sclerosis. *Brain* 129:517-526.
Boyd, A., H. Zhang, and A. Williams. 2013. Insufficient OPC migration into demyelinated lesions is a cause of poor remyelination in MS and mouse models. *Acta Neuropathol* 125:841-859.
Bramow, S., J.M. Frischer, H. Lassmann, N. Koch-Henriksen, C.F. Lucchinetti, P.S. Sorensen, and H. Laursen. 2010. Demyelination versus remyelination in progressive multiple sclerosis. *Brain* 133:2983-2998.
Brandstadter, R., and I. Katz Sand. 2017. The use of natalizumab for multiple sclerosis. *Neuropsychiatr Dis Treat* 13:1691-1702.
Bruck, W., T. Kuhlmann, and C. Stadelmann. 2003. Remyelination in multiple sclerosis. *J Neurol Sci* 206:181-185.
Bruck, W., M. Schmied, G. Suchanek, Y. Bruck, H. Breitschopf, S. Poser, S. Piddlesden, and H. Lassmann. 1994. Oligodendrocytes in the early course of multiple sclerosis. *Ann Neurol* 35:65-73.
Buckley, C.E., P. Goldsmith, and R.J. Franklin. 2008. Zebrafish myelination: a transparent model for remyelination? *Dis Model Mech* 1:221-228.
Buckley, C.E., A. Marguerie, W.K. Alderton, and R.J. Franklin. 2010. Temporal dynamics of myelination in the zebrafish spinal cord. *Glia* 58:802-812.
Caldeira, C., A.F. Oliveira, C. Cunha, A.R. Vaz, A.S. Falcao, A. Fernandes, and D. Brites. 2014. Microglia change from a reactive to an age-like phenotype with the time in culture. *Front Cell Neurosci* 8:152.
Cantuti-Castelvetri, L., D. Fitzner, M. Bosch-Queralt, M.T. Weil, M. Su, P. Sen, T. Ruhwedel, M. Mitkovski, G. Trendelenburg, D. Lutjohann, W. Mobius, and M. Simons. 2018. Defective cholesterol clearance limits remyelination in the aged central nervous system. *Science* 359:684-688.
Cardona, A., S. Saalfeld, J. Schindelin, I. Arganda-Carreras, S. Preibisch, M. Longair, P. Tomancak, V. Hartenstein, and R.J. Douglas. 2012. TrakEM2 software for neural circuit reconstruction. *PLoS One* 7:e38011.
Chari, D.M., C. Zhao, M.R. Kotter, W.F. Blakemore, and R.J. Franklin. 2006. Corticosteroids delay remyelination of experimental demyelination in the rodent central nervous system. *J Neurosci Res* 83:594-605.
Chung, A.Y., P.S. Kim, S. Kim, E. Kim, D. Kim, I. Jeong, H.K. Kim, J.H. Ryu, C.H. Kim, J. Choi, J.H. Seo, and H.C. Park. 2013. Generation of demyelination models by targeted ablation of oligodendrocytes in the zebrafish CNS. *Mol Cells* 36:82-87.
Church, J.S., L.M. Milich, J.K. Lerch, P.G. Popovich, and D.M. McTigue. 2017. E6020, a synthetic TLR4 agonist, accelerates myelin debris clearance, Schwann cell infiltration, and remyelination in the rat spinal cord. *Glia* 65:883-899.
Crawford, A.H., R.B. Tripathi, W.D. Richardson, and R.J.M. Franklin. 2016. Developmental Origin of Oligodendrocyte Lineage Cells Determines Response to Demyelination and Susceptibility to Age-Associated Functional Decline. *Cell Rep* 15:761-773.
Crockett, D.P., M. Burshteyn, C. Garcia, M. Muggironi, and P. Casaccia-Bonnefil. 2005. Number of oligodendrocyte progenitors recruited to the lesioned spinal cord is modulated by the levels of the cell cycle regulatory protein p27Kip-1. *Glia* 49:301-308.

Cui, Q.L., T. Kuhlmann, V.E. Miron, S.Y. Leong, J. Fang, P. Gris, T.E. Kennedy, G. Almazan, and J. Antel. 2013. Oligodendrocyte progenitor cell susceptibility to injury in multiple sclerosis. *Am J Pathol* 183:516-525.

Cunha, M.I., M. Su, L. Cantuti-Castelvetri, S.A. Muller, M. Schifferer, M. Djannatian, I. Alexopoulos, F. van der Meer, A. Winkler, T.J. van Ham, B. Schmid, S.F. Lichtenthaler, C. Stadelmann, and M. Simons. 2020. Pro-inflammatory activation following demyelination is required for myelin clearance and oligodendrogenesis. *J Exp Med* 217:

Czopka, T. 2016. Insights into mechanisms of central nervous system myelination using zebrafish. *Glia* 64:333-349.

Czopka, T., and D.A. Lyons. 2011. Dissecting mechanisms of myelinated axon formation using zebrafish. *Methods Cell Biol* 105:25-62.

Dawson, M.R., A. Polito, J.M. Levine, and R. Reynolds. 2003. NG2-expressing glial progenitor cells: an abundant and widespread population of cycling cells in the adult rat CNS. *Mol Cell Neurosci* 24:476-488.

De Stefano, N., P.M. Matthews, L. Fu, S. Narayanan, J. Stanley, G.S. Francis, J.P. Antel, and D.L. Arnold. 1998. Axonal damage correlates with disability in patients with relapsing-remitting multiple sclerosis. Results of a longitudinal magnetic resonance spectroscopy study. *Brain* 121 (Pt 8):1469-1477.

Deguine, J., and G.M. Barton. 2014. MyD88: a central player in innate immune signaling. *F1000Prime Rep* 6:97.

Dendrou, C.A., L. Fugger, and M.A. Friese. 2015. Immunopathology of multiple sclerosis. *Nat Rev Immunol* 15:545-558.

Dheen, S.T., C. Kaur, and E.A. Ling. 2007. Microglial activation and its implications in the brain diseases. *Curr Med Chem* 14:1189-1197.

Dillenburg, A., G. Ireland, R.K. Holloway, C.L. Davies, F.L. Evans, M. Swire, M.E. Bechler, D. Soong, T.J. Yuen, G.H. Su, J.C. Becher, C. Smith, A. Williams, and V.E. Miron. 2018. Activin receptors regulate the oligodendrocyte lineage in health and disease. *Acta Neuropathol* 135:887-906.

Djannatian, M., S. Timmler, M. Arends, M. Luckner, M.T. Weil, I. Alexopoulos, N. Snaidero, B. Schmid, T. Misgeld, W. Mobius, M. Schifferer, E. Peles, and M. Simons. 2019. Two adhesive systems cooperatively regulate axon ensheathment and myelin growth in the CNS. *Nat Commun* 10:4794.

Dobson, R., and G. Giovannoni. 2019. Multiple sclerosis - a review. *Eur J Neurol* 26:27-40.

Doring, A., S. Sloka, L. Lau, M. Mishra, J. van Minnen, X. Zhang, D. Kinniburgh, S. Rivest, and V.W. Yong. 2015. Stimulation of monocytes, macrophages, and microglia by amphotericin B and macrophage colony-stimulating factor promotes remyelination. *J Neurosci* 35:1136-1148.

Doussau, F., J.L. Dupont, D. Neel, A. Schneider, B. Poulain, and J.L. Bossu. 2017. Organotypic cultures of cerebellar slices as a model to investigate demyelinating disorders. *Expert Opin Drug Discov* 12:1011-1022.

Duncan, I.D., R.L. Marik, A.T. Broman, and M. Heidari. 2017. Thin myelin sheaths as the hallmark of remyelination persist over time and preserve axon function. *Proc Natl Acad Sci U S A* 114:E9685-E9691.

Early, J.J., K.L. Cole, J.M. Williamson, M. Swire, H. Kamadurai, M. Muskavitch, and D.A. Lyons. 2018. An automated high-resolution in vivo screen in zebrafish to identify chemical regulators of myelination. *Elife* 7:

Erridge, C. 2010. Endogenous ligands of TLR2 and TLR4: agonists or assistants? *J Leukoc Biol* 87:989-999.

Faizi, M., A. Salimi, E. Seydi, P. Naserzadeh, M. Kouhnavard, A. Rahimi, and J. Pourahmad. 2016. Toxicity of cuprizone a Cu(2+) chelating agent on isolated mouse brain mitochondria: a justification for demyelination and subsequent behavioral dysfunction. *Toxicol Mech Methods* 26:276-283.

Fancy, S.P., C. Zhao, and R.J. Franklin. 2004. Increased expression of Nkx2.2 and Olig2 identifies reactive oligodendrocyte progenitor cells responding to demyelination in the adult CNS. *Mol Cell Neurosci* 27:247-254.
Fang, Y., X. Lei, X. Li, Y. Chen, F. Xu, X. Feng, S. Wei, and Y. Li. 2014. A novel model of demyelination and remyelination in a GFP-transgenic zebrafish. *Biol Open* 4:62-68.
Fard, M.K., F. van der Meer, P. Sanchez, L. Cantuti-Castelvetri, S. Mandad, S. Jakel, E.F. Fornasiero, S. Schmitt, M. Ehrlich, L. Starost, T. Kuhlmann, C. Sergiou, V. Schultz, C. Wrzos, W. Bruck, H. Urlaub, L. Dimou, C. Stadelmann, and M. Simons. 2017. BCAS1 expression defines a population of early myelinating oligodendrocytes in multiple sclerosis lesions. *Sci Transl Med* 9:
Filippi, M., A. Bar-Or, F. Piehl, P. Preziosa, A. Solari, S. Vukusic, and M.A. Rocca. 2018. Multiple sclerosis. *Nat Rev Dis Primers* 4:43.
Forn-Cuni, G., M. Varela, P. Pereiro, B. Novoa, and A. Figueras. 2017. Conserved gene regulation during acute inflammation between zebrafish and mammals. *Sci Rep* 7:41905.
Franco, P.G., L. Silvestroff, E.F. Soto, and J.M. Pasquini. 2008. Thyroid hormones promote differentiation of oligodendrocyte progenitor cells and improve remyelination after cuprizone-induced demyelination. *Exp Neurol* 212:458-467.
Franklin, R.J., and C. Ffrench-Constant. 2008. Remyelination in the CNS: from biology to therapy. *Nat Rev Neurosci* 9:839-855.
Franklin, R.J., and S.A. Goldman. 2015. Glia Disease and Repair-Remyelination. *Cold Spring Harb Perspect Biol* 7:a020594.
Freeman, S.A., A. Desmazieres, D. Fricker, C. Lubetzki, and N. Sol-Foulon. 2016. Mechanisms of sodium channel clustering and its influence on axonal impulse conduction. *Cell Mol Life Sci* 73:723-735.
Friese, M.A., and L. Fugger. 2007. T cells and microglia as drivers of multiple sclerosis pathology. *Brain* 130:2755-2757.
Gao, K. 2019. The genetic architecture of multiple sclerosis. *Nat Med* 25:1647.
Ginhoux, F., M. Greter, M. Leboeuf, S. Nandi, P. See, S. Gokhan, M.F. Mehler, S.J. Conway, L.G. Ng, E.R. Stanley, I.M. Samokhvalov, and M. Merad. 2010. Fate mapping analysis reveals that adult microglia derive from primitive macrophages. *Science* 330:841-845.
Glatigny, S., and E. Bettelli. 2018. Experimental Autoimmune Encephalomyelitis (EAE) as Animal Models of Multiple Sclerosis (MS). *Cold Spring Harb Perspect Med* 8:
Glezer, I., A. Lapointe, and S. Rivest. 2006. Innate immunity triggers oligodendrocyte progenitor reactivity and confines damages to brain injuries. *FASEB J* 20:750-752.
Godwin, J.W., A.R. Pinto, and N.A. Rosenthal. 2013. Macrophages are required for adult salamander limb regeneration. *Proc Natl Acad Sci U S A* 110:9415-9420.
Grajchen, E., J.J.A. Hendriks, and J.F.J. Bogie. 2018. The physiology of foamy phagocytes in multiple sclerosis. *Acta Neuropathol Commun* 6:124.
Gregg, C., V. Shikar, P. Larsen, G. Mak, A. Chojnacki, V.W. Yong, and S. Weiss. 2007. White matter plasticity and enhanced remyelination in the maternal CNS. *J Neurosci* 27:1812-1823.
Gudi, V., S. Gingele, T. Skripuletz, and M. Stangel. 2014. Glial response during cuprizone-induced de- and remyelination in the CNS: lessons learned. *Front Cell Neurosci* 8:73.
Hadas, S., M. Spira, U.K. Hanisch, F. Reichert, and S. Rotshenker. 2012. Complement receptor-3 negatively regulates the phagocytosis of degenerated myelin through tyrosine kinase Syk and cofilin. *J Neuroinflammation* 9:166.
Hagemeyer, N., K.M. Hanft, M.A. Akriditou, N. Unger, E.S. Park, E.R. Stanley, O. Staszewski, L. Dimou, and M. Prinz. 2017. Microglia contribute to normal myelinogenesis and to oligodendrocyte progenitor maintenance during adulthood. *Acta Neuropathol* 134:441-458.
Hall, S.M. 1972. The effect of injections of lysophosphatidyl choline into white matter of the adult mouse spinal cord. *J Cell Sci* 10:535-546.

Hammond, T.R., C. Dufort, L. Dissing-Olesen, S. Giera, A. Young, A. Wysoker, A.J. Walker, F. Gergits, M. Segel, J. Nemesh, S.E. Marsh, A. Saunders, E. Macosko, F. Ginhoux, J. Chen, R.J.M. Franklin, X. Piao, S.A. McCarroll, and B. Stevens. 2019. Single-Cell RNA Sequencing of Microglia throughout the Mouse Lifespan and in the Injured Brain Reveals Complex Cell-State Changes. *Immunity* 50:253-271 e256.

Harbo, H.F., R. Gold, and M. Tintore. 2013. Sex and gender issues in multiple sclerosis. *Ther Adv Neurol Disord* 6:237-248.

Hare, N.C., D.P. Hunt, K. Venugopal, G.T. Ho, T. Beez, C.W. Lees, R. Gibson, B. Weller, and J. Satsangi. 2014. Multiple sclerosis in the context of TNF blockade and inflammatory bowel disease. *QJM* 107:51-55.

Harris, J., J.C. Hope, and J. Keane. 2008. Tumor necrosis factor blockers influence macrophage responses to Mycobacterium tuberculosis. *J Infect Dis* 198:1842-1850.

Herbomel, P., B. Thisse, and C. Thisse. 2001. Zebrafish early macrophages colonize cephalic mesenchyme and developing brain, retina, and epidermis through a M-CSF receptor-dependent invasive process. *Dev Biol* 238:274-288.

Hinks, G.L., and R.J. Franklin. 2000. Delayed changes in growth factor gene expression during slow remyelination in the CNS of aged rats. *Mol Cell Neurosci* 16:542-556.

Hlavica, M., A. Delparente, A. Good, N. Good, P.S. Plattner, M.S. Seyedsadr, M.E. Schwab, D.P. Figlewicz, and B.V. Ineichen. 2017. Intrathecal insulin-like growth factor 1 but not insulin enhances myelin repair in young and aged rats. *Neurosci Lett* 648:41-46.

Hsieh, J., J.B. Aimone, B.K. Kaspar, T. Kuwabara, K. Nakashima, and F.H. Gage. 2004. IGF-I instructs multipotent adult neural progenitor cells to become oligodendrocytes. *J Cell Biol* 164:111-122.

Hu, X., R.K. Leak, Y. Shi, J. Suenaga, Y. Gao, P. Zheng, and J. Chen. 2015. Microglial and macrophage polarization-new prospects for brain repair. *Nat Rev Neurol* 11:56-64.

Jakimovski, D., C. Kolb, M. Ramanathan, R. Zivadinov, and B. Weinstock-Guttman. 2018. Interferon beta for Multiple Sclerosis. *Cold Spring Harb Perspect Med* 8:

Jarjour, A.A., C. Manitt, S.W. Moore, K.M. Thompson, S.J. Yuh, and T.E. Kennedy. 2003. Netrin-1 is a chemorepellent for oligodendrocyte precursor cells in the embryonic spinal cord. *J Neurosci* 23:3735-3744.

Jeffery, N.D., and W.F. Blakemore. 1995. Remyelination of mouse spinal cord axons demyelinated by local injection of lysolecithin. *J Neurocytol* 24:775-781.

Kanther, M., X. Sun, M. Muhlbauer, L.C. Mackey, E.J. Flynn, 3rd, M. Bagnat, C. Jobin, and J.F. Rawls. 2011. Microbial colonization induces dynamic temporal and spatial patterns of NF-kappaB activation in the zebrafish digestive tract. *Gastroenterology* 141:197-207.

Karamita, M., C. Barnum, W. Mobius, M.G. Tansey, D.E. Szymkowski, H. Lassmann, and L. Probert. 2017. Therapeutic inhibition of soluble brain TNF promotes remyelination by increasing myelin phagocytosis by microglia. *JCI Insight* 2:

Karttunen, M.J., T. Czopka, M. Goedhart, J.J. Early, and D.A. Lyons. 2017. Regeneration of myelin sheaths of normal length and thickness in the zebrafish CNS correlates with growth of axons in caliber. *PLoS One* 12:e0178058.

Keough, M.B., S.K. Jensen, and V.W. Yong. 2015. Experimental demyelination and remyelination of murine spinal cord by focal injection of lysolecithin. *J Vis Exp*

Kierdorf, K., and M. Prinz. 2017. Microglia in steady state. *J Clin Invest* 127:3201-3209.

Kigerl, K.A., J.C. Gensel, D.P. Ankeny, J.K. Alexander, D.J. Donnelly, and P.G. Popovich. 2009. Identification of two distinct macrophage subsets with divergent effects causing either neurotoxicity or regeneration in the injured mouse spinal cord. *J Neurosci* 29:13435-13444.

Kinchen, J.M., and K.S. Ravichandran. 2008. Phagosome maturation: going through the acid test. *Nat Rev Mol Cell Biol* 9:781-795.

Koellhoffer, E.C., L.D. McCullough, and R.M. Ritzel. 2017. Old Maids: Aging and Its Impact on Microglia Function. *Int J Mol Sci* 18:

Kondo, Y., J.M. Adams, M.T. Vanier, and I.D. Duncan. 2011. Macrophages counteract demyelination in a mouse model of globoid cell leukodystrophy. *J Neurosci* 31:3610-3624.
Kotter, M.R., W.W. Li, C. Zhao, and R.J. Franklin. 2006. Myelin impairs CNS remyelination by inhibiting oligodendrocyte precursor cell differentiation. *J Neurosci* 26:328-332.
Kotter, M.R., A. Setzu, F.J. Sim, N. Van Rooijen, and R.J. Franklin. 2001. Macrophage depletion impairs oligodendrocyte remyelination following lysolecithin-induced demyelination. *Glia* 35:204-212.
Kotter, M.R., C. Zhao, N. van Rooijen, and R.J. Franklin. 2005. Macrophage-depletion induced impairment of experimental CNS remyelination is associated with a reduced oligodendrocyte progenitor cell response and altered growth factor expression. *Neurobiol Dis* 18:166-175.
Kremer, D., R. Akkermann, P. Kury, and R. Dutta. 2019. Current advancements in promoting remyelination in multiple sclerosis. *Mult Scler* 25:7-14.
Kroehne, V., V. Tsata, L. Marrone, C. Froeb, S. Reinhardt, A. Gompf, A. Dahl, J. Sterneckert, and M.M. Reimer. 2017. Primary Spinal OPC Culture System from Adult Zebrafish to Study Oligodendrocyte Differentiation In Vitro. *Front Cell Neurosci* 11:284.
Kubota, Y., J. Sohn, S. Hatada, M. Schurr, J. Straehle, A. Gour, R. Neujahr, T. Miki, S. Mikula, and Y. Kawaguchi. 2018. A carbon nanotube tape for serial-section electron microscopy of brain ultrastructure. *Nat Commun* 9:437.
Kuhlmann, T., V. Miron, Q. Cui, C. Wegner, J. Antel, and W. Bruck. 2008. Differentiation block of oligodendroglial progenitor cells as a cause for remyelination failure in chronic multiple sclerosis. *Brain* 131:1749-1758.
Kuhn, S., L. Gritti, D. Crooks, and Y. Dombrowski. 2019. Oligodendrocytes in Development, Myelin Generation and Beyond. *Cells* 8:
Kutzelnigg, A., C.F. Lucchinetti, C. Stadelmann, W. Bruck, H. Rauschka, M. Bergmann, M. Schmidbauer, J.E. Parisi, and H. Lassmann. 2005. Cortical demyelination and diffuse white matter injury in multiple sclerosis. *Brain* 128:2705-2712.
Lam, S.H., H.L. Chua, Z. Gong, T.J. Lam, and Y.M. Sin. 2004. Development and maturation of the immune system in zebrafish, Danio rerio: a gene expression profiling, in situ hybridization and immunological study. *Dev Comp Immunol* 28:9-28.
Lampron, A., A. Larochelle, N. Laflamme, P. Prefontaine, M.M. Plante, M.G. Sanchez, V.W. Yong, P.K. Stys, M.E. Tremblay, and S. Rivest. 2015. Inefficient clearance of myelin debris by microglia impairs remyelinating processes. *J Exp Med* 212:481-495.
Lassmann, H., W. Bruck, C. Lucchinetti, and M. Rodriguez. 1997. Remyelination in multiple sclerosis. *Mult Scler* 3:133-136.
Levin, R., S. Grinstein, and J. Canton. 2016. The life cycle of phagosomes: formation, maturation, and resolution. *Immunol Rev* 273:156-179.
Levine, J.M., and R. Reynolds. 1999. Activation and proliferation of endogenous oligodendrocyte precursor cells during ethidium bromide-induced demyelination. *Exp Neurol* 160:333-347.
Levine, J.M., F. Stincone, and Y.S. Lee. 1993. Development and differentiation of glial precursor cells in the rat cerebellum. *Glia* 7:307-321.
Li, F., W.C. Liu, Q. Wang, Y. Sun, H. Wang, and X. Jin. 2020. NG2-glia cell proliferation and differentiation by glial growth factor 2 (GGF2), a strategy to promote functional recovery after ischemic stroke. *Biochem Pharmacol* 171:113720.
Li, W.W., A. Setzu, C. Zhao, and R.J. Franklin. 2005. Minocycline-mediated inhibition of microglia activation impairs oligodendrocyte progenitor cell responses and remyelination in a non-immune model of demyelination. *J Neuroimmunol* 158:58-66.
Liu, T., L. Zhang, D. Joo, and S.C. Sun. 2017. NF-kappaB signaling in inflammation. *Signal Transduct Target Ther* 2:
Liu, Y., W. Hao, M. Letiembre, S. Walter, M. Kulanga, H. Neumann, and K. Fassbender. 2006. Suppression of microglial inflammatory activity by myelin phagocytosis: role

of p47-PHOX-mediated generation of reactive oxygen species. *J Neurosci* 26:12904-12913.
Lively, S., and L.C. Schlichter. 2018. Microglia Responses to Pro-inflammatory Stimuli (LPS, IFNgamma+TNFalpha) and Reprogramming by Resolving Cytokines (IL-4, IL-10). *Front Cell Neurosci* 12:215.
Lloyd, A.F., C.L. Davies, R.K. Holloway, Y. Labrak, G. Ireland, D. Carradori, A. Dillenburg, E. Borger, D. Soong, J.C. Richardson, T. Kuhlmann, A. Williams, J.W. Pollard, A. des Rieux, J. Priller, and V.E. Miron. 2019. Central nervous system regeneration is driven by microglia necroptosis and repopulation. *Nat Neurosci* 22:1046-1052.
Lloyd, A.F., and V.E. Miron. 2019. The pro-remyelination properties of microglia in the central nervous system. *Nat Rev Neurol* 15:447-458.
Locatelli, G., D. Theodorou, A. Kendirli, M.J.C. Jordao, O. Staszewski, K. Phulphagar, L. Cantuti-Castelvetri, A. Dagkalis, A. Bessis, M. Simons, F. Meissner, M. Prinz, and M. Kerschensteiner. 2018. Mononuclear phagocytes locally specify and adapt their phenotype in a multiple sclerosis model. *Nat Neurosci* 21:1196-1208.
Lucchinetti, C., W. Bruck, J. Parisi, B. Scheithauer, M. Rodriguez, and H. Lassmann. 1999. A quantitative analysis of oligodendrocytes in multiple sclerosis lesions. A study of 113 cases. *Brain* 122 (Pt 12):2279-2295.
Mantovani, A., A. Sica, S. Sozzani, P. Allavena, A. Vecchi, and M. Locati. 2004. The chemokine system in diverse forms of macrophage activation and polarization. *Trends Immunol* 25:677-686.
Mason, J.L., K. Suzuki, D.D. Chaplin, and G.K. Matsushima. 2001. Interleukin-1beta promotes repair of the CNS. *J Neurosci* 21:7046-7052.
Mazaheri, F., O. Breus, S. Durdu, P. Haas, J. Wittbrodt, D. Gilmour, and F. Peri. 2014. Distinct roles for BAI1 and TIM-4 in the engulfment of dying neurons by microglia. *Nat Commun* 5:4046.
Mazzolini, J., S. Le Clerc, G. Morisse, C. Coulonges, L.E. Kuil, T.J. van Ham, J.F. Zagury, and D. Sieger. 2020. Gene expression profiling reveals a conserved microglia signature in larval zebrafish. *Glia* 68:298-315.
McKinnon, R.D., G. Piras, J.A. Ida, Jr., and M. Dubois-Dalcq. 1993. A role for TGF-beta in oligodendrocyte differentiation. *J Cell Biol* 121:1397-1407.
McMurran, C.E., C.A. Jones, D.C. Fitzgerald, and R.J. Franklin. 2016. CNS Remyelination and the Innate Immune System. *Front Cell Dev Biol* 4:38.
Mi, S., B. Hu, K. Hahm, Y. Luo, E.S. Kam Hui, Q. Yuan, W.M. Wong, L. Wang, H. Su, T.H. Chu, J. Guo, W. Zhang, K.F. So, B. Pepinsky, Z. Shao, C. Graff, E. Garber, V. Jung, E.X. Wu, and W. Wu. 2007. LINGO-1 antagonist promotes spinal cord remyelination and axonal integrity in MOG-induced experimental autoimmune encephalomyelitis. *Nat Med* 13:1228-1233.
Michalski, J.P., and R. Kothary. 2015. Oligodendrocytes in a Nutshell. *Front Cell Neurosci* 9:340.
Miron, V.E. 2017. Microglia-driven regulation of oligodendrocyte lineage cells, myelination, and remyelination. *J Leukoc Biol* 101:1103-1108.
Miron, V.E., A. Boyd, J.W. Zhao, T.J. Yuen, J.M. Ruckh, J.L. Shadrach, P. van Wijngaarden, A.J. Wagers, A. Williams, R.J.M. Franklin, and C. Ffrench-Constant. 2013. M2 microglia and macrophages drive oligodendrocyte differentiation during CNS remyelination. *Nat Neurosci* 16:1211-1218.
Miron, V.E., and R.J. Franklin. 2014. Macrophages and CNS remyelination. *J Neurochem* 130:165-171.
Miron, V.E., T. Kuhlmann, and J.P. Antel. 2011. Cells of the oligodendroglial lineage, myelination, and remyelination. *Biochim Biophys Acta* 1812:184-193.
Mirza, R., L.A. DiPietro, and T.J. Koh. 2009. Selective and specific macrophage ablation is detrimental to wound healing in mice. *Am J Pathol* 175:2454-2462.
Mitchell, D.M., A.G. Lovel, and D.L. Stenkamp. 2018. Dynamic changes in microglial and macrophage characteristics during degeneration and regeneration of the zebrafish retina. *J Neuroinflammation* 15:163.

Mohan, N., E.T. Edwards, T.R. Cupps, P.J. Oliverio, G. Sandberg, H. Crayton, J.R. Richert, and J.N. Siegel. 2001. Demyelination occurring during anti-tumor necrosis factor alpha therapy for inflammatory arthritides. *Arthritis Rheum* 44:2862-2869.

Mosimann, C., A.C. Puller, K.L. Lawson, P. Tschopp, A. Amsterdam, and L.I. Zon. 2013. Site-directed zebrafish transgenesis into single landing sites with the phiC31 integrase system. *Dev Dyn* 242:949-963.

Munzel, E.J., C.G. Becker, T. Becker, and A. Williams. 2014. Zebrafish regenerate full thickness optic nerve myelin after demyelination, but this fails with increasing age. *Acta Neuropathol Commun* 2:77.

Natrajan, M.S., A.G. de la Fuente, A.H. Crawford, E. Linehan, V. Nunez, K.R. Johnson, T. Wu, D.C. Fitzgerald, M. Ricote, B. Bielekova, and R.J. Franklin. 2015. Retinoid X receptor activation reverses age-related deficiencies in myelin debris phagocytosis and remyelination. *Brain* 138:3581-3597.

Nave, K.A., and B.D. Trapp. 2008. Axon-glial signaling and the glial support of axon function. *Annu Rev Neurosci* 31:535-561.

Neumann, H., M.R. Kotter, and R.J. Franklin. 2009. Debris clearance by microglia: an essential link between degeneration and regeneration. *Brain* 132:288-295.

Newcombe, E.A., J. Camats-Perna, M.L. Silva, N. Valmas, T.J. Huat, and R. Medeiros. 2018. Inflammation: the link between comorbidities, genetics, and Alzheimer's disease. *J Neuroinflammation* 15:276.

Novoa, B., and A. Figueras. 2012. Zebrafish: model for the study of inflammation and the innate immune response to infectious diseases. *Adv Exp Med Biol* 946:253-275.

Oosterhof, N., L.E. Kuil, H.C. van der Linde, S.M. Burm, W. Berdowski, W.F.J. van Ijcken, J.C. van Swieten, E.M. Hol, M.H.G. Verheijen, and T.J. van Ham. 2018. Colony-Stimulating Factor 1 Receptor (CSF1R) Regulates Microglia Density and Distribution, but Not Microglia Differentiation In Vivo. *Cell Rep* 24:1203-1217 e1206.

Ousman, S.S., and S. David. 2000. Lysophosphatidylcholine induces rapid recruitment and activation of macrophages in the adult mouse spinal cord. *Glia* 30:92-104.

Palazuelos, J., M. Klingener, and A. Aguirre. 2014. TGFbeta signaling regulates the timing of CNS myelination by modulating oligodendrocyte progenitor cell cycle exit through SMAD3/4/FoxO1/Sp1. *J Neurosci* 34:7917-7930.

Pasquini, L.A., V. Millet, H.C. Hoyos, J.P. Giannoni, D.O. Croci, M. Marder, F.T. Liu, G.A. Rabinovich, and J.M. Pasquini. 2011. Galectin-3 drives oligodendrocyte differentiation to control myelin integrity and function. *Cell Death Differ* 18:1746-1756.

Pauwels, A.M., M. Trost, R. Beyaert, and E. Hoffmann. 2017. Patterns, Receptors, and Signals: Regulation of Phagosome Maturation. *Trends Immunol* 38:407-422.

Peri, F., and C. Nusslein-Volhard. 2008. Live imaging of neuronal degradation by microglia reveals a role for v0-ATPase a1 in phagosomal fusion in vivo. *Cell* 133:916-927.

Perry, V.H. 1998. A revised view of the central nervous system microenvironment and major histocompatibility complex class II antigen presentation. *J Neuroimmunol* 90:113-121.

Plemel, J.R., S.B. Manesh, J.S. Sparling, and W. Tetzlaff. 2013. Myelin inhibits oligodendroglial maturation and regulates oligodendrocytic transcription factor expression. *Glia* 61:1471-1487.

Plemel, J.R., J.A. Stratton, N.J. Michaels, K.S. Rawji, E. Zhang, S. Sinha, C.S. Baaklini, Y. Dong, M. Ho, K. Thorburn, T.N. Friedman, S. Jawad, C. Silva, A.V. Caprariello, V. Hoghooghi, J. Yue, A. Jaffer, K. Lee, B.J. Kerr, R. Midha, P.K. Stys, J. Biernaskie, and V.W. Yong. 2020. Microglia response following acute demyelination is heterogeneous and limits infiltrating macrophage dispersion. *Sci Adv* 6:eaay6324.

Poirier, V., and Y. Av-Gay. 2012. Mycobacterium tuberculosis modulators of the macrophage's cellular events. *Microbes Infect* 14:1211-1219.

Preston, M.A., and W.B. Macklin. 2015. Zebrafish as a model to investigate CNS myelination. *Glia* 63:177-193.

Prinz, M., and J. Priller. 2014. Microglia and brain macrophages in the molecular age: from origin to neuropsychiatric disease. *Nat Rev Neurosci* 15:300-312.
Pu, A., E.L. Stephenson, and V.W. Yong. 2018. The extracellular matrix: Focus on oligodendrocyte biology and targeting CSPGs for remyelination therapies. *Glia* 66:1809-1825.
Rasmussen, S., Y. Wang, P. Kivisakk, R.T. Bronson, M. Meyer, J. Imitola, and S.J. Khoury. 2007. Persistent activation of microglia is associated with neuronal dysfunction of callosal projecting pathways and multiple sclerosis-like lesions in relapsing--remitting experimental autoimmune encephalomyelitis. *Brain* 130:2816-2829.
Redwine, J.M., K.L. Blinder, and R.C. Armstrong. 1997. In situ expression of fibroblast growth factor receptors by oligodendrocyte progenitors and oligodendrocytes in adult mouse central nervous system. *J Neurosci Res* 50:229-237.
Reich, D.S., C.F. Lucchinetti, and P.A. Calabresi. 2018. Multiple Sclerosis. *N Engl J Med* 378:169-180.
Rifkin, I.R., E.A. Leadbetter, L. Busconi, G. Viglianti, and A. Marshak-Rothstein. 2005. Toll-like receptors, endogenous ligands, and systemic autoimmune disease. *Immunol Rev* 204:27-42.
Robinson, A.P., C.T. Harp, A. Noronha, and S.D. Miller. 2014. The experimental autoimmune encephalomyelitis (EAE) model of MS: utility for understanding disease pathophysiology and treatment. *Handb Clin Neurol* 122:173-189.
Robinson, S., and R.H. Miller. 1999. Contact with central nervous system myelin inhibits oligodendrocyte progenitor maturation. *Dev Biol* 216:359-368.
Roh-Johnson, M., A.N. Shah, J.A. Stonick, K.R. Poudel, J. Kargl, G.H. Yang, J. di Martino, R.E. Hernandez, C.E. Gast, L.R. Zarour, S. Antoku, A.M. Houghton, J.J. Bravo-Cordero, M.H. Wong, J. Condeelis, and C.B. Moens. 2017. Macrophage-Dependent Cytoplasmic Transfer during Melanoma Invasion In Vivo. *Dev Cell* 43:549-562 e546.
Rossi, F., A.M. Casano, K. Henke, K. Richter, and F. Peri. 2015. The SLC7A7 Transporter Identifies Microglial Precursors prior to Entry into the Brain. *Cell Rep* 11:1008-1017.
Ruckh, J.M., J.W. Zhao, J.L. Shadrach, P. van Wijngaarden, T.N. Rao, A.J. Wagers, and R.J. Franklin. 2012. Rejuvenation of regeneration in the aging central nervous system. *Cell Stem Cell* 10:96-103.
Ruggieri, S., C. Tortorella, and C. Gasperini. 2017. Anti lingo 1 (opicinumab) a new monoclonal antibody tested in relapsing remitting multiple sclerosis. *Expert Rev Neurother* 17:1081-1089.
Ruland, J. 2011. Return to homeostasis: downregulation of NF-kappaB responses. *Nat Immunol* 12:709-714.
Safaiyan, S., N. Kannaiyan, N. Snaidero, S. Brioschi, K. Biber, S. Yona, A.L. Edinger, S. Jung, M.J. Rossner, and M. Simons. 2016. Age-related myelin degradation burdens the clearance function of microglia during aging. *Nat Neurosci* 19:995-998.
Saijo, K., and C.K. Glass. 2011. Microglial cell origin and phenotypes in health and disease. *Nat Rev Immunol* 11:775-787.
Sasaki, T., S. Lian, A. Khan, J.R. Llop, A.V. Samuelson, W. Chen, D.J. Klionsky, and S. Kishi. 2017. Autolysosome biogenesis and developmental senescence are regulated by both Spns1 and v-ATPase. *Autophagy* 13:386-403.
Schafer, D.P., E.K. Lehrman, A.G. Kautzman, R. Koyama, A.R. Mardinly, R. Yamasaki, R.M. Ransohoff, M.E. Greenberg, B.A. Barres, and B. Stevens. 2012. Microglia sculpt postnatal neural circuits in an activity and complement-dependent manner. *Neuron* 74:691-705.
Scott, L.J. 2011. Fingolimod: a review of its use in the management of relapsing-remitting multiple sclerosis. *CNS Drugs* 25:673-698.
Seixas, A.I., M.M. Azevedo, J. Paes de Faria, D. Fernandes, I. Mendes Pinto, and J.B. Relvas. 2019. Evolvability of the actin cytoskeleton in oligodendrocytes during central nervous system development and aging. *Cell Mol Life Sci* 76:1-11.

Setzu, A., J.D. Lathia, C. Zhao, K. Wells, M.S. Rao, C. Ffrench-Constant, and R.J. Franklin. 2006. Inflammation stimulates myelination by transplanted oligodendrocyte precursor cells. *Glia* 54:297-303.

Shen, S., J. Sandoval, V.A. Swiss, J. Li, J. Dupree, R.J. Franklin, and P. Casaccia-Bonnefil. 2008. Age-dependent epigenetic control of differentiation inhibitors is critical for remyelination efficiency. *Nat Neurosci* 11:1024-1034.

Sicotte, N.L., and R.R. Voskuhl. 2001. Onset of multiple sclerosis associated with anti-TNF therapy. *Neurology* 57:1885-1888.

Sim, F.J., C. Zhao, J. Penderis, and R.J. Franklin. 2002. The age-related decrease in CNS remyelination efficiency is attributable to an impairment of both oligodendrocyte progenitor recruitment and differentiation. *J Neurosci* 22:2451-2459.

Simone, I.L., D. Carrara, C. Tortorella, A. Ceccarelli, and P. Livrea. 2000. Early onset multiple sclerosis. *Neurol Sci* 21:S861-863.

Simons, M., and K.A. Nave. 2015. Oligodendrocytes: Myelination and Axonal Support. *Cold Spring Harb Perspect Biol* 8:a020479.

Skaper, S.D. 2019. Oligodendrocyte precursor cells as a therapeutic target for demyelinating diseases. *Prog Brain Res* 245:119-144.

Slauch, J.M. 2011. How does the oxidative burst of macrophages kill bacteria? Still an open question. *Mol Microbiol* 80:580-583.

Sloane, J.A., C. Batt, Y. Ma, Z.M. Harris, B. Trapp, and T. Vartanian. 2010. Hyaluronan blocks oligodendrocyte progenitor maturation and remyelination through TLR2. *Proc Natl Acad Sci U S A* 107:11555-11560.

Snaidero, N., W. Mobius, T. Czopka, L.H. Hekking, C. Mathisen, D. Verkleij, S. Goebbels, J. Edgar, D. Merkler, D.A. Lyons, K.A. Nave, and M. Simons. 2014. Myelin membrane wrapping of CNS axons by PI(3,4,5)P3-dependent polarized growth at the inner tongue. *Cell* 156:277-290.

Snaidero, N., and M. Simons. 2014. Myelination at a glance. *J Cell Sci* 127:2999-3004.

Stadelmann, C., S. Timmler, A. Barrantes-Freer, and M. Simons. 2019. Myelin in the Central Nervous System: Structure, Function, and Pathology. *Physiol Rev* 99:1381-1431.

Stanley, E.R., and V. Chitu. 2014. CSF-1 receptor signaling in myeloid cells. *Cold Spring Harb Perspect Biol* 6:

Steelman, A.J., Y. Zhou, H. Koito, S. Kim, H.R. Payne, Q.R. Lu, and J. Li. 2016. Activation of oligodendroglial Stat3 is required for efficient remyelination. *Neurobiol Dis* 91:336-346.

Streit, W.J., Q.S. Xue, J. Tischer, and I. Bechmann. 2014. Microglial pathology. *Acta Neuropathol Commun* 2:142.

Sun, D., Z. Yu, X. Fang, M. Liu, Y. Pu, Q. Shao, D. Wang, X. Zhao, A. Huang, Z. Xiang, C. Zhao, R.J. Franklin, L. Cao, and C. He. 2017. LncRNA GAS5 inhibits microglial M2 polarization and exacerbates demyelination. *EMBO Rep* 18:1801-1816.

Syed, Y.A., A.S. Baer, G. Lubec, H. Hoeger, G. Widhalm, and M.R. Kotter. 2008. Inhibition of oligodendrocyte precursor cell differentiation by myelin-associated proteins. *Neurosurg Focus* 24:E5.

Tepavcevic, V., C. Kerninon, M.S. Aigrot, E. Meppiel, S. Mozafari, R. Arnould-Laurent, P. Ravassard, T.E. Kennedy, B. Nait-Oumesmar, and C. Lubetzki. 2014. Early netrin-1 expression impairs central nervous system remyelination. *Ann Neurol* 76:252-268.

Thetiot, M., R. Ronzano, M.S. Aigrot, C. Lubetzki, and A. Desmazieres. 2019. Preparation and Immunostaining of Myelinating Organotypic Cerebellar Slice Cultures. *J Vis Exp*

Titelbaum, D.S., A. Degenhardt, and R.P. Kinkel. 2005. Anti-tumor necrosis factor alpha-associated multiple sclerosis. *AJNR Am J Neuroradiol* 26:1548-1550.

Torkildsen, O., L.A. Brunborg, K.M. Myhr, and L. Bo. 2008. The cuprizone model for demyelination. *Acta Neurol Scand Suppl* 188:72-76.

Torres, L., J. Danver, K. Ji, J.T. Miyauchi, D. Chen, M.E. Anderson, B.L. West, J.K. Robinson, and S.E. Tsirka. 2016. Dynamic microglial modulation of spatial learning and social behavior. *Brain Behav Immun* 55:6-16.

Town, T., V. Nikolic, and J. Tan. 2005. The microglial "activation" continuum: from innate to adaptive responses. *J Neuroinflammation* 2:24.

Trapp, B.D., J. Peterson, R.M. Ransohoff, R. Rudick, S. Mork, and L. Bo. 1998. Axonal transection in the lesions of multiple sclerosis. *N Engl J Med* 338:278-285.

Tsarouchas, T.M., D. Wehner, L. Cavone, T. Munir, M. Keatinge, M. Lambertus, A. Underhill, T. Barrett, E. Kassapis, N. Ogryzko, Y. Feng, T.J. van Ham, T. Becker, and C.G. Becker. 2018. Dynamic control of proinflammatory cytokines Il-1beta and Tnf-alpha by macrophages in zebrafish spinal cord regeneration. *Nat Commun* 9:4670.

Vacaru, A.M., G. Unlu, M. Spitzner, M. Mione, E.W. Knapik, and K.C. Sadler. 2014. In vivo cell biology in zebrafish - providing insights into vertebrate development and disease. *J Cell Sci* 127:485-495.

van der Laan, L.J., S.R. Ruuls, K.S. Weber, I.J. Lodder, E.A. Dopp, and C.D. Dijkstra. 1996. Macrophage phagocytosis of myelin in vitro determined by flow cytometry: phagocytosis is mediated by CR3 and induces production of tumor necrosis factor-alpha and nitric oxide. *J Neuroimmunol* 70:145-152.

van Deursen, J.M. 2014. The role of senescent cells in ageing. *Nature* 509:439-446.

van Horssen, J., S. Singh, S. van der Pol, M. Kipp, J.L. Lim, L. Peferoen, W. Gerritsen, E.J. Kooi, M.E. Witte, J.J. Geurts, H.E. de Vries, R. Peferoen-Baert, P.J. van den Elsen, P. van der Valk, and S. Amor. 2012. Clusters of activated microglia in normal-appearing white matter show signs of innate immune activation. *J Neuroinflammation* 9:156.

van Oosten, B.W., F. Barkhof, L. Truyen, J.B. Boringa, F.W. Bertelsmann, B.M. von Blomberg, J.N. Woody, H.P. Hartung, and C.H. Polman. 1996. Increased MRI activity and immune activation in two multiple sclerosis patients treated with the monoclonal anti-tumor necrosis factor antibody cA2. *Neurology* 47:1531-1534.

van Tilborg, E., C.G.M. de Theije, M. van Hal, N. Wagenaar, L.S. de Vries, M.J. Benders, D.H. Rowitch, and C.H. Nijboer. 2018. Origin and dynamics of oligodendrocytes in the developing brain: Implications for perinatal white matter injury. *Glia* 66:221-238.

Vela, J.M., E. Molina-Holgado, A. Arevalo-Martin, G. Almazan, and C. Guaza. 2002. Interleukin-1 regulates proliferation and differentiation of oligodendrocyte progenitor cells. *Mol Cell Neurosci* 20:489-502.

Villani, A., J. Benjaminsen, C. Moritz, K. Henke, J. Hartmann, N. Norlin, K. Richter, N.L. Schieber, T. Franke, Y. Schwab, and F. Peri. 2019. Clearance by Microglia Depends on Packaging of Phagosomes into a Unique Cellular Compartment. *Dev Cell* 49:77-88 e77.

Voet, S., C. Mc Guire, N. Hagemeyer, A. Martens, A. Schroeder, P. Wieghofer, C. Daems, O. Staszewski, L. Vande Walle, M.J.C. Jordao, M. Sze, H.K. Vikkula, D. Demeestere, G. Van Imschoot, C.L. Scott, E. Hoste, A. Goncalves, M. Guilliams, S. Lippens, C. Libert, R.E. Vandenbroucke, K.W. Kim, S. Jung, Z. Callaerts-Vegh, P. Callaerts, J. de Wit, M. Lamkanfi, M. Prinz, and G. van Loo. 2018. A20 critically controls microglia activation and inhibits inflammasome-dependent neuroinflammation. *Nat Commun* 9:2036.

Vora, P., P. Pillai, J. Mustapha, C. Kowal, S. Shaffer, R. Bose, M. Namaka, and E.E. Frost. 2012. CXCL1 regulation of oligodendrocyte progenitor cell migration is independent of calcium signaling. *Exp Neurol* 236:259-267.

Voss, E.V., J. Skuljec, V. Gudi, T. Skripuletz, R. Pul, C. Trebst, and M. Stangel. 2012. Characterisation of microglia during de- and remyelination: can they create a repair promoting environment? *Neurobiol Dis* 45:519-528.

Wade, B.J. 2014. Spatial analysis of global prevalence of multiple sclerosis suggests need for an updated prevalence scale. *Mult Scler Int* 2014:124578.

Wang, X., K. Cao, X. Sun, Y. Chen, Z. Duan, L. Sun, L. Guo, P. Bai, D. Sun, J. Fan, X. He, W. Young, and Y. Ren. 2015. Macrophages in spinal cord injury: phenotypic and functional change from exposure to myelin debris. *Glia* 63:635-651.

Wasko, N.J., M.H. Kulak, D. Paul, A.M. Nicaise, S.T. Yeung, F.C. Nichols, K.M. Khanna, S. Crocker, J.S. Pachter, and R.B. Clark. 2019. Systemic TLR2 tolerance enhances central nervous system remyelination. *J Neuroinflammation* 16:158.

Watanabe, M., T. Hadzic, and A. Nishiyama. 2004. Transient upregulation of Nkx2.2 expression in oligodendrocyte lineage cells during remyelination. *Glia* 46:311-322.

Watzlawik, J.O., A.E. Warrington, and M. Rodriguez. 2013. PDGF is required for remyelination-promoting IgM stimulation of oligodendrocyte progenitor cell proliferation. *PLoS One* 8:e55149.

Whittaker, M.T., L.J. Zai, H.J. Lee, A. Pajoohesh-Ganji, J. Wu, A. Sharp, R. Wyse, and J.R. Wrathall. 2012. GGF2 (Nrg1-beta3) treatment enhances NG2+ cell response and improves functional recovery after spinal cord injury. *Glia* 60:281-294.

Willer, C.J., D.A. Dyment, N.J. Risch, A.D. Sadovnick, G.C. Ebers, and G. Canadian Collaborative Study. 2003. Twin concordance and sibling recurrence rates in multiple sclerosis. *Proc Natl Acad Sci U S A* 100:12877-12882.

Williams, K., E. Ulvestad, A. Waage, J.P. Antel, and J. McLaurin. 1994. Activation of adult human derived microglia by myelin phagocytosis in vitro. *J Neurosci Res* 38:433-443.

Wolswijk, G. 1998. Chronic stage multiple sclerosis lesions contain a relatively quiescent population of oligodendrocyte precursor cells. *J Neurosci* 18:601-609.

Woodruff, R.H., and R.J. Franklin. 1999. Demyelination and remyelination of the caudal cerebellar peduncle of adult rats following stereotaxic injections of lysolecithin, ethidium bromide, and complement/anti-galactocerebroside: a comparative study. *Glia* 25:216-228.

Woodruff, R.H., M. Fruttiger, W.D. Richardson, and R.J. Franklin. 2004. Platelet-derived growth factor regulates oligodendrocyte progenitor numbers in adult CNS and their response following CNS demyelination. *Mol Cell Neurosci* 25:252-262.

Wooliscroft, L., E. Silbermann, M. Cameron, and D. Bourdette. 2019. Approaches to Remyelination Therapies in Multiple Sclerosis. *Curr Treat Options Neurol* 21:34.

Yamout, B.I., N.K. El-Ayoubi, J. Nicolas, Y. El Kouzi, S.J. Khoury, and M.M. Zeineddine. 2018. Safety and Efficacy of Rituximab in Multiple Sclerosis: A Retrospective Observational Study. *J Immunol Res* 2018:9084759.

Yeung, M.S.Y., M. Djelloul, E. Steiner, S. Bernard, M. Salehpour, G. Possnert, L. Brundin, and J. Frisen. 2019. Dynamics of oligodendrocyte generation in multiple sclerosis. *Nature* 566:538-542.

Yona, S., K.W. Kim, Y. Wolf, A. Mildner, D. Varol, M. Breker, D. Strauss-Ayali, S. Viukov, M. Guilliams, A. Misharin, D.A. Hume, H. Perlman, B. Malissen, E. Zelzer, and S. Jung. 2013. Fate mapping reveals origins and dynamics of monocytes and tissue macrophages under homeostasis. *Immunity* 38:79-91.

Yu, H.M., Y.M. Zhao, X.G. Luo, Y. Feng, Y. Ren, H. Shang, Z.Y. He, X.M. Luo, S.D. Chen, and X.Y. Wang. 2012. Repeated lipopolysaccharide stimulation induces cellular senescence in BV2 cells. *Neuroimmunomodulation* 19:131-136.

Yu, L., L. Wang, and S. Chen. 2010. Endogenous toll-like receptor ligands and their biological significance. *J Cell Mol Med* 14:2592-2603.

Zhang, Y., Y.P. Zhang, B. Pepinsky, G. Huang, L.B. Shields, C.B. Shields, and S. Mi. 2015. Inhibition of LINGO-1 promotes functional recovery after experimental spinal cord demyelination. *Exp Neurol* 266:68-73.

Zhou, Q., S. Wang, and D.J. Anderson. 2000. Identification of a novel family of oligodendrocyte lineage-specific basic helix-loop-helix transcription factors. *Neuron* 25:331-343.

Zoller, T., A. Schneider, C. Kleimeyer, T. Masuda, P.S. Potru, D. Pfeifer, T. Blank, M. Prinz, and B. Spittau. 2018. Silencing of TGFbeta signalling in microglia results in impaired homeostasis. *Nat Commun* 9:4011.